The role of the BMP and Toll pathways in patterning the dorsal-ventral axis of the jewel wasp *Nasonia vitripennis*.

Inaugural-Dissertation
zur
Erlangung des Doktorgrades
der Mathematisch-Naturwissenschaftlichen Fakultät
der Universität zu Köln

vorgelegt von
Orhan Özüak
aus Köln

Copy-Star Druck & Werbung GmbH | 50937 Köln

Köln, 2014

Berichterstatter/in: Prof. Dr. Siegfried Roth
Prof. Dr. Henrike Scholz

Tag der mündlichen Prüfung: 10. April 2014

Contents

1 Introduction

One of the most wonderful and fascinating aspects of life is the vast diversity of species across the entire animal kingdom. This diversity does not only include the outer appearance with its beautiful colours and different forms and shapes but also other aspects of life such as mating behaviour, reproductive strategies and different types of oogenesis. Among all animals, insects display by far the most diverse class. But despite this diversity, insects as well as all bilaterian animals share the common feature of having two orthogonal major body axes. The anterior-posterior (AP) axis, which is usually the longest axis, runs parallel to the gut from mouth to anus. Perpendicular to this is the short dorsal-ventral (DV) axis, which runs from back to belly. To establish these axes, diverse mechanisms and strategies have evolved among different lineages, using highly conserved signalling pathways and transcription factors. The establishment and patterning of the DV axis of the fruit fly *Drosophila melanogaster* is the best described embryonic patterning systems among bilateria. Therefore, when studying the evolution of axial patterning, DV specification in *Drosophila* can be considered as the gold standard to which other insects can be compared.

1.1 Oogenesis in *Drosophila melanogaster*

By the time the *Drosophila* egg is laid, a clear asymmetry is already present in the embryo due to symmetry-breaking events in the ovary during oogenesis. The two ovaries of *Drosophila* are composed of 16-20 independent ovarioles each (Spradling, 1993). The ovarioles can be considered as egg production units, which are strings of progressively maturing egg chambers (Fig. 1). Oogenesis (the development of the egg chambers) has been divided into 14 stages. Stages 1-6 are

called early, stages 7-10 mid, and stages 11-14 late oogenesis. A new egg chamber is always generated at the germarium. This is a specific region located at the anterior tip of each ovariole, which harbors germline and somatic stem cells (Fig. 1). An asymmetric division of germline stem cells (GSC) at the anterior tip of the germarium gives rise to one self-renewing GSC and one cystoblast that starts to differentiate (Fuller and Spradling, 2007).

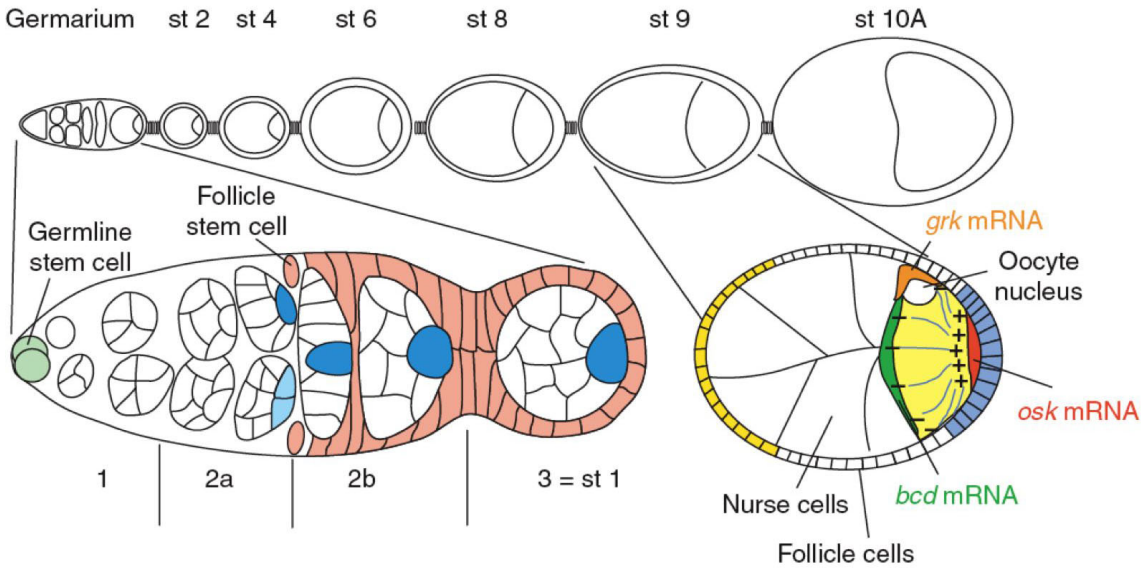

Figure 1.1 | The ovariole
Upper portion: A schematic drawing of an ovariole with the germarium and egg chambers of different stages. Lower portion: A magnified view of the germarium and stage 9 egg chamber. (Figure taken from (Roth and Lynch, 2009))

After four incomplete mitotic divisions of the cystoblast, a cyst of 16 cells (cystoytes) is formed that are connected by cytoplasmic bridges, called ring canals. A membranous branched structure called the fusome runs through the ring canals and controls the orientation of the divisions, which leads to a stereotypic pattern of cell-cell connections: eight cells of the cyst have one ring canal, four cells have two, two cells have three, and two cells have four ring canals (Spradling, 1993; Lin and Spradling, 1995; Deng and Lin, 1997; McGrail and Hays, 1997; Grieder et al., 2000).

One of the two cells with four ring canals will differentiate as the oocyte, while the remaining 15 cells of the cyst will become polyploid nurse cells that provide the oocyte with nutrients and cytoplasmic components via the ring canals. As the cyst moves down the germarium it becomes surrounded by somatic follicle cells and finally becomes rounded with the oocyte always positioned at the posterior pole (Torres et al., 2003; Assa-Kunik et al., 2007).

1.1.1 Determination of the main body axes during oogenesis

As the egg chamber leaves the germarium, it starts to increase in size and several mRNAs that were transported from the nurse cells begin to accumulate within the oocyte. Among those mRNAs is *gurken* (*grk*), which starts to accumulate within the oocyte in the germarium and is localized to the posterior cortex at the beginning of stage 1. *grk* codes for a transforming growth factor α (TGFα) homolog, which is a member of the epidermal growth factor receptor (EGFR) ligand family (Neuman-Silberberg and Schüpbach, 1993). Around stage 6/7, the oocyte starts to secrete Grk protein, which in turn activates the EGFR in the adjacent follicle cells (Fig 1.2 A) (Peri et al., 1999; Queenan et al., 1999; Chang et al., 2008). Upon this activation, the transcription of several target genes of EGF signalling is initiated (Morimoto et al., 1996; Ghiglione et al., 1999; Reich et al., 1999), which finally leads to the induction of posterior follicle cell (PFC) fate. The outcome of this first germline to soma signalling event is a clear AP polarity of the follicular epithelium in addition to the inner polarity of the germline (González-Reyes and St Johnston, 1994; González-Reyes et al., 1995; Roth et al., 1995). After PFC induction, back signalling takes place where the PFCs signal back to the germline (Fig. 1.2 B). The consequence of this is a repolarization of the oocyte at stages 7-9. A rearrangement of the microtuble (MT) cytoskeleton leads to the

localization of *bicoid* (*bcd*) mRNA to the anterior and *oskar* (*osk*) mRNA to the posterior pole of the oocyte (Fig 1.1 st9) (Ephrussi et al., 1991; Kim-Ha et al., 1991; Brendza et al., 2000; Januschke et al., 2002). In addition to mRNAs being localized, the oocyte nucleus migrates from its posterior position to the anterior margin of the oocyte (Fig. 1.2 C).

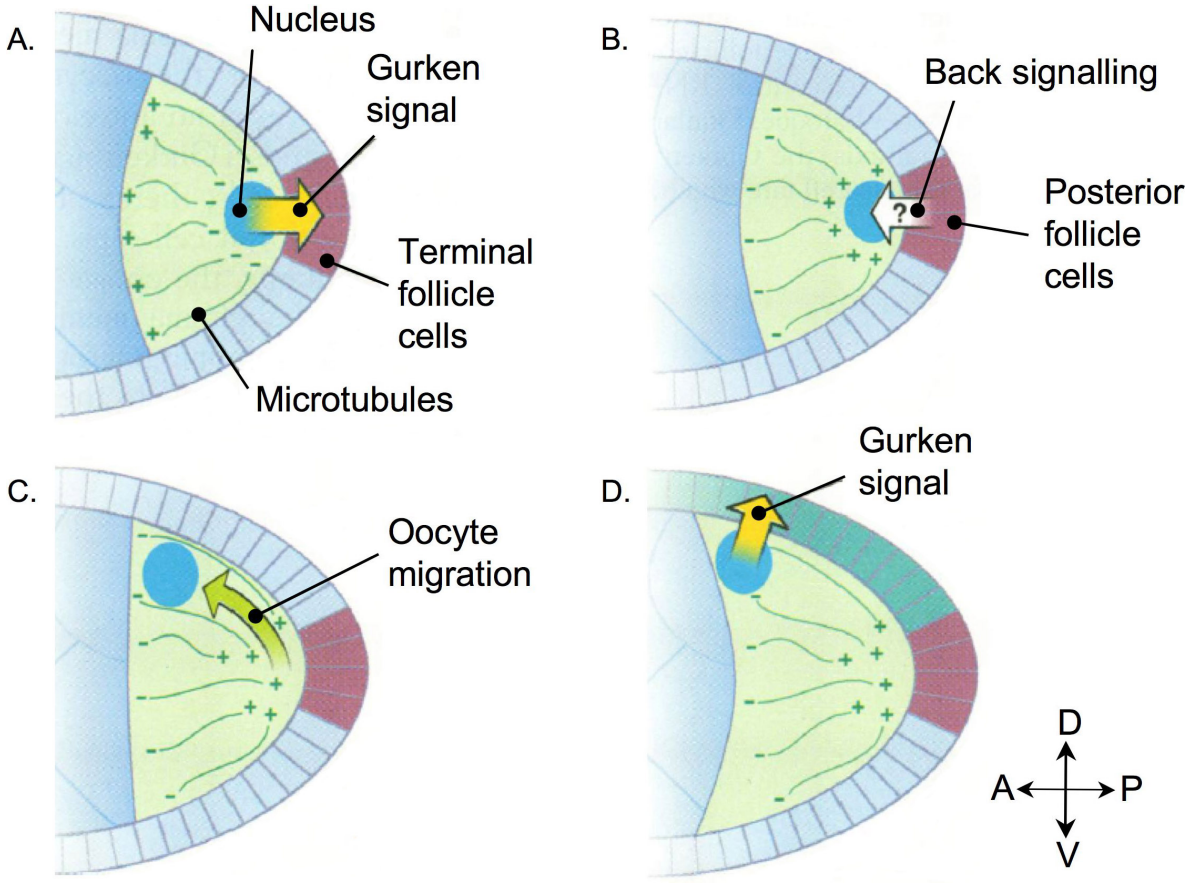

Figure 1.2 | First and second round of Gurken signalling
(A) First Gurken signal from oocyte to terminal follicle cells. (B) Posterior follicle cells establishment and back signalling to the oocyte. (C) Oocyte nucleus migration to the anterior margin. (D) Second Gurken signal to establish DV polarity. (Figure modified from (Anderson, 1995))

For a long time it was suggested that the oocyte nucleus is pulled to the anterior side along a polarized MT cytoskeleton but recent studies have revealed that the oocyte nucleus is rather pushed by growing MT towards the anterior side (Zhao et al., 2012).

Together with the oocyte nucleus, *grk* mRNA also localizes to the anterior corner, where it induces a second round of EGF signalling to establish dorso-ventral polarity (Fig. 1.2 D) (Neuman-Silberberg and Schüpbach, 1993; González-Reyes et al., 1995; Roth et al., 1995). The main target of Grk signalling that is most relevant to DV axis patterning is *pipe*, whose expression is repressed by Mirror (Mirr) in dorsal follicle cells, which in turn is induced by Grk signalling (Fig. 1.3 A) (Andreu et al., 2012). This restriction of *pipe* expression, which encodes for a sulfotransferase, to the ventral follicle cells leads to a localized activation of a protease cascade in the perivitelline space (Fig. 1.3 B) (Sen et al., 1998; Cho et al., 2010). This protease cascade is triggered by the autocatalytically processed Nudel and is composed of Gastrulation defective (Konrad et al., 1998), Snake (DeLotto and Spierer, 1986), and Easter (Chasan and Anderson, 1989; Chasan et al., 1992). The final outcome of this protease cascade is the cleavage and activation of the Toll ligand Spätzle (Spz) in the ventral portion of the perivitelline space (Fig. 1.3 B) (Moussian and Roth, 2005).

1.2 Toll signalling in the *Drosophila* embyro

As soon as the egg is laid, the cleaved (and thereby activated) form of Spz protein binds to the maternally supplied Toll receptor, which is present at the plasma membrane of the embryo (Fig. 1.3 C). The activated Toll receptor recruits and binds a complex of the adaptor proteins MyD88 and Tube via intracellular TIR (Toll and Interleukin Receptor) domains (Medzhitov et al., 1998; Horng and

Medzhitov, 2001; Kambris et al., 2003; Sun et al., 2004). These two components of the heterodimer complex bind to each other through their DEATH domains and can localize to the plasma membrane independently of a signal (Towb et al., 1998). The next step in transducing the signal is the recruitment of the serine/threonine kinase Pelle to the Toll-MyD88-Tube complex (Fig. 1.3 C1).

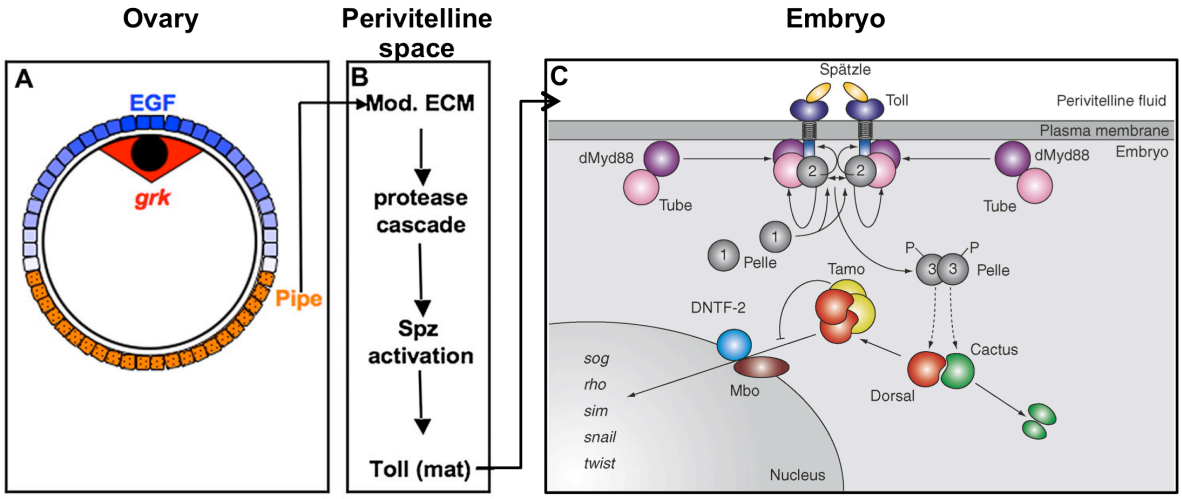

Figure 1.3 | Upstream and downstream of the Toll pathway
(A) Localization of *grk* mRNA around the oocyte nucleus (red) and activation of EGF signalling leads to restricted expression of *pipe* in the ventral follicle cells. (B) Pipe triggers a protease cascade in the perivitelline space, which finally leads to the activation of Spätzle. (C) Spätzle binds to the Toll Receptor that is located in the plasma membrane of the embryo. Activation of the Toll receptor leads to the degradation of Cactus and subsequently to the translocation of Dorsal into the nucleus where it regulates the expression of target genes. (A and B modified from (Lynch and Roth, 2011) and C modified from (Moussian and Roth, 2005))

Pelle does not interact with MyD88, but instead binds to Tube via DEATH domains (Hu et al., 2004). Upon high concentrations of the tetrameric complex of Toll-MyD88-Tube-Pelle, Pelle undergoes autophosphorylation, thus enhancing its kinase activity (Fig. 1.3 C2). The targets of Pelle are Toll and Tube and after their phosphorylation Pelle is released again from the complex and transduces the signal to downstream factors, which will lead to the degradation of the IκB homolog Cactus (Cact) (Fig. 1.3 C3) (Bergmann et al., 1996; Reach et al., 1996;

Edwards et al., 1997). In the absence of signalling, Cact binds and inhibits the NFκB transcription factor Dorsal in the cytoplasm. Once Dorsal is freed from Cact (in response to Toll activation), it binds to Tamo and enters the nucleus through a nuclear pore that contains *Drosophila* Nuclear Transport Factor-2 (DNTF-2) and Members-only (Mbo) (Uv et al., 2000; Minakhina et al., 2003).

The activation of the Toll signalling pathway finally leads to a stable nuclear Dorsal gradient with peak levels at the ventral midline (Fig. 1.4). However, it is important to point out that the nuclear Dorsal gradient is not simply a readout of the ventral *pipe* expression pattern in the ovarian follicle cells, which is uniformly expressed in its domain (compare Fig. 1.3 A and 1.4 A) (Roth, 2003). How a uniform *pipe* domain at the ventral side in the ovary is transformed into a graded domain of Dorsal nuclear uptake in the embryo is still not fully understood, but it appears that a self-regulation at the level of Spz activation plays a crucial role (Morisato, 2001). In addition it has been suggested that there might be another source of DV polarity information besides *pipe*, because egg chambers with a uniform *pipe* expression in all follicle cells still show some degree of DV polarity (Zhang et al., 2009).

All cell fates along the DV axis depend directly or indirectly on Dorsal. It acts as a morphogen and regulates over 50 target genes in a concentration dependent manner (Fig. 1.4 B) (Stathopoulos et al., 2002; Hong et al., 2008). The sensitivity of Dorsal target genes to nuclear Dorsal concentrations is, in part, determined by the arrangement and affinities of Dorsal-binding sites in their enhancers (Stathopoulos and Levine, 2004; Hong et al., 2008). Additionally Dorsal cooperates with other maternal factors such as Zelda and basic helix-loop-helix (bHLH) proteins to pattern the most dorsally extending domains (Crocker et al., 2008; Liberman and Stathopoulos, 2009). Target genes with very low affinity Dorsal binding sites are only activated by high levels of nuclear Dorsal, which restricts their expression to the ventral region of the embryo (Fig. 1.4 B). Examples for such targets are *twist* and *snail*, which both encode transcription factors that are

involved in specification and morphogenesis of the mesoderm. Moderate amounts of nuclear Dorsal concentrations turn on genes that contain high affinity Dorsal binding sites such as *ventral neuroblasts defective* (*vnd*), which patterns the neuroectoderm. In addition, *vnd* is repressed at the ventral side by *snail*, which leads to a lateral, stripe like expression domain of *vnd*.

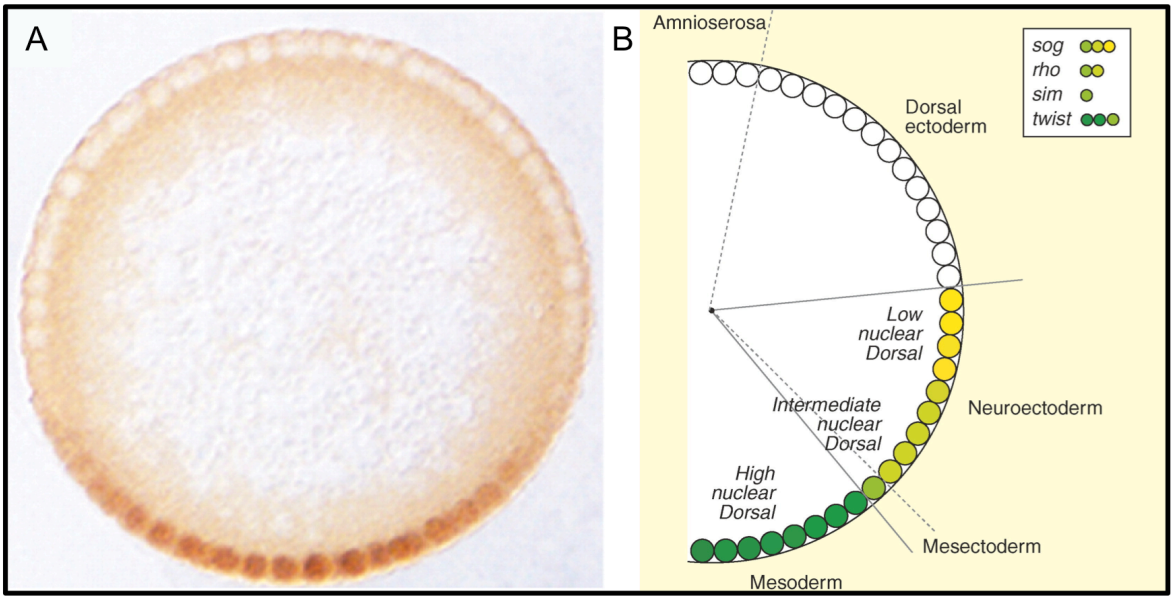

Figure 1.4 | Dorsal gradient and the positional information along the DV axis
(A) A cross-section of a syncytial blastoderm embryo of *Drosophila* stained for Dorsal protein (red). (B) A schematic half cross-section of a syncytial blastoderm embryo of *Drosophila*. A graded activation of the Toll pathway leads to the subdivision of the embryo in three major regions along the DV axis: Mesoderm, neuroectoderm, and the non-neurogenic ectoderm. (A modified from (Roth, 2003) and B modified from (Moussian and Roth, 2005))

Finally, target genes that respond to low levels of nuclear Dorsal concentrations are characterized by high affinity Dorsal binding sites. Depending on the presence of closely linked co-activators or co-repressors, these target genes can be activated, e.g. *short gastrulation* (*sog*), or repressed, e.g. *zerknüllt* (*zen*) (Rusch and Levine, 1996; Reeves and Stathopoulos, 2009).

However, Dorsal does not only pattern the ventral and lateral parts of the *Drosophila* embryo, but it also regulates the expression of genes that are components of the Bone Morphogenic Protein (BMP) signalling pathway, which patterns the dorsal half of the embryo.

1.3 BMP signalling in the *Drosophila* embryo

The BMP signalling pathway patterns the dorsal half of the *Drosophila* embryo, which consists of the dorsal non-neurogenic ectoderm and the extra embryonic region. The morphogen Dorsal controls this pathway by regulating several of its components. The BMP inhibitor *sog* is activated in a broad lateral domain, while the BMP2/4 ligand *decapentaplegic* (*dpp*) and the metalloprotease *tolloid* (*tld*) are repressed by Dorsal, thereby restricting their expression domains to the dorsal side of the embryo. *sog* codes for a large secreted protein, which contains four copies of a cysteine repeat (CR) and is structurally and functionally homologous to *Xenopus* Chordin (François and Bier, 1995). The protein acts as an inhibitor of BMP signalling by binding to BMP ligands and preventing them from activating their receptors. Heterodimers of the ligands Dpp and Screw (Scw) are preferentially bound by Sog, while homodimers of Dpp are only bound in a trimeric complex with another antagonist called Twisted gastrulation (Tsg) (Fig. 1.5) (Mason et al., 1994; Oelgeschläger et al., 2000, 2003; Ross et al., 2001; Scott et al., 2001). As the Sog/ligand complex diffuses towards the dorsal half of the embryo, Sog is cleaved by Tld (Shimell et al., 1991; Marqués et al., 1997; Shimmi and O'Connor, 2003). Released Dpp can then either bind to its receptor and activate signalling, or it can be recaptured by another Sog/Tsg complex. The probability to bind the receptor becomes more likely towards the dorsal midline, where Sog levels are low (Eldar et al., 2002; Mizutani et al., 2005). These complex interactions

of BMP pathway components initially lead to a gradient of BMP activation at the dorsal side of the embryo. Later on, transcriptional feedback (Wang and Ferguson, 2005) as well as complex protein-protein interactions among BMP components (O'Connor et al., 2006) resolve the gradient into a sharp peak at the dorsal midline.

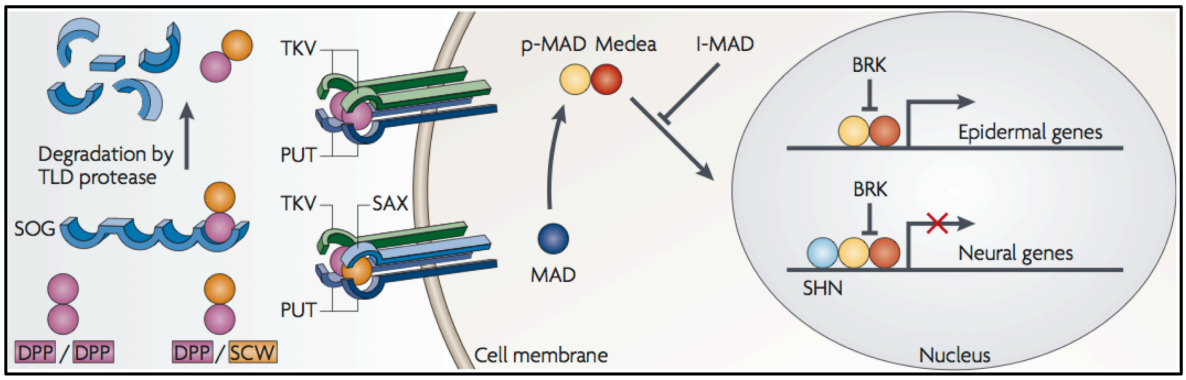

Figure 1.4 | The BMP signalling pathway
The BMP antagonist Sog binds the ligands and prevents them from signalling. In addition, it diffuses towards the dorsal half where it is cleaved by the metalloprotease Tld. Released Dpp and Scw can then bind to a heterotetrameric receptor complex, which leads to the phosphorylation and activation of Mad. pMad forms a complex with Medea and translocates into the nucleus where it regulates target gene expression. This can be inhibited by inhibitory-MADs. The transcription factor Brk can also inhibit BMP signalling by binding to sequences that overlap with those of pMad. Schnurri (Shn) can form a trimeric complex with pMad/Medea and efficiently repress expression of neural genes.

The Dpp and Scw ligands either bind as Dpp-Dpp homodimers or as Dpp-Scw heterodimers to a specific combination of a heterotetrameric receptor complex, which consists of two type I and two type II serine-threonine kinase receptors (Fig. 1.5) (Shimmi et al., 2005). Both homo- and heterodimers use the type II receptor Punt (Put), while specificity is generated by the type I receptors (Letsou et al., 1995). Dpp homodimers bind to a combination of two Thick veins (Tkv) type I receptors, whereas Dpp-Scw heterodimers bind to a combination of one Tkv receptor and one Saxophone (Sax) type I receptor (Brummel et al., 1994; Penton et al., 1994). Upon ligand binding, the type II receptors become activated and their chains phosphorylate the type I chains. These activated type I receptors in turn

transduce the signal into the cell by phosphorylating and thereby activating Mothers against Dpp (Mad) (Raftery et al., 1995; Sekelsky et al., 1995). The activated form of Mad, called phospho-Mad (pMad), forms a complex with the co-Mad Medea, which can then enter the nucleus and alter the expression of several different target genes (Raftery and Wisotzkey, 1996; Das et al., 1998; Hudson et al., 1998; Wisotzkey et al., 1998).

In addition to the extracellular control of BMP signalling in form of Sog, Tsg, and Tld there is also a strict intracellular control of BMP signalling. The formation of the pMad-Medea complex can for example be inhibited by an inhibitory-Mad (I-Mad) like Daughters against Dpp (Dad). This can either be by targeting the active receptors or at the transcriptional level (Schmierer and Hill, 2007). Another transcriptional repressor called Brinker (Brk) can also block BMP signalling by binding to sequences that overlap with those of pMad (Jaźwińska et al., 1999; Kirkpatrick et al., 2001; Winter and Campbell, 2004).

1.4 The misleading gold standard

To summarize the introduction so far, the DV axis of *Drosophila* is established during oogenesis, and is patterned by two conserved signalling pathways, although the BMP pathway is clearly dominated by the Toll pathway. This patterning system is by far the best understood gene regulatory network (GRN), and therefore it is tempting to consider this as the gold standard to which other insects can be compared to. However, this may be a mistake, as *Drosophila* exhibits several highly derived features, which are not typical of insects in general. For example, *Drosophila* undergoes a mode of embryogenesis, which is called long-germ, where all segments are specified simultaneously within the blastoderm stage

embryo (Davis and Patel, 2002). This mode of embryogenesis is only found among holometabolous insects (fully metamorphosing insects), and it is believed that this mode has been evolved independently multiple times. In contrast to this, the short germ mode of embryogenesis is found among all hemimetabolous and some holometabolous insects such as the flour beetle *Tribolium castaneum*. In this type of embryogenesis, which is considered to be the ancestral mode, only some of the anterior segments are present at the blastoderm stage, while the rest is generated and patterned progressively after gastrulation from a posterior growth zone (Davis and Patel, 2002). Thus, short germ embryogenesis requires at least two steps in patterning the DV axis, with one being active during the blastoderm stage and one operating in the growth zone after gastrulation.

Cell fates along the DV axis of the early *Tribolium* embryo are also patterned by a Dorsal protein gradient, which is however different compared to *Drosophila* (Chen et al., 2000; Nunes da Fonseca et al., 2008). While the shape of the *Drosophila* Dorsal gradient is relatively stable, the *Tribolium* gradient is dynamic over developmental time. It starts as a shallow gradient and then progressively shrinks to a sharply graded stripe along the ventral midline until it finally disappears completely just prior to gastrulation (Chen et al., 2000; Nunes da Fonseca et al., 2008; Kanodia et al., 2009; Liberman et al., 2009).

In addition to these differences between *Drosophila* and *Tribolium* in patterning the DV axis, outside the insects, only the BMP pathway patterns the DV axis. The Toll pathway (which dominates DV patterning in *Drosphila*) has an ancestral, highly conserved role in innate immunity but plays no role in DV patterning outside the insects. Thus, the employment of the Toll signalling pathway to pattern the DV axis must be a novelty of insects. This raises the question of when did the transition from using only the BMP pathway to using both the BMP + Toll pathways occur within the insects?

To address this question and to understand which characteristics of DV patterning systems are truly representative of the ancestral mode of insects, more

insect species have to be examined. One appropriate candidate is the parasitoid jewel wasp *Nasonia vitripennis*. During the last years of research, the wasp has emerged more and more as an import model organism with the advantages of a fully sequenced genome, the ability to create transgenic wasps, and the use of parental RNA interference (pRNAi) technique to manipulate gene function (Lynch and Desplan, 2006; Werren et al., 2010). In addition, the wasp undergoes the long germ mode of embryogensis, which is similar to, but probably independently derived from that of *Drosophila*. Finally, it is a member of the Hymenoptera, the most basally branching order of the Holometabola, which makes *Nasonia* a representative of a key phylogenetic sampling point for reconstructing features of the ancestral DV patterning system.

1.5 Objectives

The main goal of this thesis is to find out how the DV axis of the wasp *Nasonia vitripennis* is established and patterned. To achieve this goal, three main projects were carried out: first, a detailed analysis of the expression of DV marker genes that cover the entire embryonic axis; second, functional analysis of the Toll and BMP pathways that pattern the DV axis; and third, an approach to identify new target genes and possible components of the pathways. With the outcome of these experiments we expect to gain new insights regarding the ancestral mode of axial patterning in insects.

2 Published and submitted manuscripts

2.1 Patterning the dorsal-ventral axis of the wasp *Nasonia vitripennis*

Developmental Biology 381 (2013) 189–202

Contents lists available at ScienceDirect

Developmental Biology

journal homepage: www.elsevier.com/locate/developmentalbiology

Patterning the dorsal–ventral axis of the wasp *Nasonia vitripennis*

Thomas Buchta [a,1], Orhan Özüak [a,1], Dominik Stappert [a], Siegfried Roth [a,*], Jeremy A. Lynch [a,b,**]

[a] Institute for Developmental Biology, University of Cologne, Zülpichstrasse 47b, 50674 Cologne, Germany
[b] Department of Biological Sciences, University of Illinois at Chicago, 900S Ashland Ave., Chicago, IL 60607, USA

ARTICLE INFO

Article history:
Received 29 November 2012
Received in revised form
14 May 2013
Accepted 24 May 2013
Available online 2 June 2013

Keywords:
Nasonia
Tribolium
Fate map
Dorsal–ventral patterning
Mesoderm
Extraembryonic
Patterning
Embryo

ABSTRACT

Regulatory networks composed of interacting genes are responsible for pattern formation and cell type specification in a wide variety of developmental contexts. Evolution must act on these regulatory networks in order to change the proportions, distribution, and characteristics of specified cells. Thus, understanding how these networks operate in homologous systems across multiple levels of phylogenetic divergence is critical for understanding the evolution of developmental systems. Among the most thoroughly characterized regulatory networks is the dorsal–ventral patterning system of the fly *Drosophila melanogaster*. Due to the thorough understanding of this system, it is an ideal starting point for comparative analyses. Here we report an analysis of the DV patterning system of the wasp, *Nasonia vitripennis*. This wasp undergoes a mode of long germ embryogenesis that is superficially nearly identical to that of *Drosophila*, but one that was likely independently derived. We have found that while the expression of genes just prior to the onset of gastrulation is almost identical in *Nasonia* and *Drosophila*, both the upstream network responsible for generating this pattern, and the downstream morphogenetic movements that it sets in motion, are significantly diverged. From this we conclude that many network structures are available to evolution to achieve particular developmental ends.

Introduction

All bilaterally symmetric animals face the problem of setting up two orthogonal body axes during embryogenesis. The mechanisms employed in these processes are variable across evolutionary time, with embryological and environmental factors influencing the strategies employed in various lineages. In order to understand how axis determination and patterning processes can change in the course of evolution, a comparative approach that incorporates highly detailed descriptions of homologous developmental processes is required. The establishment and patterning of the dorsal–ventral axis of the fruit fly *Drosophila melanogaster* is one of the most thoroughly described embryonic patterning systems among the bilateria, and thus serves as a valuable point of comparison for studies focused on the evolution of patterning processes.

The chain of events that leads to cell fate determination along the DV axis of the *Drosophila* (and other insects (Lynch et al., 2010)) embryo begins in the ovary (reviewed in (Roth and Schüpbach, 1994)). Here, *gurken* mRNA localized anteriorly and asymmetrically with regard to the short axis of the oocyte, leads to the localized activation of EGF signaling in the overlying follicle cells, and this signal specifies the future dorsal side of the egg (Neuman-Silberberg and Schüpbach, 1993; Roth, 2003). EGF signaling also precisely restricts the expression of the sulfotransferase *pipe* to the ventral follicle cells, which in turn leads to a localized activation of a protease cascade in the perivitelline space (Sen et al., 1998; Cho et al., 2010). The outcome of the activated protease cascade is the graded cleavage, and thus activation, of the Toll ligand Spätzle (Spz) in the ventral half of the perivitelline space (Moussian and Roth, 2005).

In the early embryo, cleaved Spz protein binds the maternally provided Toll receptor present in the plasma membrane. Upon Toll activation by Spz the IκB homolog Cactus (Cact) becomes phosphorylated and degraded, which in turn leads to the release and translocation of the NF-κB transcription factor Dorsal to the nucleus, creating a stable DV gradient of nuclear Dorsal with peak levels at the ventral midline (Moussian and Roth, 2005). Dorsal acts as a morphogen, directly regulating around 50 genes in a concentration dependent manner (Stathopoulos et al., 2002; Hong et al., 2008).

Dorsal target genes contain enhancers that vary in the number, affinity, and arrangement of Dorsal binding sites and determine their sensitivity to nuclear Dorsal concentrations (Stathopoulos and Levine, 2004; Hong et al., 2008). The expression of genes with

* Corresponding author.
** Corresponding author.
E-mail addresses: siegfried.roth@uni-koeln.de (S. Roth).
jlynch42@uic.edu (J.A. Lynch).
[1] These authors contributed equally.

0012-1606/$ - see front matter © 2013 Elsevier Inc. All rights reserved.
http://dx.doi.org/10.1016/j.ydbio.2013.05.026

enhancers containing low affinity Dorsal binding sites can only be activated by high levels of nuclear Dorsal, and are thereby restricted to the ventral region of the embryo. Examples are genes like *twist* and *snail*, which are involved in the specification and morphogenesis of mesoderm. Genes such as *ventral neuroblasts defective (vnd)* and *brinker (brk)* that react to moderate and low nuclear Dorsal concentrations are characterized by enhancers containing high affinity affinity Dorsal binding sites in combination with binding sites for bHLH, Supressor of Hairless and/or ETS domain transcription factors. They have lateral, stripe like expression domains, due to repression by Snail ventrally. Finally, genes like *short gastrulation (sog)* and *zerknuellt (zen)*, that react to low levels of Dorsal, are characterized by enhancers containing high affinity Dorsal binding sites with either activating (e.g. *sog* enhancer) or repressing influence (e.g. *zen* enhancer) depending on the presence of closely linked co-activator or co-repressor binding sites, respectively (Rusch and Levine, 1996; Reeves and Stathopoulos, 2009).

Several Dorsal target genes are transcription factors that interact with each other and which further refine and elaborate the expression of downstream target genes. Dorsal not only patterns the ventral and lateral parts of the *Drosophila* embryo, but also plays a major role in regulating the BMP signaling pathway, which patterns the dorsal half of the embryo. By activating the BMP inhibitor *sog* in a broad lateral domain and repressing the BMP2/4-like ligand *decapentaplegic (dpp)* and the metalloprotease *tolloid (tld)* in the ventral half of the embryo, Dorsal facilitates the establishment of a gradient of BMP activation with a sharp peak at the dorsal midline (O'Connor et al., 2006).

Althoughh the *Drosophila* DV patterning system is one of the best understood gene regulatory networks (GRNs), and thus is the gold standard to which other insects will be compared, the fly is not typical of insects in many respects. It shows highly derived features and undergoes a long germ mode of embryogenesis, which is only found among holometabolous insects. In this type of embryogenesis all segments are specified simultaneously within the blastoderm stage embryo (Davis and Patel, 2002). In contrast, all hemimetabolous and some holometabolous insects, such as the beetle *Tribolium castaneum*, undergo a short germ mode of embryogenesis. In this mode of embryogenesis only the head and thoracic segments are specified prior to gastrulation, while the remaining segments are generated and patterned progressively after gastrulation (Davis and Patel, 2002). Thus, short germ patterning requires at least two steps in DV patterning: one acting at the blastoderm stage which partitions the head and thoracic segments, and a second one being active in the post-gastrulation growth zone.

The Dorsal protein of *Tribolium* (Tc-Dorsal), like its *Drosophila* counterpart, forms a gradient during early embryogenesis, and is involved in patterning cell fates along the DV axis of the early embryo (Chen et al., 2000; Nunes da Fonseca et al., 2008). However, the function of Tc-Dorsal differs from that of fly Dorsal in two fundamental ways. First, the Tc-Dorsal gradient is dynamic over developmental time, while the shape of the *Drosophila* gradient is relatively stable (Chen et al., 2000; Kanodia et al., 2009; Liberman et al., 2009). The domain of nuclear Tc-Dorsal is initially weak and shallowly graded, then progressively shrinks to form a steeply graded stripe straddling the ventral midline, before finally disappearing completely just prior to gastrulation. The dynamics of the Tc-Dorsal gradient are a result of a feedback loop of zygotic target genes of Tc-Dorsal, which include both its upstream activating receptor Tc-Toll, and its inhibitor, Tc-Cactus (Nunes da Fonseca et al., 2008). *Tc-Toll*, *Tc-cactus*, and at least one additional zygotic target of Tc-Dorsal (*Tc-twist*) are expressed in dynamic patterns that seem to follow the changes in the Tc-Dorsal gradient (Nunes da Fonseca et al., 2008).

A second difference between the fly and beetle systems is that Tc-Dorsal is only directly involved in specifying cell fates along the DV axis in a fraction of the embryo, since the Tc-Dorsal nuclear gradient is only present prior to gastrulation, and does not operate in the growth zone (Chen et al., 2000). In contrast, fly Dorsal assigns DV cell fates to all segmental primordia prior to gastrulation.

These differences between *Tribolium* and *Drosophila* Dorsal function lead to questions about which characteristics of the *Drosophila* DV patterning system are due to its mode of embryogenesis, and which characteristics of the *Tribolium* system are truly representative of the ancestral mode for insects.

To begin to address these questions, we have initiated an examination of the DV patterning process of the wasp *Nasonia vitripennis*. This wasp has a mode of long germ embryogenesis similar to, but independently derived from, that of the fly, which makes it an ideal model for understanding the patterning requirements for long germ embryogenesis (Lynch et al., 2012). On the other hand, it is a member of the Hymenoptera, the most basally branching order of the Holometabola (fully metamorphosing insects), and *Nasonia* thus represents a key phylogenetic sampling point for reconstructing features of the ancestral DV patterning mechanism within this clade (Lynch et al., 2012).

To fully understand how establishment and patterning of the DV axis come about at a functional level, the process must first be well described observationally. Only after such a thorough description can perturbations of the system be robustly interpreted. Thus, to provide a basis for future functional experiments, and to gain insights into how DV axial patterning comes about in *Nasonia*, we have cloned and analyzed the expression of *Nasonia* orthologs of *Drosophila* DV marker genes covering the entire embryonic axis. We have found that the expression patterns of these genes just prior to gastrulation are highly similar between *Nasonia* and *Drosophila*. However, our results also show that some aspects of the gene regulatory networks both upstream and downstream of this conserved arrangement have diverged significantly between the wasp and the fly. Finally, incorporation of gene expression data from the beetle *Tribolium* into this comparative work has shed light onto features and components of DV patterning that were likely present in the last common ancestor of the Holometabola.

Results

Characterization of early Nasonia embryogenesis

In order to best be able to interpret the dynamics of gene expression, the process of *Nasonia* embryogenesis needed further characterization. We took two approaches to this end. One was timed egg collections and DAPI staining to characterize the stages present at different time points at 29 °C (the temperature at which embryos were laid and incubated) (Fig. S1). The other was to take advantage of the optically clear embryo of *Nasonia* to make time lapse DIC movies of embryogenesis (supplemental movie 1). These two approaches were complementary, and led us to the same conclusions about early *Nasonia* embryogenesis, that were generally consistent with previous work (Bull, 1982). Like *Drosophila*, there are rapid, synchronous syncytial divisions of nuclei before the onset of gastrulation. In *Nasonia*, there are 12 of these divisions, rather than 13 observed in *Drosophila*. The initial pole cell bud occurs after 6 divisions (02:00, supplemental movie 1), one cycle prior to the appearance of the rest of the nuclei on the egg surface (02:20, supplemental movie 1). This is in contrast to *Drosophila*, where the pole cells form simultaneously with the arrival of nuclei to the embryo surface.

Supplementary material related to this article can be found online at doi:10.1016/j.ydbio.2013.05.026.

Once nuclei have arrived at the egg surface, they undergo 5 division cycles of increasing duration. Once the 12th division has been completed, there is a long period before gastrulation (~1 h), during which membrane furrows form between the nuclei, and a clear boundary forms between the nuclei and the yolk sac, completing the process of cellularization (07:00, supplemental movie 1). Once this boundary is completed the embryo begins the process of gastrulation with the mesoderm internalizing ventrally starting at the anterior, and progressing posteriorly, and the posterior gut invaginating posterior-dorsally. As these processes complete, cells on the dorsal side differentiate and migrate ventrally over the ectoderm, forming the serosa (onset at 09:00, supplemental movie 1). All of these morphogenetic movements are distinct from equivalent events occurring in the *Drosophila* embryo (see Discussion).

These observations were made with embryos deriving from both mated and virgin females, which should give rise to mostly female embryos, and all male embryos, respectively. We could not detect any differences between male or female embryos in our time lapse, or in our DAPI analyses. This was somewhat surprising, since in *Drosophila*, haploid embryos undergo an additional, and triploid embryos undergo one less, division cycle prior to gastrulation (Erickson and Quintero, 2007). It may be that since *Nasonia* is obligately haplodiploid, it has developed means to ensure a consistent number of blastoderm nuclei prior to gastrulation between the sexes.

Aside from the morphological movements, the structure of the blastoderm and the arrangement of cell fates prior to gastrulation appear to be almost identical between *Nasonia* and *Drosophila* as described above. Since this similarity is likely due to convergent evolution, it is of interest to compare the molecular patterning processes occurring during this time. We have identified and examined *Nasonia* orthologs of genes known to play a crucial role in DV patterning in other insects, and examined their expression to understand how the mesoderm (ventral region), ectoderm (lateral regions) and extraembryonic membranes (dorsal region) are specified and patterned.

Dynamic gene expression on the ventral side

Two transcription factors, Twist and Snail, are critical factors both in patterning the *Drosophila* DV axis and in specifying the ventral most tissue, the mesoderm (Leptin, 1991). Both of these transcription factors are direct targets of Dorsal, and are expressed in broad overlapping stripes that are initiated weakly and slightly narrower than their broad, largely overlapping final domains (Fig. 1A″–C″).

Orthologs of these genes were cloned, and their expression was observed in the blastoderm embryo of *Nasonia*. Like their fly counterparts, both of these genes are expressed ventrally. However the dynamics of their patterns over time are distinct. Both *Nv-twi* and *sna* are initially detected at cycle 11 in very narrow stripes covering 3–4 ventral nuclei (Fig. 1D″). Over the course of cycle 11, *Nv-twi* and *sna* expression domains expand more or less in concert (Fig. 1E″), until they reach their finally width (16–17 nuclei) and take on their characteristic "slug" shape in cycle 12 (Fig. 1F″). We do not observe any major differences between patterns of *Nv-sna* and *twi* expression during the dynamic or final domain stages, in contrast to the graded *twi* and extremely sharp "on/off" character of *sna* (Fig. 1C and C′) in *Drosophila*. Aside from its expression on the blastoderm, *Nv-sna* is expressed in the yolk nuclei (Fig. 1D″–F″).

Given the apparent dynamic nature of the ventral patterning system in *Nasonia*, it was of interest to compare our wasp results with another system with known dynamic patterning properties: the beetle *T. castaneum*. It is known that the Dorsal gradient and the expression of its early target genes are dynamic in the early *Tribolium* embryo, and it was of interest to determine whether the pattern of simultaneous gene expression in the beetle resembled that of *Nasonia*.

In *Tribolium*, both the temporal and spatial relationship between *Tc-twi* and *Tc-sna* appear to be quite different from that found in either *Nasonia* or *Drosophila*. *Tc-twist* is a very early target of the dynamic Tc-Dorsal gradient, and is first easily detectable as a fairly broad ventral stripe (approximately 9 nuclei wide) expressed over most (Fig. 1G), or the entire length (see Fig. 2G) of the AP axis. This stripe then retracts from the anterior pole, narrows and increases in intensity (Fig. 1H and I). *Tc-sna* expression is not detectable in the early stages of development (Fig. 1G′), and was only seen after *Tc-twi* expression retracts from the anterior pole (Fig. 1H′). *Tc-sna* is not only expressed later, but it is initially expressed in a domain that is significantly narrower than the concurrent *Tc-twi* domain (Fig. 1H″). Prior to gastrulation the *Tc-sna* domain becomes nearly coincident with the slightly broader *Tc-twi* domain (Fig. 1I″).

In the course of our analysis of DV marker genes in *Nasonia*, we unexpectedly observed that the temporal and spatial pattern of *Nv-sim* early expression resembled strongly those of *Nv-sna* and *twi*. The *Nv-sim* stripe starts narrowly, just as the *Nv-sna* and *twi* stripes do (Fig. 2D″, S2E″), and undergoes expansion and refinement as well. The *Nv-sim* domain is consistently wider than both the *Nv-twi* and *Nv-sna* domains, but is largely coexpressed with the other two markers during cycle 11 and a portion of cycle 12 (Fig. 2D″ and E″). In the latter portion of cycle 12 *Nv-sim* begins to clear ventrally (Fig. 2F″, S2F″). The end result of this clearing is that *Nv-sim* is no longer co-expressed at any position with *Nv-twi* or *Nv-sna*, and is found in stripes of 1–2 cells wide flanking the domains of the mesodermal genes (Fig. 2F″, S2H″). After gastrulation, these stripes will constitute the leading edge of the migrating ectoderm, and eventually fuse, forming the ventral midline (Fig. S3A and B).

The early and dynamic expression of *Nv-sim* is in stark contrast to the pattern of *sim* expression in *Drosophila*. Here, *sim* is not detected prior to cycle 14 (Fig. 2A′), and is initially expressed only in a posterior domain (Fig. 2B′). Only after *sna* and *twi* achieve their final domains, is striped *sim* expression observed (Fig. 2C″, S2C″). Theses stripes emerge somewhat gradually in the cells directly adjacent to the lateral edges of the *sna* domain (Fig. 2B′, S2C′).

The *Tribolium* mode of generating *sim* stripes contains elements of both the *Nasonia* and *Drosophila* systems, but also differs from both. Like *Drosophila*, *Tc-sim* expression is initiated well after the first appearance of a ventral *Tc-twi* domain (Fig. 2G″). Like *Nasonia*, *Tc-sim* appears at a slightly later stage and is expressed in a stripe that is slightly broader than, and completely covering the *Tc-twi* domain (Fig. 2H″). Later, *Tc-sim* is repressed in the most ventral regions, leading to the production of two stripes of 1–4 cells wide flanking the mesoderm (Fig. 2I″). The clearing of *Tc-sim* from the ventral region seems to be correlated with the onset of *Tc-sna* expression (Fig. S2K″–M″), in contrast to *Nasonia*, where *Nv-sim* and *Nv-sna* are initially completely overlapping ventrally (Fig. S2E).

In *Tribolium*, the *cactus* gene was an important marker that gave great insight into how the dynamic, self-regulatory DV patterning system functions in the beetle embryo. It is initially expressed very broadly, then narrows progressively over time, mimicking the pattern of nuclear Tc-Dorsal (Nunes da Fonseca et al., 2008). Given the apparent dynamic nature of ventral patterning in *Nasonia*, as indicated by the behavior of *Nv-twi*, *Nv-sna*, and *Nv-sim*, it was of interest to determine how the

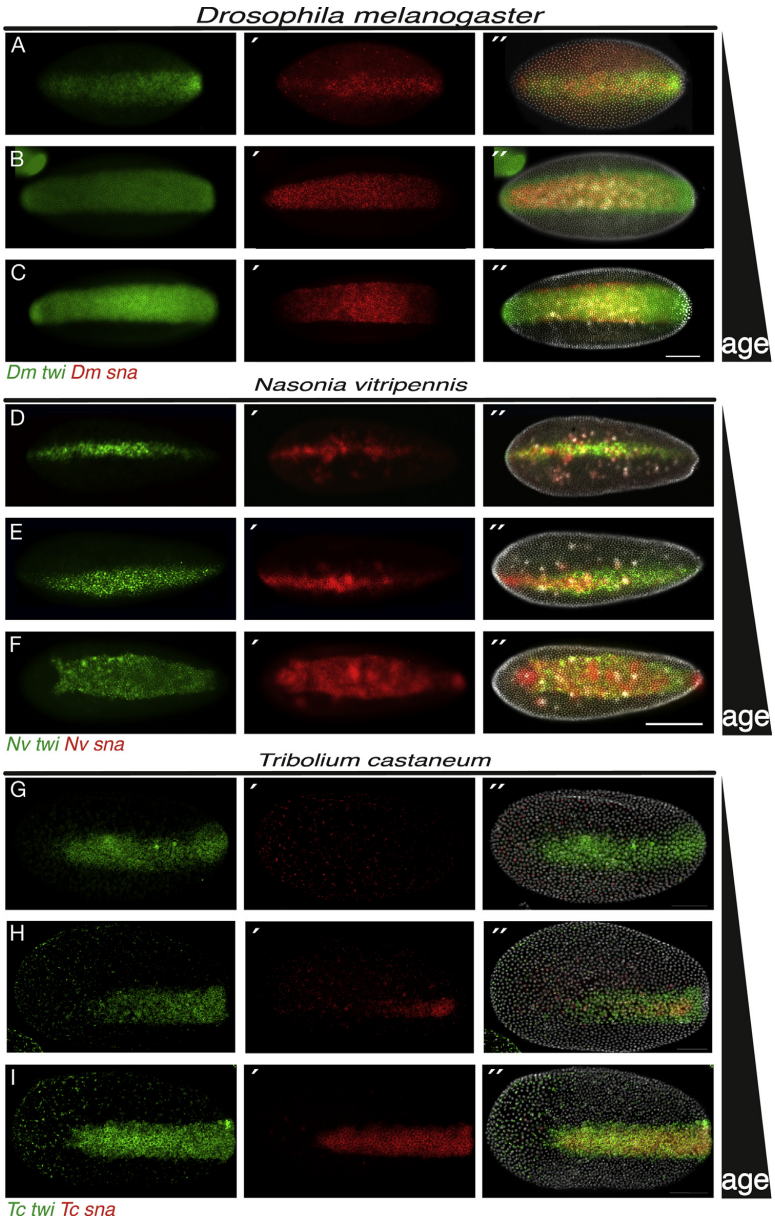

Fig. 1. Simultaneous detection of *twist* and *snail* in *Nasonia*, *Drosophila* and *Tribolium* embryos. (A)–(C″) Ventral views of *Drosophila* embryos in cycle 13 (A)–(A″) and cycle 14 (B)–(C″) comparing *Dm-twi* (A)–(C) and *Dm-sna* (A′)–(C′). Overlays with DAPI (white) (A″)–(C″). (D)–(F″) Ventral views of *Nasonia* embryos in cycle 11 (D)–(E″) and cycle 12 (F)–(F″) comparing *Nv-twi* (D)–(F) with *Nv-sna* (D′)–(F′). Overlays with DAPI (white) (D″)–(F″). (G)–(I″) Ventral views of *Tribolium* embryos in undifferentiated blastoderm (G)–(G″), early differentiated blastoderm (H)–(H″) and late differentiated blastoderm (I)–(I″) comparing *Tc-twi* (G)–(I) and *Tc-sna* (G′)–(I′) expression. Overlays with DAPI (white) (G″)–(I″). Embryos in panels (A″), (D″), (E″), and (G″) are at an equivalent developmental stage (penultimate nuclear division before gastrulation). Embryos in (B″), (C″), (F″), (H″), and (I″) are also at an equivalent stage in the last division directly preceding gastrulation. Scale bar 100 μm. Anterior is left.

Nasonia cactus gene behaves in the early embryo, as it could provide insight into the potential for feedback regulation in the *Nasonia* embryo.

In *Nasonia* there are three *cact* paralogs tandemly arrayed in the genome. Only one of these (XM_001602977) is differentially expressed along the DV axis. In the early stages, (cycle 11) this gene is expressed in a narrow ventral stripe (Fig. 3A′), similar to the early narrow stripes of *Nv-twi, sna*, and *sim* (Fig. 1D–D′, Fig. 2D–D′). In contrast to the other *Nasonia* ventral genes, the *Nv-cact1* expression domain does not expand over the course of development

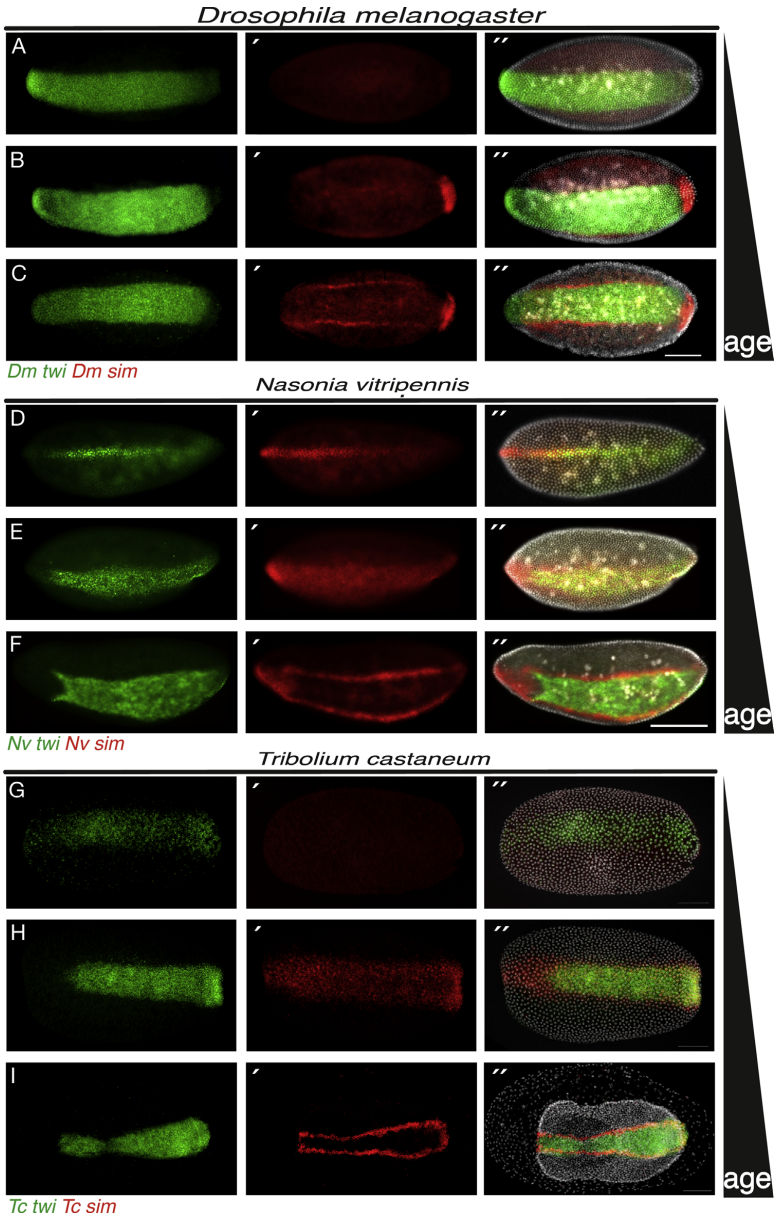

Fig. 2. Simultaneous detection of *twist* and *single-minded* in *Nasonia*, *Drosophila* and *Tribolium* embryos. (A)–(C″) Ventral views of *Drosophila* embryos in cycle 14 (A)–(A″) and (B)–(B″) and at initiation of gastrulation (C)–(C″) comparing *Dm-twi* (A)–(C) and *Dm-sim* (A′)–(C′). Overlays with DAPI (white) (A″)–(C″). (D)–(F″) Ventral views of *Nasonia* embryos in cycle 10 (D)–(D″), cycle 11 (E)–(E″) and cycle 12 (F)–(F″) comparing *Nv-twi* (D)–(F) and *Nv-sim* (D′)–(F′). Overlays with DAPI (white) (D″)–(F″). (G)–(I″) Ventral views of *Tribolium* embryos in undifferentiated blastoderm (G)–(G″), start of primitive pit formation (H)–(H″) and before serosal window closes (I)–(I″) comparing *Tc-twi* (G)–(I) and *Tc-sim* (G′)–(I′). Overlays with DAPI (white) (G″)–(I″). Embryos in (A″), (B″), (F″), (H″) are at equivalent stages, while (D″), (E″), and (G″) are at earlier stages, and (C″) and (I″) are at later (post-gastrulation) stages. Scale bar 100 μm. Anterior is left.

(Fig. 3B′). Rather, the narrow stripe disappears, leaving two terminal spots at each of the AP poles, during cycle 12, prior to gastrulation (Fig. 3C′). Thus unlike *Tc-cact*, *Nv-cact* is not dynamic in early development, which may have implications for the nature of the Dorsal gradient behavior in *Nasonia*.

Lateral markers

The specification and pattern of the neurogenic ectoderm is another function of DV pattering in insect embryos. In *Drosophila*, genes involved in this process are typically expressed in symmetric

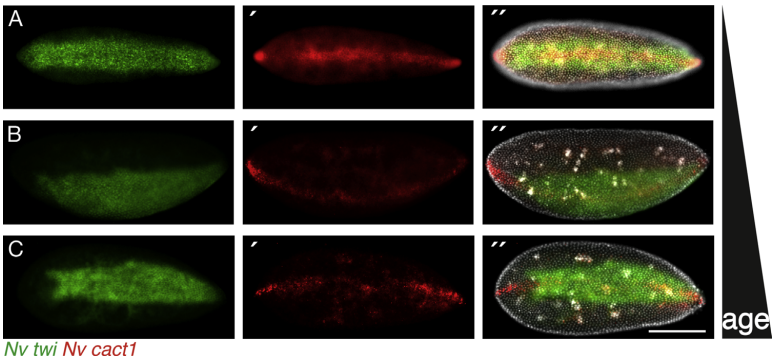

Fig. 3. Characterization of the expression and dynamics of *cact* in *Nasonia*. (A)–(A″) Ventral view of a *Nasonia* embryo in cycle 11 comparing *Nv-twi* (green) and *Nv-cact1* (red) and DAPI (white). (B)–(B″) Ventro-lateral view of a *Nasonia* embryo in cycle 12 comparing *Nv-twi* (green) and *Nv-cact1* (red) and DAPI (white). (C)–(C″) Ventral view of a *Nasonia* embryo in late cycle 12 comparing *Nv-twi* (green) and *Nv-cact1* (red) and DAPI (white). Scale bar 100 μm. Anterior is left. (For interpretation of the references to color in this figure legend, the reader is referred to the web version of this article.)

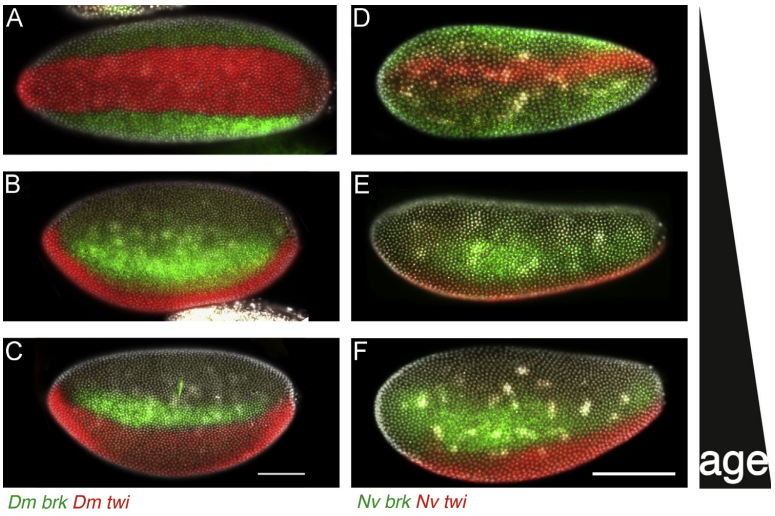

Fig. 4. Comparison of *brinker* expression dynamics in *Drosophila* and *Nasonia*. (A) Ventral, and (B) and (C) lateral views of *Drosophila* embryos comparing *Dm-brk* (green) mRNA and *Dm-twi* (red) expression with DAPI (white) in *Drosophila* during cycle 14. (D) Ventral, and (E) and (F) lateral views of *Nv-brk* mRNA expression with DAPI (white) in cycle 10 (D), cycle 11 (E) and cycle 12 (F) in *Nasonia*. Scale bar 100 μm. Embryos arranged from youngest to oldest from top to bottom in each species panel. Anterior is left. (For interpretation of the references to color in this figure legend, the reader is referred to the web version of this article.)

lateral stripes, reflecting their activation by low to moderate levels of nuclear Dorsal, as well as repression on the ventral side by Snail. Here three markers of differential fates within the neuroectoderm were examined in *Nasonia*: *ventral neuroblasts defective (vnd)*, *intermediate neuroblasts defective (ind)* and *muscle segment homeobox (msh)* (Von Ohlen and Doe, 2000). In addition, an important specifier of general neuroectoderm fate, *brinker (brk)* was also examined in the wasp.

In *Drosophila*, *brk* (Jaźwińska et al., 1999) is expressed in two lateral stripes with sharp ventral borders adjacent to the mesoderm and with relatively fuzzy dorsal borders extending into the region of the dorsal neurogenic ectoderm (Fig. 4A and B). This pattern is somewhat dynamic, being initially broad (Fig. 4A and B), narrowing early in cycle 14 (Fig. 4C), then expanding again just prior to gastrulation (not shown, (Jaźwińska et al., 1999)).

In *Nasonia*, *Nv-brk* is the only neurogenic gene examined that shows expression at the time when the ventral markers (e.g., *Nv-twi*) are expressed in early, very narrow stripes (Fig. 4D). At this stage *Nv-brk* is expressed in broad ventro-lateral domains with relatively fuzzy borders on both the ventral and dorsal edges, and is excluded from the domain of the ventral markers (Fig. 4D). As the embryo ages and the expression domain of *Nv-twi* expands, *Nv-brk* expression is correspondingly cleared from the ventral side (Fig. 4E). During this time, the dorsal border of the *Nv-brk* domain becomes more defined, until the domains of *Nv-twi* and *Nv-brk* are very similar to their counterparts in *Drosophila* (Fig. 4C and F).

The neurogenic ectoderm in *Drosophila* is subdivided by a set of factors known as the columnar genes (*vnd*, *ind*, and *msh*, listed in order of expression from ventral to dorsal). *vnd* is a direct target of the Dorsal gradient, is expressed in stripes of 7–8 nuclei (Jiménez et al., 1995) that lie just dorsally to the stripes of sim expression, and its expression is stable at the blastoderm stage. Expression can be detected early in cycle 14 in stripes that correspond well with the AP and DV extent of the final domain prior to gastrulation

(Fig. 5A). These stripes intensify and become more refined in the time approaching gastrulation (Fig. 5B and C).

ind is expressed just dorsal of *vnd*, in a stripe of approximately the same width, and with limited dynamics (Fig. 5B and C). Like *vnd*, *ind* expression is initiated in a stripe that is complete along the AP axis (Fig. 5B). *ind* initiation occurs later than *vnd*, as we have observed multiple embryos with *vnd* stripes lacking the *ind* domain (Fig. 5A).

In *Nasonia*, the final domain of *Nv-vnd* is also in the form of two broad stripes directly dorsal to the *Nv-sim* domain (not shown). Unlike *Drosophila vnd* and *Nv-brk*, the *Nv-vnd* domain appears relatively late in embryogenesis, just prior to gastrulation. In addition, *Nv-vnd* expression is dynamic with respect to the AP axis. It is first observed at the anterior in stripes extending to approximately 40% egg length (Fig. 5D). These stripes progressively lengthen over time, finally extending to the posterior pole of the embryo just prior to the initiation of gastrulation (Fig. 5E and F, S3C). During gastrulation, *Nv-vnd* marks most of the ectoderm that migrates over the mesoderm (Fig. S3D). Once gastrulation is completed, *Nv-vnd* is expressed in two stripes flanking the ventral midline (S3E).

Nv-ind is initiated later than *Nv-vnd*, and is first detected after the *Nv-vnd* stripe has extended most of the way toward the posterior pole (Fig. 5E). Like *Nv-vnd*, *Nv-ind* expression is also

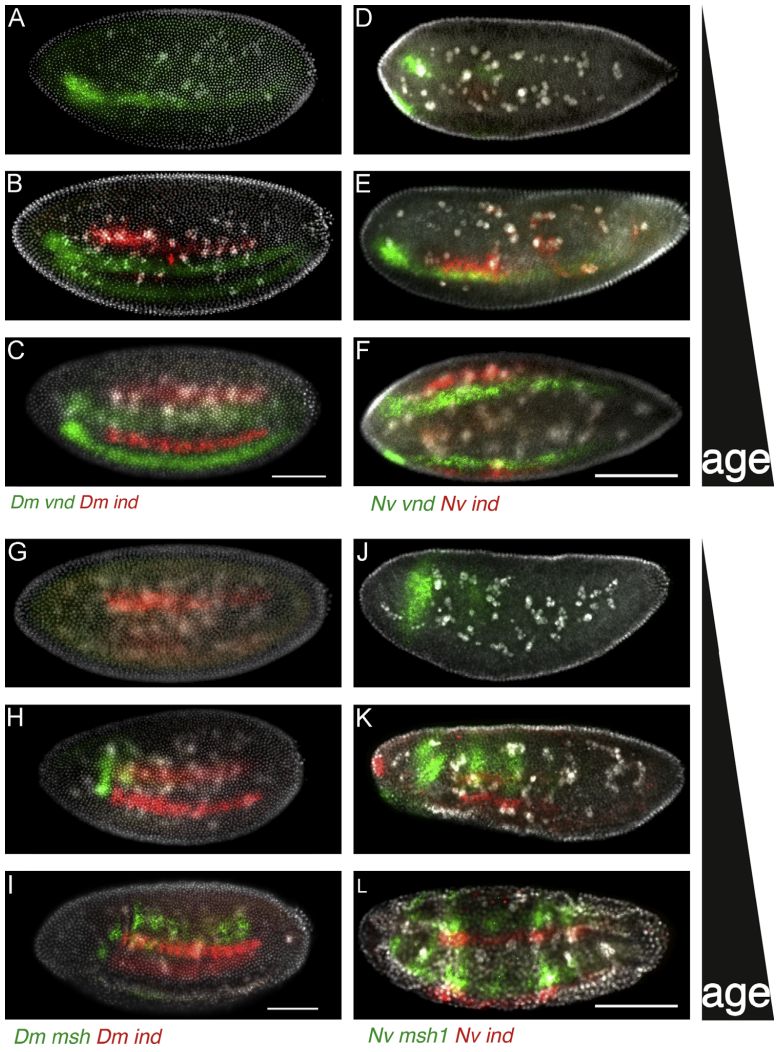

Fig. 5. Comparsion of columnar gene dynamics in *Drosophila* and *Nasonia*. (A)–(C) Lateral views of *Drosophila* embryos in cycle 14 comparing *Dm-vnd* (green) and *Dm-ind* (red) mRNA expression with DAPI (white) in *Drosophila*. (D) and (E) Lateral and (F) ventral views of *Nasonia* embryos in cycle 11–12 comparing *Nv-vnd* (green) and *Nv-ind* (red) mRNA expression with DAPI (white) in *Nasonia*. (G)–(I) Lateral views of *Drosophila* embryos in cycle 14 (G) and (H) and early gastrulating embryo (I) comparing *Dm-msh* (green) and *Dm-ind* (red) mRNA expression with DAPI (white). (J)–(L) Lateral views of *Nasonia* embryos in cycle 11–12 (J), early gastrulation (K) and ongoing gastrulation (L) comparing *Nv-msh1* (green) and *Nv-ind* (red) mRNA expression with DAPI (white). Scale bar 100 μm. Embryos arranged from youngest to oldest from top to bottom in each species panel. Anterior is left. (For interpretation of the references to color in this figure legend, the reader is referred to the web version of this article.)

initially restricted to the anterior portion of the embryo, and then extends over time toward the posterior pole (Fig. 5E, F, K and L). This process of extension is not completed until after gastrulation has been initiated at the anterior of the embryo.

The most dorsally expressed of the *Drosophila* columnar genes is *msh*, which is initiated still later than *ind* (Fig. 5G). The first evidence of *msh* expression is in the form of a stripe in the head region of the embryo, that extends ventrally in nuclei just anterior to the *ind* domain (Fig. 5H). Subsequently to this, a segmentally modulated stripe of *msh* appears dorsally to the *ind* domain (Fig. 5I). Again this stripe appears all at once, with no detectable AP progression.

As is the case in *Tribolium*, there are two msh-like genes in the *Nasonia* genome (Wheeler et al., 2005; Nunes da Fonseca et al., 2008). Only one of these genes is expressed in a columnar pattern in *Nasonia*, and we refer to this gene as *Nv-msh1*. *Nv-msh1* expression shares characteristics with both fly msh expression, and with the other *Nasonia* columnar genes, but also exhibits some differences. The first evidence of *Nv-msh1* is a stripe covering the dorsal part of the embryonic head anlage, quite similar to that seen in the fly (Fig. 5J). At the time of the appearance of this stripe, a second stripe can be seen arising toward the posterior. This indicates that the initiation of the neurogenic ectoderm domain of *Nv-msh1* occurs prior to the onset of *Nv-ind*, which is in contrast to the pattern observed for both *Drosophila* and *Tribolium ind* and *msh* (Fig. 5K) (Von Ohlen and Doe, 2000; Wheeler et al., 2005). Over time, the full *Nv-msh1* expression domain appears progressively, again, from anterior to posterior, in segmental blocks (Fig. 5K). The full extent of the *Nv-msh1* domain is not completed until well after the initiation of gastrulation (Fig. 5L).

Complexity of dorsal ectodermal and extraembryonic patterning

In *Drosophila* a set of genes is expressed in the dorsal part of the embryo that is used to pattern and differentiate the dorsal ectoderm and amnioserosa (the single extraembryonic tissue in the fly embryo) (Ashe et al., 2000). The novelty of the higher dipteran amnioserosa (Schmidt-Ott, 2000) makes a comparison to *Nasonia* dorsal genes significant, as this wasp which exhibits an independently derived mode of long germ embryogenesis, but has been proposed to posses the ancestral complement of extraembryonic tissues (amnion+serosa) (Bull, 1982; Fleig and Sander, 1988). These two tissues have been described to arise from a narrow dorsal domain that is more similar to the fly amnioserosal anlage than to the typical pattern for amnion and serosa specification found in short and intermediate germ insects, such as *Tribolium* (Van der Zee et al., 2005).

The homeodomain transcription factor *zerknuellt* (*zen*) is a highly conserved marker of extraembryonic fate throughout the insects so far examined (Falciani et al., 1996; Dearden et al., 2000; Panfilio et al., 2006). In *Drosophila* it is initially expressed in a very broad domain covering most of the dorsal side of the embryo (Fig. S4A′). This broad domain later resolves into a narrow stripe that corresponds to the future amnioserosal cells (Fig. S4B′ and C′) (Rushlow et al., 1987).

Drosophila zen is part of a BMP signaling dependent gene regulatory network that produces different threshold outputs of gene expression on the dorsal half of the embryo, which leads to the patterning and subdivision of the amnioserosa and dorsal ectoderm. Genes such as *pannier* (*pnr*) are expressed in broad domains covering most of the dorsal surface of the embryo, and respond to the lowest threshold levels of BMP signaling+zen

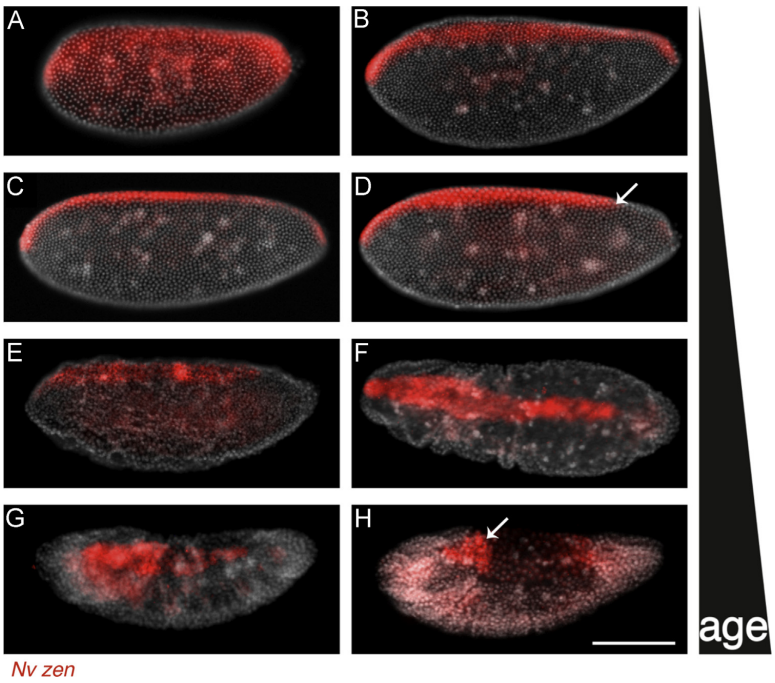

Fig. 6. Dynamics of *Nv-zen* expression in *Nasonia* embryos. (A)–(E) Lateral and (F)–(H) dorso-lateral views of *Nasonia* embryos expressing *Nv-zen* with DAPI (white) in cycle 9 (A), cycle 12 (B)–(D), initiation of gastrulation (E), continuation of gastrulation (F), onset of germ band extension (G) and completion of germ band extension (H). Arrow in D indicates retraction of *Nv-zen* on the posterior pole. Arrow in H indicates *Nv-zen* expression in anterior portion of the serosa. Scale bar 100 μm. Anterior is left.

(Fig. S5A′–C′). Genes such as *tail-up* (*tup*) and *dorsocross* (*doc*) respond to moderate to high levels of BMP+Zen (Fig. S6B and C). Peak levels of BMP signaling are required to activate a third class of genes that includes genes such as *RACE* and *hindsight* (*hnt*) (Fig. S4A–C). In other insects, many of these have conserved roles in the amnion and/or serosa (Van der Zee et al., 2006; Goltsev et al., 2007; Rafiqi et al., 2010). We have cloned and analyzed orthologs of the above mentioned genes from *Nasonia* in order to understand the patterning and tissue specification of the extraembryonic membranes and dorsal ectoderm of the wasp.

Nasonia zen, like its *Drosophila* ortholog is expressed in a narrow stripe over the dorsal midline in the last nuclear cycle before gastrulation. *Nv-zen* is one of the earliest detectable dorsal genes in the embryo. We have detected it in cycle 9 where it is weakly expressed in a rather broad domain (Fig. 6A). In the next cycle, the *Nv-zen* domain is found in a narrow stripe with fuzzy borders that extends from the extreme anterior to posterior pole (Fig. 6B). After the 12th nuclear division, the *Nv-zen* stripe further refines, gains sharp borders and retracts from the posterior pole (Fig. 6C and D). After gastrulation, *Nv-zen* expression is initially strong, then progressively reduced in the presumptive serosa, with strong staining remaining only in the anterior portion of the tissue (Fig. 6E–H).

RACE has a strong requirement both for peak levels of BMP signaling, and for the late phase of narrow zen expression to be fully expressed in the *Drosophila* embryo (Ashe et al., 2000). To determine whether a similar gene regulatory network may be operating in the *Nasonia* embryo, we cloned the *Nasonia* ortholog of this gene, and examined its expression. *Nv-RACE* appears late relative to *Nv-zen*, just before gastrulation, in a stripe that mostly overlaps the *Nv-zen* domain (Fig. 7A″). After gastrulation, *Nv-RACE* expressing cells of the serosa break their epithelial continuity with ectodermal cells, and spread over the surface of the embryo (Fig. S7). The function of RACE in the fly amnioserosa is not clear, but our results indicate that this factor was included in the extraembryonic GRN in the common ancestor of the holometabolous insects.

Another high level target of the BMP+Zen GRN in *Drosophila* is hnt. This gene is expressed in a narrow stripe similar in width to the zen domain, but restricted to the posterior half of the embryo (Fig. S4C″). *Nv-hnt* is unique among the DV genes examined so far. It is initially detected ubiquitously in embryos at cycle 11 (Fig. 7B) and earlier stages (not shown). In cycle 12, most of the transcript disappears leaving a continuous stripe covering both the ventral and dorsal midlines (Fig. 7C). Eventually, the ventral half of this ring disappears, and what remains is a dorsal narrow stripe that corresponds exactly with the *Nv-zen* domain (Fig. 7D″). Again, this gene remains expressed in the presumptive serosa after gastrulation (not shown).

We examined two *Nasonia* orthologs of genes that respond to moderate levels of BMP+*Zen*, *Nv-tup* and *Nv-doc*. *tup* is expressed in a moderately broad stripe in *Drosophila*, similar to that of *doc*. In the wasp, however, the *Nv-tup* expression is quite dynamic, and rather different from *Nv-doc*. *Nv-tup* is first detected in spot-like domains just anterior and posterior to the *Nv-zen* expression stripe, just prior to gastrulation (Fig. 8A). As gastrulation proceeds, and the presumptive serosa begins to expand, *Nv-tup* expression becomes localized to the lateral margins of the serosal region, which may represent the Nasonia amnion (Fig. 8B and C).

Nv-doc also has a rather complex expression pattern in *Nasonia* (Fig. 8D and F). Dorsally, the *Nv-doc* stripe is variable in width. It is broader than the *Nv-zen* domain anteriorly (Fig. 8E″). Starting at about 50% egg length, the *Nv-doc* domain gets narrower than the *Nv-zen* domain. Then, close to the posterior pole, it is wider again. In addition, its domain extends over the extreme anterior pole of the embryo and continues on the ventral side in the presumptive head region (Fig. 8E), unlike most of the dorsally expressed genes that we have examined. This stripe terminates in a broad domain on the ventral side (Fig. 8F).

We next describe the expression of *Nv-pnr*, whose *Drosophila* ortholog is expressed broadly, covering most of the dorsal surface of the embryo (Fig. S5A′). Just before gastrulation, *Nv-pnr* is expressed in a very broad domain straddling the dorsal midline, and extending several cell rows wider than *Nv-zen* (Fig. 9A″ and B″).

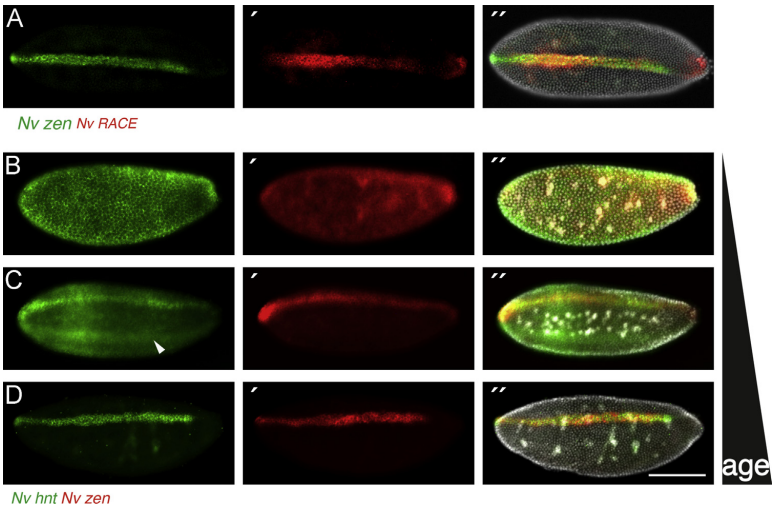

Fig. 7. Dynamics of *Nv-RACE* and *Nv-hnt* in relation to those of *Nv-zen*. (A)–(A″) Dorsal view of a *Nasonia* embryo between cycle 11 and 12 comparing *Nv-zen* (green) and *Nv-RACE* (red) expression with DAPI (white). (B)–(B″) Lateral view of a *Nasonia* embryo in cycle 11–12 comparing *Nv-hnt* (green) and *Nv-zen* (red) expression with DAPI (white). (C)–(C″) Dorso-lateral view of a *Nasonia* embryo in cycle 11 comparing *Nv-hnt* (green) and *Nv-zen* (red) expression with DAPI (white). Note the ventral stripe of *Nv-hnt* is still discernable (arrowhead in C), despite being out of focus. Dorsal view of a *Nasonia* embryo in cycle 12 comparing *Nv-hnt* (green) and *Nv-zen* (red) expression with DAPI (white). Scale bar 100 μm. Anterior is left. (For interpretation of the references to color in this figure legend, the reader is referred to the web version of this article.)

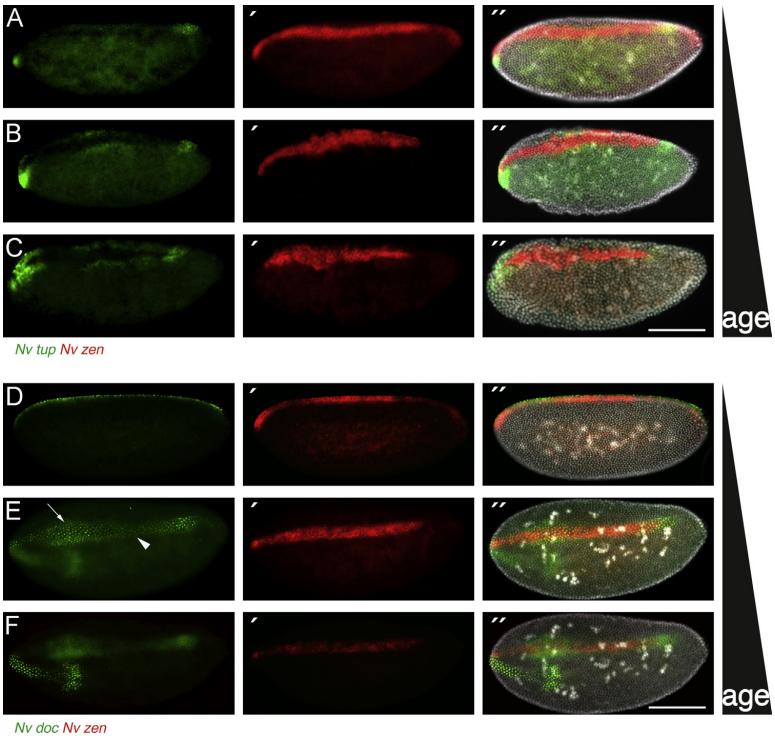

Fig. 8. Dynamics of *Nv-tup* and *Nv-doc* in relation to those of *Nv-zen*. (A″)–(C″) Lateral views of *Nasonia* embryos in cycle 11 (A″), at initiation of gastrulation (B″) and completion of gastrulation (C″) comparing *Nv-tup* (A)–(C) and *Nv-zen* (A′)–(C′) with DAPI (white). (D)–(D″) Lateral view of a *Nasonia* embryo in cycle 11 comparing *Nv-doc* (green) and *Nv-zen* (red) with DAPI (white). (E″)–(F″) Ventro-lateral views of a *Nasonia* embryo in cycle 11–12 comparing *Nv-doc* (green) and *Nv-zen* (red) with DAPI (white) focusing on the dorsal side (E)–(E″) and ventral side (F)–(F″). Arrow in E indicates broadened area of *Nv-doc* expression, arrowhead in E indicates narrowed area. Scale bar 100 μm. Anterior is left. (For interpretation of the references to color in this figure legend, the reader is referred to the web version of this article.)

As development proceeds, *Nv-pnr* is cleared from the presumptive serosal region, and flanks the expanding *Nv-zen* domain in a very similar way to *Nv-tup* (Fig. 9C″).

Finally, we examined the expression of the single *Nasonia* ortholog of the *Drosophila iro-c* genes *araucan/caupolican* (referred to here as *Nv-ara*). In the fly, these genes are expressed late in the dorsal ectodermal region, but the single *Tribolium* ortholog (referred to as *Tc-iroquois*) has served as a useful marker for the amnion (Nunes da Fonseca et al., 2010). *Nv-ara* expression is first detected in two broad patches toward the posterior end of the embryo that flank the domain of *Nv-zen* (Fig. 9D″). As the embryo nears gastrulation, the stripe-like expression extends anteriorly, until the *Nv-ara* domain completely flanks the presumptive serosa, with the stripes being narrow at the anterior, and becoming quite broad at the posterior (Fig. 9E″). After gastrulation, *Nv-ara* refines to two broad, even stripes flanking the serosa (Fig. 9F″).

Discussion

With our analyses of time lapse movies and DAPI stainings in *Nasonia* embryos, we have shown that in general the cellular processes leading up to gastrulation are quite similar, with some interesting differences, between *Nasonia* and *Drosophila*. In our gene expression analyses, we have uncovered points of strong convergence between these embryos, and also cases of major divergence between them in the three main DV domains (ventral (mesoderm), lateral (ectoderm), dorsal (extraembryonic)).

Ventral side

One of our striking results is the observation that the expression of *Nv-cact1*, *twi*, *sna*, and *sim* all start out as very narrow stripes at the ventral midline. The latter three expand over time until they reach their full domains, while *Nv-cact* remains the same width until it is cleared from most of the ventral side. This result gives some insights into the patterning system operating in the *Nasonia* blastoderm embryo. First, it appears that there is a very restricted peak of initial gene activation in early (cycle 11) embryos, covering only a few nuclei at the ventral midline. The sharp edges of these early stripes indicate that the activation is either very steeply graded with a sharp peak at the ventral side, or that these target genes are exquisitely sensitive to specific threshold levels of activation that are only present in this region (or a combination of both). This differs from *Drosophila*, where the early DV regulated domains of *twi* and *sna* are only slightly narrower, weaker, and more graded than their mature domains, likely reflecting the increasing amplitude of the broad, stably shaped nuclear Dorsal gradient (Liberman et al., 2009).

The expansion of the *Nv-twi*, *sim*, and *sna* domains from their initial very narrow domains to their broad, final shape indicates that the ventral patterning GRN has strong dynamic, and possibly self-regulatory, properties. In this respect, the *Nasonia* system has

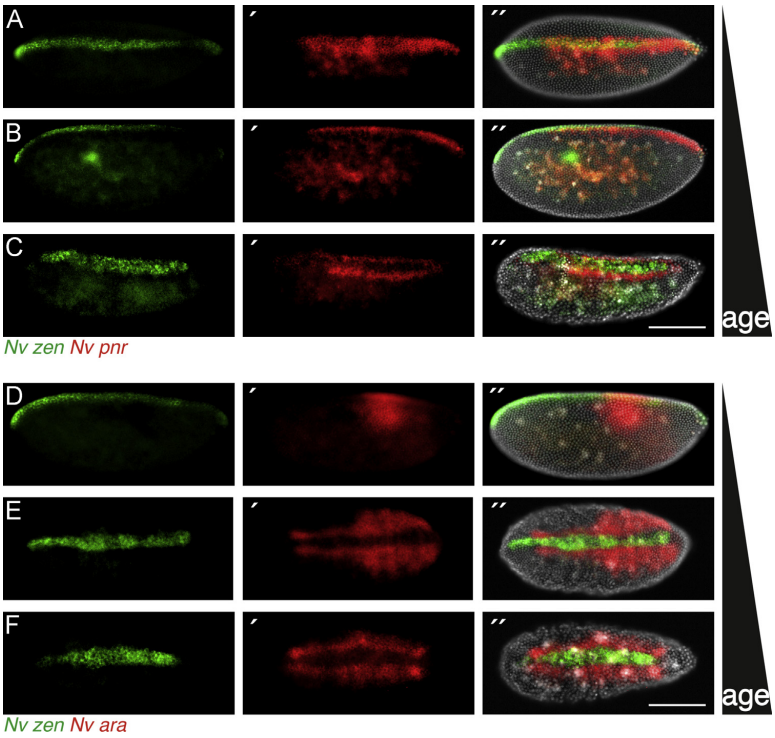

Fig. 9. Dynamics of *Nv-pnr* and *Nv-ara* expression in relation to those of *Nv-zen*. (A)–(A″) Dorsal view of a *Nasonia* embryo in cycle 11 comparing *Nv-zen* (green) and *Nv-pnr* (red) with DAPI (white). (B)–(B″) Lateral view of a *Nasonia* embryo in cycle 12 comparing *Nv-zen* (green) and *Nv-pnr* (red) with DAPI (white). (C)–(C″) Dorso-lateral view of a *Nasonia* embryo in continuation of gastrulation comparing *Nv-zen* (green) and *Nv-pnr* (red) with DAPI (white). (D)–(D″) Lateral view of a *Nasonia* embryo in cycle 11 comparing *Nv-zen* (green) and *Nv-ara* (red) with DAPI (white). (E)–(E″ and F)–(F″) Dorsal view of *Nasonia* embryos in continuation of gastrulation comparing *Nv-zen* (green) and *Nv-ara* (red) with DAPI (white). Scale bar 100 μm. Embryos arranged from youngest to oldest from top to bottom in each species panel. Anterior is left. (For interpretation of the references to color in this figure legend, the reader is referred to the web version of this article.)

more in common with that of *Tribolium* than with *Drosophila*. In *Tribolium*, a self-regulatory loop composed of components and direct targets of the Toll signaling pathway leads to a dynamic source of DV patterning information in the form of a gradient of nuclear Dorsal that progressively narrows over the course of embryonic development (Nunes da Fonseca et al., 2008). In contrast, while there is quite some crosstalk among Dorsal target genes in the process of refinement of their domains, the *Drosophila* system does not appear to have significant dynamic self-regulatory properties downstream of Toll activation.

While the apparent use of a highly dynamic, and self-regulatory system for patterning the ventral side appears to be conserved between *Tribolium* and *Nasonia*, it is clear that the regulatory mechanism responsible for these features are not the same. In *Tribolium*, the changes in dynamic ventral genes such as *Tc-twist* are due to the shrinking and refinement of the Dorsal nuclear gradient toward the ventral side. In *Nasonia*, the changes in gene expression domains proceeds in the opposite direction, from narrow to broad.

At present it is not clear at which level the dynamic behavior of ventral genes in the *Nasonia* embryo is generated. Preliminary evidence indicates that Toll signaling is required for the activation of ventral genes in *Nasonia* (in preparation), so one explanation could be that the Dorsal gradient is itself dynamic in *Nasonia*. Other possibilities include the presence of feed-forward or feed-back interactions among ventrally expressed genes. A more complete characterization of all of the genes expressed in the ventral region, the distribution of protein products, and the functional connections among genes expressed in this region, are needed to differentiate among these possibilities.

Our analyses also provide insights into the evolution of *sim* regulation among the insects. In *Drosophila*, the sim stripes appear very late in embryogenesis, and seem to arise de novo in a single row of cells flanking the presumptive mesoderm (Fig. 2A′–C′). The pattern is very different in *Nasonia*, where *Nv-sim* appears simultaneously with *Nv-twi* and *sna* in a stripe that is narrow, but noticeably broader than the expression of *Nv-twi* and *sna*. The *Nv-sim* stripe remains broader than *Nv-sna* and *twi* and is largely coexpressed with them throughout most of blastodermal development. Only toward the end of cycle 12 is *Nv-sim* finally cleared from the ventral side of the embryo, leading to the production of two stripes that in the end cover a single row of nuclei flanking the mesoderm (Fig. 2D″–F″, S2E″–H″).

A similar pattern is seen in *Tribolium*, where *Tc-sim* is a relatively early target of the Tc-Dorsal gradient, appearing later than *Tc-twist* but before *Tc-snail* (Fig. 2G″, S2I′–J″). The initial domain of *Tc-sim* is similar to that of its *Nasonia* counterpart, in that it initially covers the ventral side of the embryo in an unbroken domain, and persists in being coexpressed with *Tc-sna* for a significant period of time, before being cleared from the ventral side at the onset of gastrulation (Fig. S2I″–M″). Thus, an early broad stripe of *sim* expression is likely ancestral for at least the holometabolous insects.

Lateral genes

Nv-brk is the first of the lateral genes to be expressed, and appears at about the same time as the early, narrow stripes of *Nv-twi*, sim and *sna* (Fig. 4D). This indicates that *Nv-brk* might have an important role in the early interpretation and further refinement of positional information in the *Nasonia* embryo.

Our results also raise an interesting question about the origin of the use of *brinker* in insect embryonic patterning, since *brinker* is not expressed in the embryo of *Tribolium*. (R.N. da Fonseca, personal communication). Thus, either embryonic *brinker* was present in the common ancestor of the Holometabola, and was lost in the beetle lineage, or it was independently recruited for DV patterning in the wasp and fly lineages.

In contrast to the early expression of *Nv-brk*, genes involved in the partitioning of the neurogenic ectoderm are expressed relatively late in embryogenesis, at about the time just preceding gastrulation. The first of these to appear is *Nv-vnd*, which is the ventral-most of the columnar genes. Unlike the fly *vnd* domain, the *Nv-vnd* domain is initially incomplete along the AP axis, and is only present in presumptive thoracic regions (Fig. 5D). As development progresses, this stripe extends to the posterior end of the embryo, just as the morphogenetic movements of gastrulation are beginning (Fig. 5E and F). *Nv-ind* and *msh1* columnar expression is initiated later, and again in an anteriorly restricted pattern, at a stage where *Nv-vnd* is extended most of the way to the posterior pole (Fig. 5F and K). Thus, there appear to be two temporal gradients of gene activation that affect columnar gene expression: one along the DV axis and one along the AP axis.

Another potentially useful marker for ectoderm fate would have been *short-gastrulation (sog)*, which is a BMP inhibitor, and responds to the lowest levels of nuclear Dorsal in the fly embryo (Rusch and Levine, 1996; Reeves and Stathopoulos, 2009). To date we have found no evidence that this gene exists in *Nasonia*. It is absent from all three *Nasonia* genome sequences and was not detected in any of the numerous EST and next generation sequencing projects deposited in Genbank. In addition, we have sequenced the transcriptome of the *Nasonia* embryo between blastoderm formation and gastrulation, and were not able to detect any *sog* expression. Together, these data indicate that *sog* has been lost from the *Nasonia* genome. This may not be so surprising, as *sog* appears to have no role in establishing early polarity in honeybee (Wilson and Dearden, 2011). In addition the other known function of *Drosophila sog* is in patterning the wing veins. These structures are strongly reduced in *Nasonia*, a trait that is diagnostic for the Chalcid family of wasps (Grissell and Schauff, 1990), to which *Nasonia* belongs. Thus, the combination of a loss of a role in embryonic patterning early in hymenopteran evolution (prior to the divergence of *Nasonia* and *Apis* lineages), and the lineage specific reduction in wing veins, may have allowed the loss of *sog* somewhere along the lineage leading to *Nasonia*.

Dorsal side

One of the characteristic features of the insect embryo is the presence of extra-embryonic membranes, which are critical for the protection of the embryo from the environment, and for morphogenetic movements taking place after gastrulation. Insects vary widely in regard to the proportion of the egg surface which is dedicated to the production of these membranes, as well as where these structures are specified within the coordinates of the egg axes. *Drosophila* is one extreme, where the extraembryonic membranes are reduced to a single tissue type (the amnioserosa), which is restricted to the extreme dorsal pole of the embryo. On the other hand, most other insects generate two distinct extraembryonic tissues, the amnion and the serosa. In short germ insects, these tissues typically derive from both anterior and dorsal egg regions (Panfilio, 2008).

At first glance the *Nasonia* embryo looks very much like that of *Drosophila* in terms of its arrangement of, and egg surface area commitment to, extraembryonic membranes. The best known *Drosophila* marker for this tissue, *zen*, is expressed initially in a very broad pattern, which then refines to a narrow stripe at the dorsal midline (Fig. S4A′–C′). A similar pattern is observed for *Nv-zen*, which in a very early division cycle (10) is expressed in a fairly broad domain restricted to the dorsal side of the embryo (Fig. 6A), and very quickly refines to a narrow stripe of about 4 nuclei wide covering the dorsal midline in the next nuclear division cycle (Fig. 6B and C). It is not yet clear whether the same molecular mechanisms for generating the two phases of *zen* expression in the fly (ubiquitous activation+repression by Dorsal, followed by refinement and amplification of BMP signaling) are also employed in *Nasonia*.

The expression patterns of two of our dorsal marker genes give an intriguing insight into the possible mechanisms used to generate DV polarity in the wasp. Both *Nv-hnt* and *Nv-doc* show expression in a stripe that covers the dorsal midline and continues over one or both poles onto the ventral side of the embryo (Fig. 7C, Fig. 8E–F). *Nv-hnt* is particularly striking, since it has a transient stripe completely covering the embryo circumference, before disappearing from the ventral side (Fig. 7C and D). The above observations indicate that there is a shared characteristic of both the dorsal and ventral midlines of *Nasonia* that allows the initial circumpolar expression of *Nv-hnt* and *Nv-doc*, and that breaking of DV asymmetry allows differential expression at the two midlines.

BMP signaling in *Drosophila* has three threshold outputs on the dorsal side of the embryo, with genes such as *RACE* and *hnt* expressed in narrow dorsal domains, genes such as *tup* and *doc* expressed in somewhat broader stripes, while genes such as *pnr* are expressed quite broadly, and can be activated in the presence of low levels of BMP activity (Ashe et al., 2000). We have also found that there are genes expressed very narrowly (*Nv-RACE, Nv-hnt*), moderately more broadly (*Nv-tup, Nv-doc*), and significantly more broadly (*Nv-ara*) along the dorsal surface of the *Nasonia*. This indicates that there might be a gradient of positional information on the dorsal side of the *Nasonia* embryo with threshold outputs similar in nature to the one found in *Drosophila*. It is clear that while the location and width of the *Nv-zen* stripe is quite similar to that of its fly counterpart, the behavior of the tissue in which it is expressed is quite different. The fly amnioserosa maintains a border with the surrounding ectoderm throughout development until the end of dorsal closure. In contrast, *Nasonia* serosal cells eventually migrate and surround the entire embryo. This latter behavior is typical of the serosal coverings present in most insects. However the *Nasonia* serosal behavior differs from that of most insects, in that its movement involves a severing of this tissue from the flanking epithelium, and the migration of a free edge over the surface of the ectoderm. This behavior is similar to that observed in the honeybee (Fleig and Sander, 1988), indicating that this type of migration is an ancestral character of the higher hymenoptera. Interestingly, this mode of serosal migration is also found in some fly species, such as the scuttlefly *Megaselia* (Rafiqi et al., 2008). This may be an additional case of convergent evolution between hymenoptera and dipterans.

Many of the dorsal/extraembryonic markers analyzed here have also been examined in other insect species, and have been used as indicators of serosa or amnion fate. *zen* orthologs are generally reliable markers of the serosa, but also have roles in the amnion in *Tribolium* and *Megaselia* (Van der Zee et al., 2005; Rafiqi et al., 2010). *hnt* orthologs seem to vary in their expression, with a narrow, *zen*-like, serosal expression in *Nasonia*, a broader domain encompassing both the amnion and serosa in *Megaselia* (Rafiqi

et al., 2012), and a domain flanking the presumptive serosa in the mosquito *Anopheles* (Goltsev et al., 2007). Expression of *hnt* has so far not been reported in *Tribolium*. In both *Megaselia* and *Anopheles*, *tup* and *doc* are expressed in domains flanking the serosa, which will give rise to the amnion (Goltsev et al., 2007; Rafiqi et al., 2010). While *Nasonia tup* matches this pattern, and likely also is an amnion marker in the wasp, *Nv-doc* differs in that it is only slightly broader than the serosal primordium, and is not repressed at the dorsal midline. *Tribolium doc* is also exceptional, as it is expressed in the dorsal serosa (Van der Zee et al., 2006). *Tribolium pnr* and *ara* are both specific amnion markers, and the expression of *Nv-pnr* and *ara* are also consistent with amniotic roles (Van der Zee et al., 2006; Nunes da Fonseca et al., 2008), with *Nv-ara* likely also having a significant role in the dorsal ectoderm.

Thus it is clear that there is much plasticity in gene regulatory systems in the insect extraembryonic and dorsal ectoderm, but that there also may be a conserved core of factors that are crucial for the specification of amnion, serosa, and dorsal embryonic ectoderm across insects.

Conclusion

In this work we have shown that the arrangement of cell fates, and the expression of genes that mark these fates, are strongly convergent along the DV axis of the long germ embryo of *Nasonia* just prior to gastrulation when compared to those of *Drosophila* at an equivalent stage (Fig. 10). Given the large evolutionary distances between the wasp and the fly this may represent a developmental constraint impinging on the evolution of rapid long germ embryonic patterning among the holometabolous insects. The stringency and true nature of this constraint can be explored by further sampling additional cases of independent evolution of the long germ mode of embryogenesis in other insect orders. Only in this way can lineage specific traits (which are in themselves interesting) and mere coincidence be distinguished from a true signal of constraint.

In contrast to the similarity seen at the stage just prior to gastrulation, we have found that the dynamics of the generation and interpretation of positional information before this stage is quite diverged (Fig. 10). In addition, the behaviors of cells and tissues during and after gastrulation are also quite different between *Drosophila* and *Nasonia* (Fig. S3, Fig. 10). Together these observations indicate that the GRN governing DV patterning and cell type specification in *Nasonia* is structured rather differently and could have novel components that are not found in the *Drosophila* DV GRN. For these reasons, a comprehensive characterization of the *Nasonia* DV patterning system, at the level of its components, their interactions, and the output of the preceding in regard to cell fate and behavior, will give major insights into how convergent traits can evolve.

Methods

Embryo collection and fixation

All *N. vitripennis* embryos were collected using the Waspinator (Fig. S8). This modified petri dish harbors 19 hosts, which can be accessed by up to 120 *Nasonia* females at the same time only from the anterior side. To collect the embryos, parasitized hosts were cracked open at the anterior side and dipped into the fixing solution (5 mL heptane, 2 mL 10% methanol-free formaldehyde, 2 mL 1xPBS, in a 15 mL scintillation vial). Fixation and subsequent hand devitellinization were done as described in Lynch and Desplan (2006).

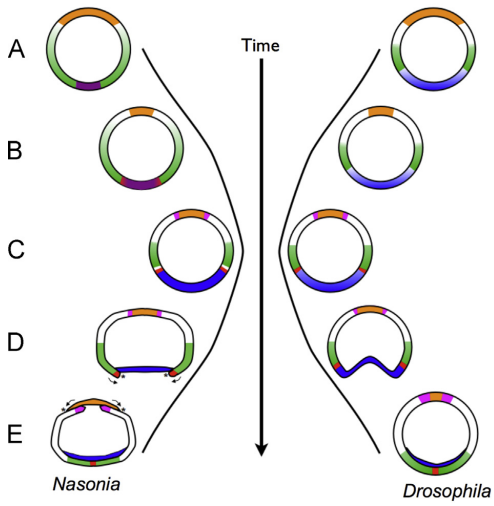

Fig. 10. Summary of convergences and divergences between *Nasonia* and *Drosophila* embryos. Schematic representations of embryogenesis of *Nasonia* (left) and *Drosophila* (right) from mid-blastoderm stage (A) until after the completion of gastrulation (E). Colored regions correspond to different exemplar gene expression patterns: blue=*twi*, red=*sim*, green=*brk*, orange=*zen*, magenta=*tup*, purple=blue(*twi*)+red(*sim*). (A) The *Nasonia* embryo diverges from *Drosophila* in that *Nv-twi* and *sim* are expressed in a very narrow, overlapping (red+blue=purple) domain, while in *Drosophila* twi expression is broad and sim is not yet detected. *Nv-brk* is found quite ventrally, while *Dm-brk* is restricted to the lateral sides. (B) As development proceeds the *Nv-twi+sim* domain dynamically expands, while the *Drosophila* pattern remains for the most part static. In both species, zen expression retracts to a very narrow dorsal stripe. (C) *Dm-sim* becomes expressed in two lateral stripes and *Nv-sim* expression is cleared from the *Nv-twi* expression domain resulting in two lateral stripes of *Nv-sim* expression, too. Hence the arrangement of markers of tissue fates are basically identical between *Nasonia* and *Drosophila* just before gastrulation. (D) *Nasonia* and *Drosophila* embryos diverge again at the onset of gastrulation. *Drosophila* mesoderm is internalized through a ventral furrow, whereas the embryonic epithelium remains intact. In contrast, *Nasonia* mesoderm is internalized by a rupturing of the epithelium at the border between *Nv-sim* and *Nv-twi* expressing cells, leading to free edges (*) that migrate over the mesoderm, and eventually fuse at the midline (see E). (E) After the completion of gastrulation, morphogenetic movements differ on the dorsal side between *Nasonia* and *Drosophila*. In *Nasonia*, the border between serosal cells and putative amnion is ruptured, leading again to free edges (*) that move over the ectodermal surface. In contrast, the fly amnioserosa gradually shrinks as the embryonic flanks expand dorsally. (For interpretation of the references to color in this figure legend, the reader is referred to the web version of this article.)

In situ hybridization

Single in Situ hybridizations for *Nasonia* and *Drosophila* were performed as previously described (Brent et al., 2003).

Double fluorescent in situ hybridizations in *Nasonia* were performed as described in Lynch et al. (2010). In brief, digoxigenin and biotin labeled probes were hybridized simultaneously. They were detected by anti-dig::POD (Roche, 1:100), and anti-Biotin::AP (Roche, 1:2000) antibodies respectively. Fluorescence was generated with the AlexaFluor 488 TSA kit (Invitrogen), and a modification of the HNPP/Fast Red (Roche) protocol, respectively.

Double fluorescent in situ hybridizations in *Tribolium* were performed using a modified version of the protocol described in Lynch and Desplan (2010). Digoxigen-labelled and dinitrophenyl (DNP)-labeled probes were added simultaneously and were detected using anti-digoxigenin::AP antibody (1:2500, Roche) coupled with HNPP Fluorescent detection (Roche), and 1st anti-DNP-rabbit antibody (1:400, Molecular Probes) plus 2nd anti-rabbit-HRP antibody (1:100) combined with AlexaFluor 488 TSA

kit (Invitrogen), respectively. A step by step protocol is available at: http://www.uni-koeln.de/math-nat-fak/ebio/Research/Roth/Protocols/protocols.html.

Probes were produced as in Lynch et al. (2010), using the gene specific primers listed in the Supplementary Table.

Acknowledgements

This work was funded and supported by the Collaborative Research Grant "Molecular Basis of Evolutionary Innovations" (SFB 680) from the German Research Foundation (DFG). We also thank Boehringer Ingelheim Fonds for supporting Dominik Stappert with a B.I.F. Ph.D. Fellowship.

Appendix A. Supporting information

Supplementary data associated with this article can be found in the online version at http://dx.doi.org/10.1016/j.ydbio.2013.05.026.

References

Ashe, H.L., Mannervik, M., Levine, M., 2000. Dpp signaling thresholds in the dorsal ectoderm of the Drosophila embryo. Development (Cambridge, England) 127, 3305–3312.
Brent, A.E., Schweitzer, R., Tabin, C.J., 2003. A somitic compartment of tendon progenitors. Cell 113, 235–248.
Bull, A.L., 1982. Stages of living embryos in the jewel wasp Mormoniella (nasonia) vitripennis (walker) (hymenoptera: pteromalidae). Int. J. Insect Morphol. Embryol. 11, 1–23.
Chen, G., Handel, K., Roth, S., 2000. The maternal NF-kappaB/dorsal gradient of *Tribolium castaneum*: dynamics of early dorsoventral patterning in a short-germ beetle. Development (Cambridge, England) 127, 5145–5156.
Cho, Y.S., Stevens, L.M., Stein, D., 2010. Pipe-dependent ventral processing of Easter by Snake is the defining step in Drosophila embryo DV axis formation. Curr. Biol.: CB 20, 1133–1137.
Davis, G.K., Patel, N.H., 2002. Short, long, and beyond: molecular and embryological approaches to insect segmentation. Annu. Rev. Entomol. 47, 669–699.
Dearden, P., Grbic, M., Falciani, F., Akam, M., 2000. Maternal expression and early zygotic regulation of the Hox3/zen gene in the grasshopper Schistocerca gregaria. Evol. Dev. 2, 261–270.
Erickson, J.W., Quintero, J.J., 2007. Indirect effects of ploidy suggest X chromosome dose, not the X:A ratio, signals sex in Drosophila. PLoS Biol. 5, e332.
Falciani, F., Hausdorf, B., Schröder, R., Akam, M., Tautz, D., Denell, R., Brown, S., 1996. Class 3 Hox genes in insects and the origin of zen. Proc. Nat. Acad. Sci. U.S.A. 93, 8479–8484.
Fleig, R., Sander, K., 1988. Honeybee morphogenesis: embryonic cell movements that shape the larval body 534, 525–534.
Goltsev, Y., Fuse, N., Frasch, M., Zinzen, R.P., Lanzaro, G., Levine, M., 2007. Evolution of the dorsal–ventral patterning network in the mosquito, Anopheles gambiae. Development (Cambridge, England) 134, 2415–2424.
Grissell, E.E., Schauff, M., 1990. A Handbook of the Families of Nearctic Chalcidoidea (Hymenoptera). 1. Entomological Society of Washington, Washington, D.C., pp. 1–85, Handbook.
Hong, J.-W., Hendrix, D.a., Papatsenko, D., Levine, M.S., 2008. How the Dorsal gradient works: insights from postgenome technologies. Proc. Nat. Acad. Sci. U.S.A. 105, 20072–20076.
Jaźwińska, A., Rushlow, C., Roth, S., 1999. The role of brinker in mediating the graded response to Dpp in early Drosophila embryos. Development (Cambridge, England) 126, 3323–3334.
Jiménez, F., Martin-Morris, L.E., Velasco, L., Chu, H., Sierra, J., Rosen, D.R., White, K., 1995. vnd, a gene required for early neurogenesis of Drosophila, encodes a homeodomain protein. EMBO J. 14, 3487–3495.
Kanodia, J.S., Rikhy, R., Kim, Y., Lund, V.K., DeLotto, R., Lippincott-Schwartz, J., Shvartsman, S.Y., 2009. Dynamics of the Dorsal morphogen gradient. Proc. Nat. Acad. Sci. U.S.A. 106, 21707–21712.
Leptin, M., 1991. twist and snail as positive and negative regulators during Drosophila mesoderm development. Genes Dev. 5, 1568–1576.
Liberman, L.M., Reeves, G.T., Stathopoulos, A., 2009. Quantitative imaging of the Dorsal nuclear gradient reveals limitations to threshold-dependent patterning in Drosophila. Proc. Nat. Acad. Sci. U.S.A. 106, 22317–22322.
Lynch, J.A., Desplan, C., 2010. Novel modes of localization and function of nanos in the wasp Nasonia. Development (Cambridge, England) 137, 3813–3821.
Lynch, J.A., El-Sherif, E., Brown, S.J., 2012. Comparisons of the embryonic development of Drosophila, Nasonia, and Tribolium. Wiley Interdisciplinary Reviews. Dev. Biol. 1, 16–39.
Lynch, J.A., Desplan, C., 2006. A method for parental RNA interference in the wasp *Nasonia vitripennis* Nature Protocols 1, 486–494.
Lynch, J.A., Peel, A.D., Drechsler, A., Averof, M., Roth, S., 2010. EGF signaling and the origin of axial polarity among the insects. Curr. Biol.: CB 20, 1042–1047.
Moussian, B., Roth, S., 2005. Dorsoventral axis formation in the Drosophila embryo—shaping and transducing a morphogen gradient. Curr. Biol.: CB 15, R887–R899.
Nunes da Fonseca, R., Van der Zee, M., Roth, S., 2010. Evolution of extracellular Dpp modulators in insects: the roles of tolloid and twisted-gastrulation in dorsoventral patterning of the Tribolium embryo. Dev. Biol. 345, 80–93.
Neuman-Silberberg, F.S., Schüpbach, T., 1993. The Drosophila dorsoventral patterning gene gurken produces a dorsally localized RNA and encodes a TGF alpha-like protein. Cell 75, 165–174.
Nunes da Fonseca, R., Von Levetzow, C., Kalscheuer, P., Basal, A., Van der Zee, M., Roth, S., 2008. Self-regulatory circuits in dorsoventral axis formation of the short-germ beetle *Tribolium castaneum*. Dev. Cell 14, 605–615.
O'Connor, M.B., Umulis, D., Othmer, H.G., Blair, S.S., 2006. Shaping BMP morphogen gradients in the Drosophila embryo and pupal wing. Development (Cambridge, England) 133, 183–193.
Panfilio, K.A., 2008. Extraembryonic development in insects and the acrobatics of blastokinesis. Dev. Biol. 313, 471–491.
Panfilio, K.a., Liu, P.Z., Akam, M., Kaufman, T.C., 2006. Oncopeltus fasciatus zen is essential for serosal tissue function in katatrepsis. Dev. Biol. 292, 226–243.
Rafiqi, A.M., Lemke, S., Ferguson, S., Stauber, M., Schmidt-Ott, U., 2008. Evolutionary origin of the amnioserosa in cyclorrhaphan flies correlates with spatial and temporal expression changes of zen. Proc. Nat. Acad. Sci. U.S.A. 105, 234–239.
Rafiqi, A.M., Lemke, S., Schmidt-Ott, U., 2010. Postgastrular zen expression is required to develop distinct amniotic and serosal epithelia in the scuttle fly Megaselia. Dev. Biol. 341, 282–290.
Rafiqi, A.M., Park, C.-H., Kwan, C.W., Lemke, S., Schmidt-Ott, U., 2012. BMP-dependent serosa and amnion specification in the scuttle fly Megaselia abdita. Development. (Cambridge, England).
Reeves, G.T., Stathopoulos, A., 2009. Graded dorsal and differential gene regulation in the Drosophila embryo. Cold Spring Harbor Perspect. Biol. 1, a000836.
Roth, S., 2003. The origin of dorsoventral polarity in Drosophila. Philos. Trans. R. Soc. London, Ser. B 358, 1317–1329, discussion 1329.
Roth, S., Schüpbach, T., 1994. The relationship between ovarian and embryonic dorsoventral patterning in Drosophila. Development (Cambridge, England) 120, 2245–2257.
Rusch, J., Levine, M., 1996. Threshold responses to the dorsal regulatory gradient and the subdivision of primary tissue territories in the Drosophila embryo. Curr. Opin. Genetics Dev. 6, 416–423.
Rushlow, C., Frasch, M., Doyle, H., Levine, M., 1987. Maternal regulation of zerknüllt: a homoeobox gene controlling differentiation of dorsal tissues in Drosophila. Nature 330, 583–586.
Schmidt-Ott, U., 2000. The amnioserosa is an apomorphic character of cyclorrhaphan flies. Dev. Genes Evol. 210, 373–376.
Sen, J., Goltz, J.S., Stevens, L., Stein, D., 1998. Spatially restricted expression of pipe in the Drosophila egg chamber defines embryonic dorsal–ventral polarity. Cell 95, 471–481.
Stathopoulos, A., Levine, M., 2004. Whole-genome analysis of Drosophila gastrulation. Curr. Opin. Genetics Dev. 14, 477–484.
Stathopoulos, A., Van Drenth, M., Erives, A., Markstein, M., Levine, M., 2002. Whole-genome analysis of dorsal–ventral patterning in the Drosophila embryo. Cell 111, 687–701.
Van der Zee, M., Berns, N., Roth, S., 2005. Distinct functions of the Tribolium zerknüllt genes in serosa specification and dorsal closure. Curr. Biol.: CB 15, 624–636.
Van der Zee, M., Stockhammer, O., Von Levetzow, C., Nunes da Fonseca, R., Roth, S., 2006. Sog/Chordin is required for ventral-to-dorsal Dpp/BMP transport and head formation in a short germ insect. Proc. Nat. Acad. Sci. U.S.A. 103, 16307–16312.
Von Ohlen, T., Doe, C.Q., 2000. Convergence of dorsal, dpp, and egfr signaling pathways subdivides the drosophila neuroectoderm into three dorsal–ventral columns. Dev. Biol. 224, 362–372.
Wheeler, S.R., Carrico, M.L., Wilson, B.a., Skeath, J.B., 2005. The Tribolium columnar genes reveal conservation and plasticity in neural precursor patterning along the embryonic dorsal–ventral axis. Dev. Biol. 279, 491–500.
Wilson, M.J., Dearden, P.K., 2011. Diversity in insect axis formation: two orthodenticle genes and hunchback act in anterior patterning and influence dorsoventral organization in the honeybee (Apis mellifera). Development (Cambridge, England) 138, 3497–3507.

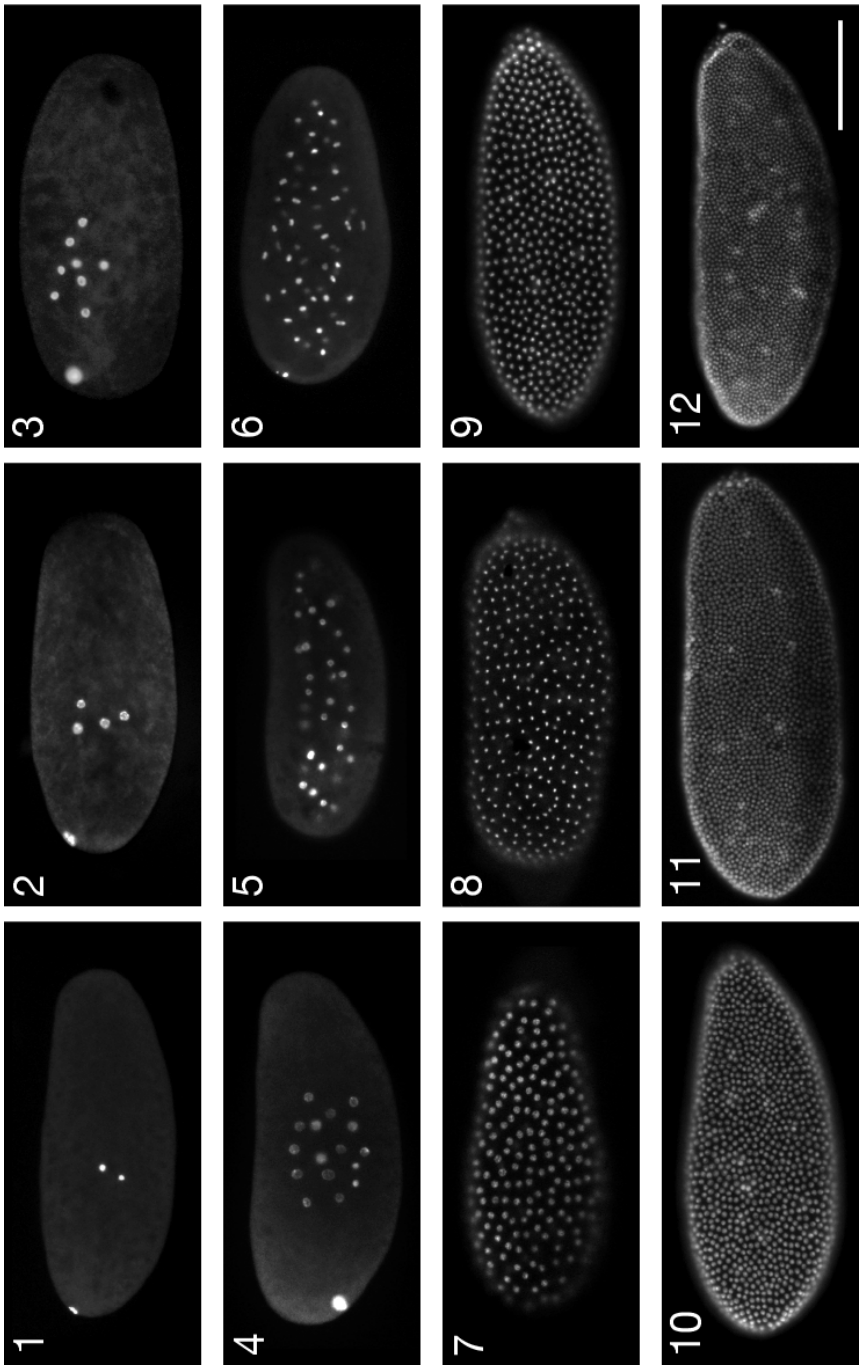

Supplementary Figure 1. Characterization of syncytial divisions in the early embryo of *Nasonia*

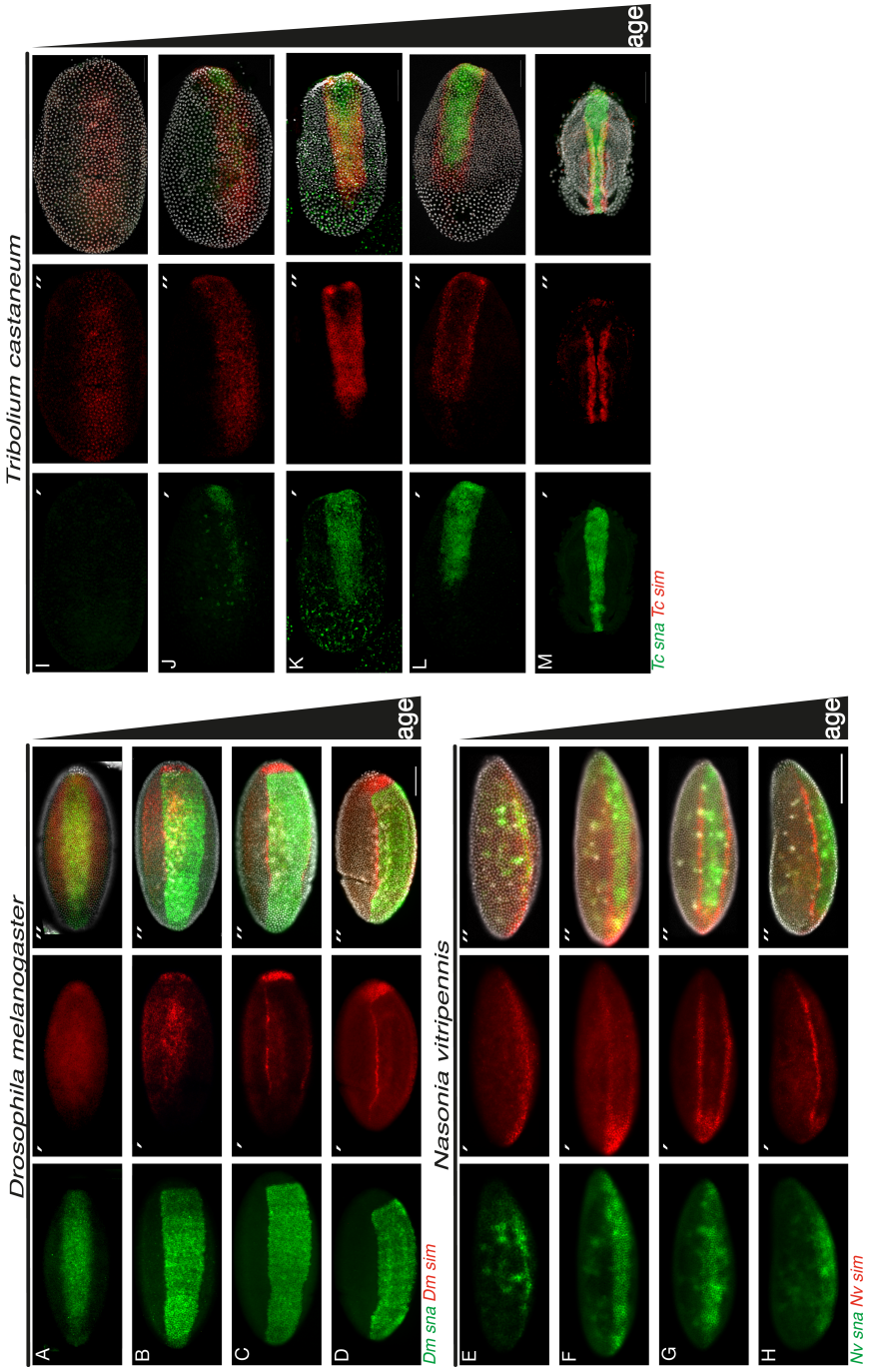

Supplementary Figure 2. Double fluorescent ISH of *snail* (green) and *sim* (red) in *Nasonia*, *Drosophila* and *Tribolium* embryos

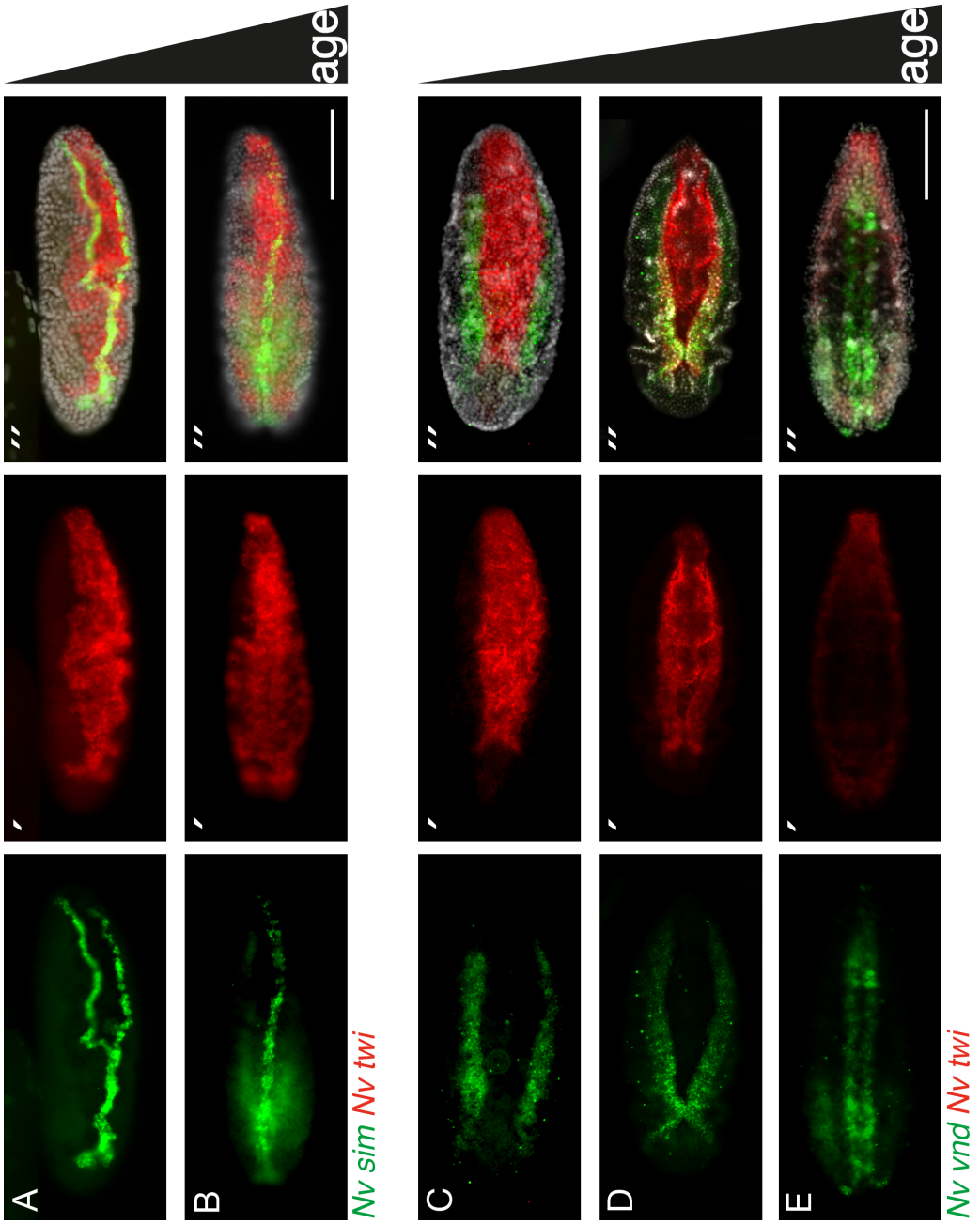

Supplementary Figure 3. Postgastrular dynamics of *Nv-vnd* and *Nv-sim*

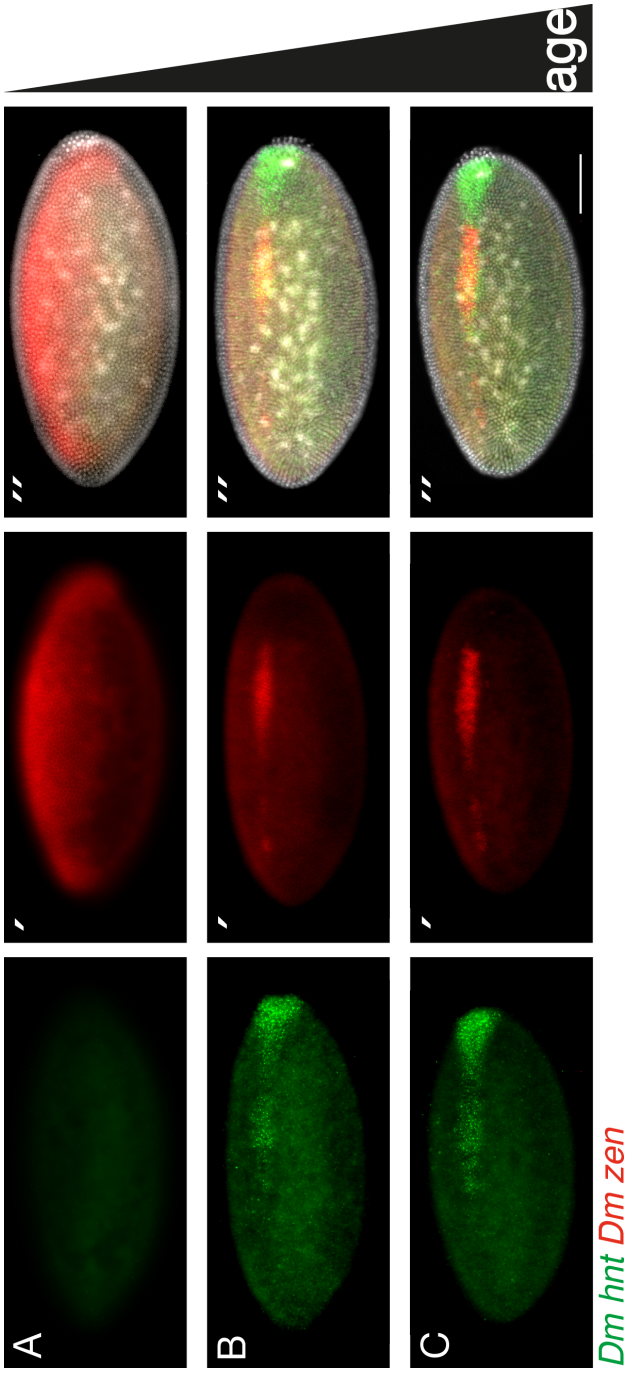

Supplementary Figure 4. Double fluorescent ISH of *hnt* (green) and *zen* (red) in *Drosophila*

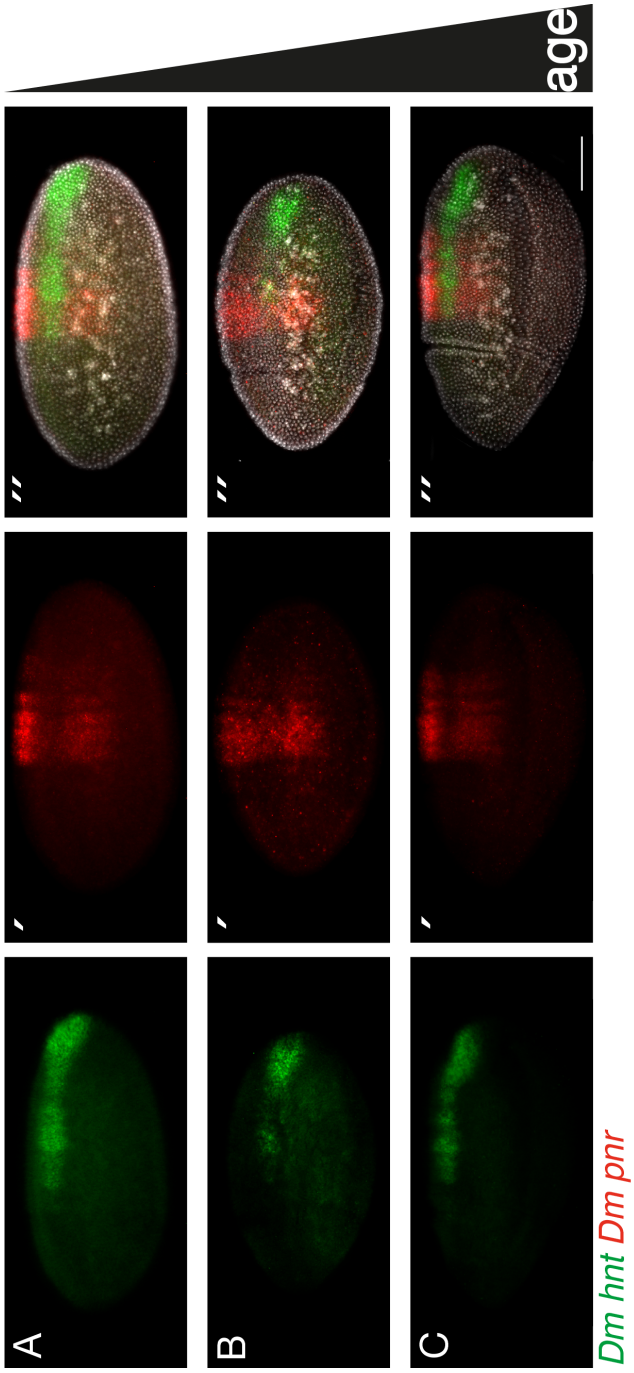

Supplementary Figure 5. Double fluorescent ISH of *hnt* (green) and *pnr* (red) in *Drosophila*

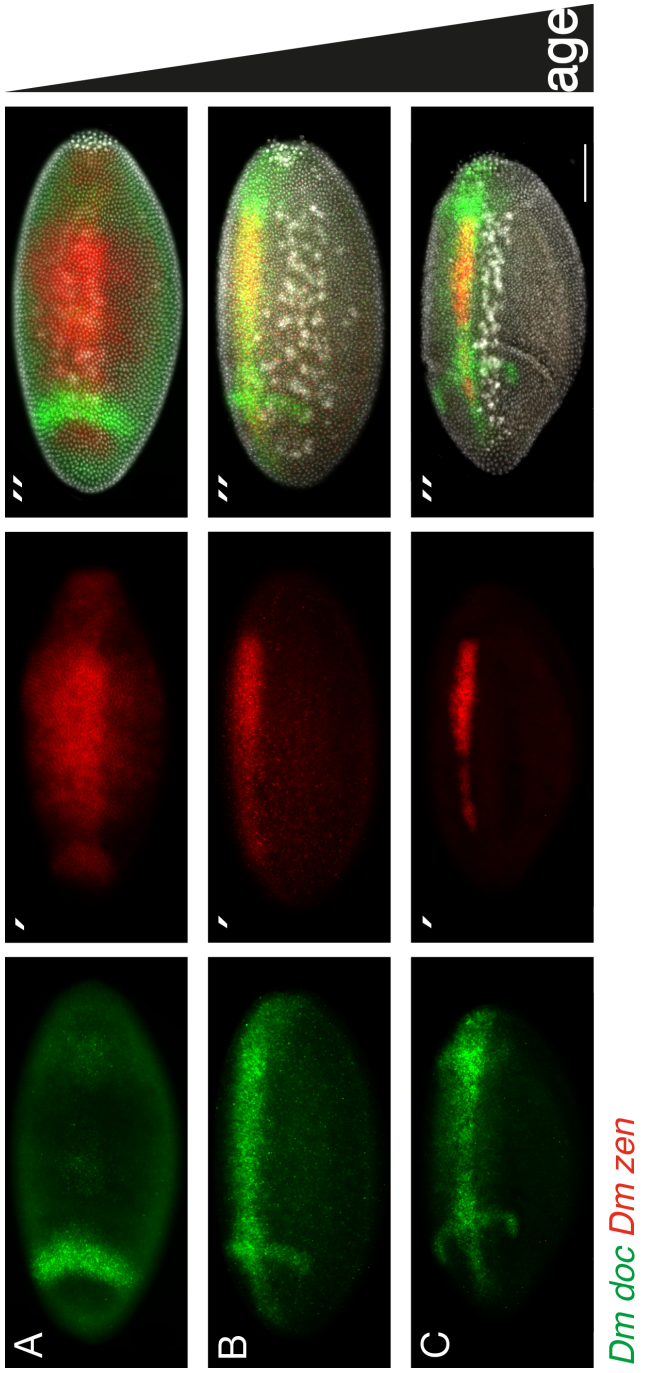

Supplementary Figure 6. Double fluorescent ISH of *doc* (green) and *zen* (red) in *Drosophila*

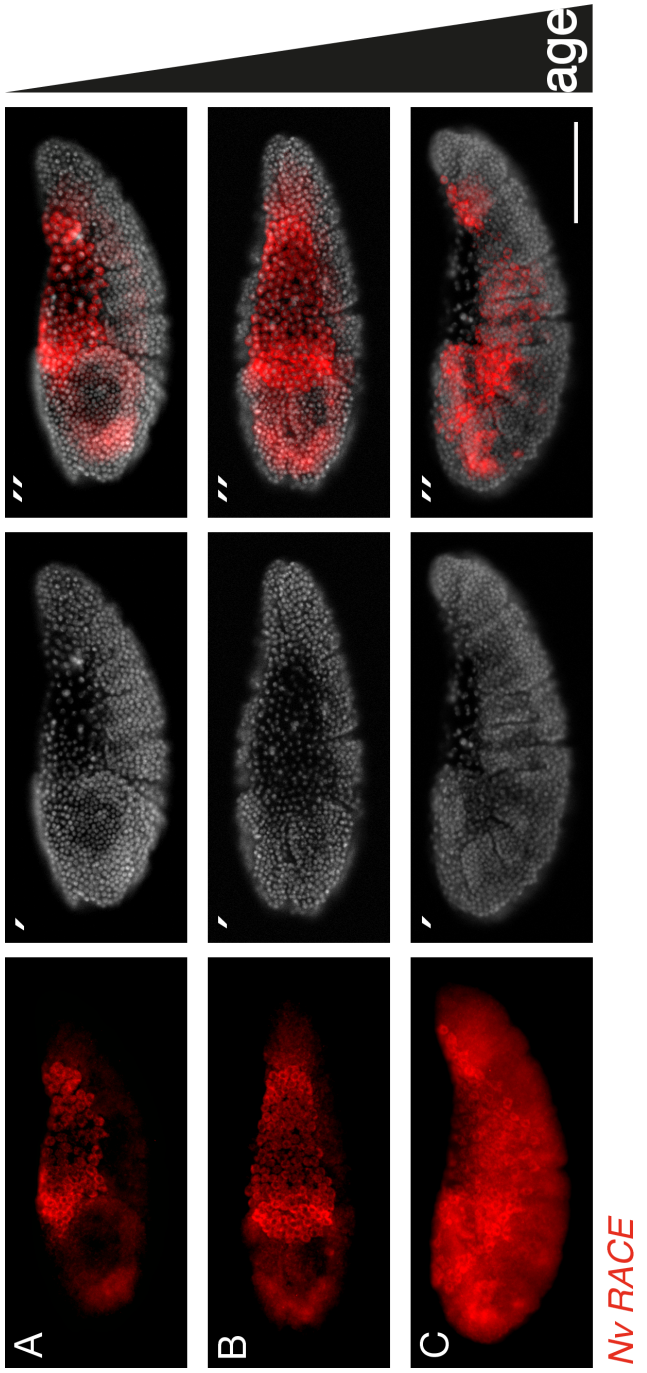

Supplementary Figure 7. fluorescent ISH of RACE (red) in late (gastrulating and post- gastrulation) *Nasonia* embryos

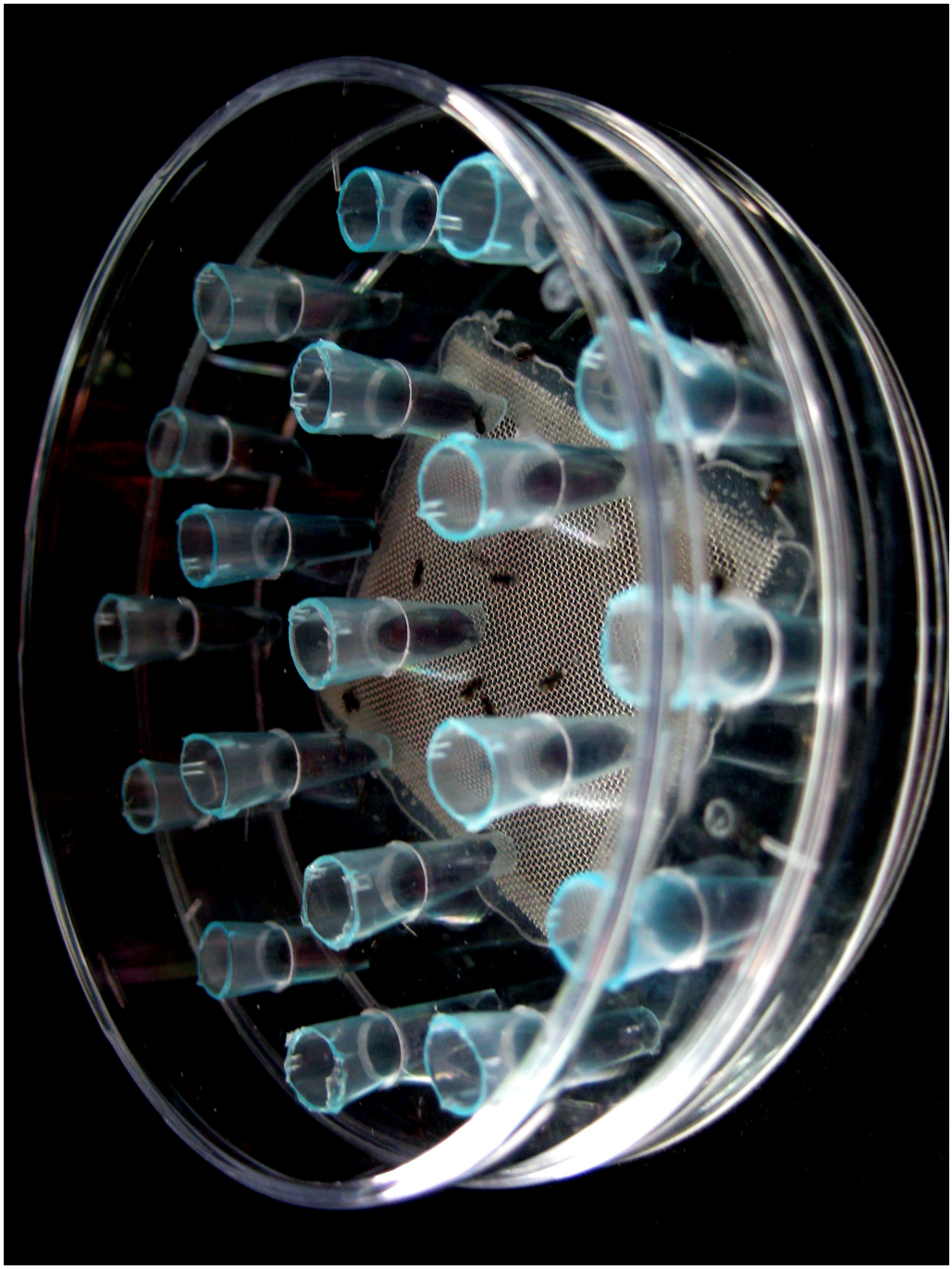

Supplementary Figure 8. The "WASPINATOR" egg laying chamber

Supplementary Figure 1. Characterization of syncytial divisions in the early embryo of *Nasonia*
Embryos at all stages stained with DAPI to demonstrate the arrangement of the nuclei. Embryos are arranged from youngest to oldest.

Supplementary Figure 2. Double fluorescent ISH of *snail* (green) and *sim* (red) in *Nasonia*, *Drosophila* and *Tribolium* embryos
(A´´-C´´) Ventral and (D´´) ventro-lateral views of *Drosophila* embryos in cycle 13 (A´´), cycle 14 (B´´), initiation of gastrulation (C´´) and ongoing gastrulation (D´´) comparing *Dm*-snail (A-D) and *Dm-sim* (A´-D´) mRNA expression with DAPI (white).
(E´´/H´´) Lateral and (F´´-G´´) ventro-lateral views of *Nasonia* embryos in cycle 10-12 (E´´-H´´) comparing *Nv-sna* (E-H) and *Nv-sim* (E´-H´) mRNA expression with DAPI (white).
(I´´-M´´) Ventral views of *Tribolium* embryos in undifferentiated blastoderm (I´´-J´´), start of pit formation (K´´), differentiated blastoderm (H´´) and before serosal window closes (M´´) comparing *Tc-sna* (I-M) and *Tc-sim* (I´-M´) mRNA expression with DAPI (white).
Scale bar 100 µm. Embryos arranged from youngest to oldest from top to bottom in each species panel. Anterior is left.

Supplementary Figure 3. Postgastrular dynamics of *Nv-vnd* and *Nv-sim*
(A-A´´) Ventro-lateral view of a gastrulating *Nasonia* embryo comparing *Nv-sim* (green) and *Nv-twi* (red) mRNA expression with DAPI (white).
(B-B´´) Ventral view of a *Nasonia* embryo comparing *Nv-sim* (green) and *Nv-twi* (red) mRNA expression with DAPI (white) after gastrulation is completed.
(C´´-E´´) Ventral views of Nasonia embryos comparing Nv-vnd (C-E) and Nv-twi (C´-E`) after initiation of gastrulation (C´´), ongoing gastrulation (D´´) and after gastrulation is completed.

Supplementary Figure 4. Double fluorescent ISH of *hnt* (green) and *zen* (red) in *Drosophila*
(A´´) Dorsal and (B´´-C´´) dorso-lateral views of *Drosophila* embryos comparing *Dm-hnt* (A-C) and *Dm-zen* (A´-C´) mRNA expression in cycle 14 (A´´-C´´)
Scale bar 100 µm. Embryos arranged from youngest to oldest from top to bottom.
Anterior is left.

Supplementary Figure 5. Double fluorescent ISH of *hnt* (green) and *pnr* (red) in *Drosophila*
(A´´-C´´) Lateral views of *Drosophila* embryos comparing *Dm-hnt* (A-C) and *Dm-pnr* (A´-C´) mRNA expression in cycle 14 (A´´), initiation of gastrulation (B´´) and ongoing gastrulation (C´´).
Scale bar 100 µm. Embryos arranged from youngest to oldest from top to bottom. Anterior is left.

Supplementary Figure 6. Double fluorescent ISH of *doc* (green) and *zen* (red) in *Drosophila*

(A´´) Dorsal and (B´´-C´´) dorso-lateral views of *Drosophila* embryos comparing *Dm-doc* (A-C) and *Dm-zen* (A´-C´) mRNA expression in cycle 14 (A´´-B´´) and initiation of gastrulation (C´´).
Scale bar 100 µm. Embryos arranged from youngest to oldest from top to bottom. Anterior is left.

Supplementary Figure 7. fluorescent ISH of RACE (red) in late (gastrulating and post- gastrulation) *Nasonia* embryos
(A´´) Dorso-lateral, (B´´) dorsal and (C´´) lateral views of *Nasonia* embryos with completed germ band extension comparing *Nv-RACE* (A-C) mRNA expression and DAPI (A´-C´). Scale bar 100 µm. Embryos arranged from youngest to oldest from top to bottom. Anterior is left.

Supplementary Figure 8. The "WASPINATOR" egg laying chamber
Modified 10 cm plastic Petri dish with cut 1 ml pipette tips to position fly hosts and a grid for airflow. See materials and methods for details.

2.2 Novel deployment of Toll and BMP signaling pathways leads to a convergent patterning output in a wasp

Novel deployment of Toll and BMP signaling pathways leads to a convergent patterning output in a wasp

Orhan Özüak*, Thomas Buchta*,Siegfried Roth, Jeremy A. Lynch

*These authors contributed equally

Abstract

In *Drosophila*, Toll signaling is the source for all dorsal-ventral (DV) patterning of the embryo. This is in contrast to the majority of the metazoa, where Toll signaling plays no role in embryonic patterning, and BMP signaling plays the major role. We have examined the DV patterning system in the wasp *Nasonia*, whose embryo has many features convergent with *Drosophila*. In contrast to the fly, wasp Toll has a limited role, and BMP is required for almost all DV patterning and polarity of the *Nasonia* embryo. Our results indicate that the ancestral role of Toll in insect embryos was to simply induce mesoderm that BMP played the morphogen role, and that significant alterations in the BMP pathway occurred in the *Nasonia* lineage.

Results/Discussion

Toll signaling, which leads to the graded nuclear uptake of the transcription factor Dorsal that acts as a morphogen, patterns the Drosophila embryo, and is required for all DV polarity (1-3). It is known that in most other animal species, Toll has no embryonic patterning role (4), and BMP signaling is the most commonly used system to generate DV polarity (5). Even in the beetle *Tribolium,* the strict hierarchy with Toll at the top is not conserved, indicating that the *Drosophila* system is not representative of the insects (6).

We have shown that while the expression of DV fate markers is almost identical in *Nasonia* and *Drosophila* embryos at the onset of gastrulation, the upstream networks responsible for these patterns are highly diverged (7). This led us to examine the functional basis of DV patterning in *Nasonia*.

Multiplex *in situ* hybridization techniques with *Nv-twist* (*-twi,* mesoderm), *Nv-brinker* (*-brk,* ventral and lateral ectoderm), and *Nv-zerknuellt* (*-zen*, extraembryonic) allow a global view of the *Nasonia* DV axis (Fig. 1A). Parental RNAi (pRNAi) targeting either the *Nasonia* Toll receptor (*Nv-Toll*) or the BMP ligand Decapentaplegic (*Nv-dpp*) allowed a test of the relative roles of the two pathways.

Nv-Toll pRNAi embryos show a complete loss *Nv-twi* expression (Fig. 1B). This indicates a conserved role of Toll in mesoderm induction. However, even the most strongly affected embryos are still highly polarized, with normal *Nv-zen* and dorsal border of *Nv-brk* expression (Fig. 1B), indicating that a Toll independent patterning system operates on the dorsal side, which is absent in *Drosophila* (1, 8). In addition, the expansion of the ventral border of *Nv-brk* to cover the ventral side (Fig. 1B) in *Nv-Toll* RNAi indicates a Toll independent mode of ventro-lateral ectoderm specification in *Nasonia* which is also absent in *Drosophila* (compare Fig. 1E to 1F) (1, 9).

Nv-dpp knockdown leads to loss of not only the dorsal fates (which is its phenotype in *Drosophila*, Fig. 1F), but also to the expansion of the mesoderm to the

dorsal side, (Fig. 1C), whereas the mesoderm is unaffected by loss of BMP in *Drosophila* (Fig. 1F*)*.

Double knockdown of *Nv-dpp* and *Nv-Toll* results in embryos expressing *Nv-brk* only (Fig. 1D). This shows that the ventralization of *Nv-dpp* RNAi embryos requires at least initial induction of mesoderm by Nv-Toll. Thus wasps and flies may share a similar ectodermal "ground state" (compare Fig. 1E to 1F) (11-12).

These phenotypes indicate that Nv-Toll signaling has a rather limited role in *Nasonia*, rather than acting as a global morphogen, while BMP signaling appears to have a broad patterning role encompassing most of the embryo. Thus, these end point phenotypes show that *Nasonia* uses novel mechanisms for patterning its DV axis, and we hoped to gain insights into the molecular bases of the differences by looking in more detail how these phenotypes come about.

Nv-ventral nervous system defective (*Nv-vnd*) is a marker of ventral ectoderm, and is expressed in stripes flanking the *Nv-twi* domain (Fig. 2A). In weak *Nv-Toll* knockdowns *Nv-twi* narrows (Fig. 2B), while *Nv-vnd* shifts in concert ventrally. In stronger knockdowns, *Nv-twi* and *Nv-vnd* retract from the poles (Fig. 2C). In some cases, *Nv-twi* is completely absent, and only a small patch of *Nv-vnd* remains (Fig. 2D). In the strongest, and by far most common case, both *Nv-twi*, and *Nv-vnd* are absent after *Nv-Toll* RNAi (not shown).

This behavior of *Nv-vnd* provides clues about the role of Toll signaling on the ventral side of the embryo. First, *Nv-vnd*, unlike *Nv-brk,* requires at least a minimal amount of Nv-Toll signaling for its expression. Second, *Nv-vnd* seems able to respond to lower levels of ventralizing influence, since it is always expressed further dorsally than *Nv-twi*. These results alone cannot distinguish whether *Nv-vnd* is directly sensing lower levels of Nv-Toll activity, or whether it is activated by a factor emanating from presumptive mesoderm. The fact that *Nv-vnd* expression is only seen well after the *Nv-twi* domain has been stably established is consistent with the latter possibility.

The almost complete ventralization of late blastoderm embryos after *Nv-dpp* RNAi (Fig. 1C) led us to examine the origin of this phenotype. Our previous analyses showed that ventral genes start from very narrow domains early (division cycles 10 & 11) and expand laterally until cycle 12 (demonstrated in detail in (7). After *Nv-dpp* RNAi, all early embryos show narrow *Nv-twi* domains that are indistinguishable from wild-type (compare Fig. 2E to 2F, BMP knockdown is confirmed by absence of *Nv-zen*, and dorsal expansion of *Nv-brk*).

This demonstrates that the Nv-Toll dependent activation of *Nv-twi* is initially independent of the state of BMP signaling. It also shows that the *Nv-dpp* pRNAi phenotypes seen at cycle 12 are the result of a dynamic process, as the mesoderm must expand massively from its initially narrow domain to eventually cover the entire embryo.

It is clear from intermediate phenotypes that BMP signaling has a strong influence on both the width of the *Nv-vnd* (compare Fig. 2G to 2C) domain, as well as the position of its dorsal edge (Fig. 2G and H). A similar strong input of BMP into the vertebrate *vnd* ortholog *Nkx2.2* has been described, as has a much weaker influence on fly *vnd* (13, 14). Subtle, but consistent differences in expansion of *Nv-twi* along the AP axis have also been observed (arrows in Fig. 2G, Fig. S1), which may indicate significant cross-talk between the axes, another hallmark of vertebrate systems (5).

These results show that patterning the ventral side of the *Nasonia* embryo involves a two-step process. First, narrow domains of genes such as *Nv-twi* are established in an Nv-Toll dependent manner in the early syncytial stage. The second phase is when the narrow domains expand and sharpen, and the later expressed lateral genes such as *Nv-vnd* are turned on. This phase is negatively regulated by BMP signaling, and indicates that robust ventral patterning is accomplished through a balance between dynamic, self-enhancing interactions among ventral genes and repressive BMP signaling emanating from the dorsal side (Fig. 4)

We next asked: what is the regulatory basis of the expansion of ventral fates in wild-type and *Nv-dpp* RNAi embryos in *Nasonia?*

If the Toll activity gradient itself were dynamic and increasing over time, one would expect all early, direct targets of Toll to expand laterally both in wild-type, and in BMP knockdown embryos. *Nv-cactus* (*Nv-cact*) is likely a direct target of Toll signaling, since: 1) its orthologs are conserved targets and components of Toll signaling (6, 15, 16), 2) its expression is lost in *Nv-Toll* RNAi (Fig. 2J), and 3) a highly significant cluster of Dorsal binding sites is found just upstream of its coding sequence (Fig. S2).

Nv-cact does not expand in *Nasonia* embryos, and remains as a narrow stripe at the ventral midline of the embryo (Fig 2I). When BMP is knocked down, *Nv-cact* expression is unaffected, indicating both that Toll signaling is not increasing in BMP knockdown, and that *Nv-cact* (and thus *Nv-Toll* signaling) is not regulated by BMP signaling (Fig. 2K). This result supports the ideas that only a subset of ventral genes participate in the expansionary feedback loop, and that the loop is both independent of further Toll input, and negatively regulated by BMP signaling (Fig. 4).

Another striking feature of the *Nasonia* DV patterning system from our initial investigation is that *Nv-zen* expression at the dorsal midline is unaffected in Toll knockdown (Figure 1B), which is in contrast to *Drosophila*. We examined a more broadly expressed dorsal marker, *Nv-araucan* (*-ara*, Fig. 2L (7)), which should be more sensitive to subtle fluctuations in BMP activity, to see if there is any weak effect of *Nv-Toll* pRNAi. In all cases, *Nv-ara* appears normal (Fig 2M), even when it is apparent that *Nv-Toll* knockdown is strong (Fig. 2M').

Since *Nasonia* DV patterning depends so strongly on BMP signaling, we used a cross-reactive phosphorylated MAD antiserum to monitor the pattern of BMP activity (17, 18). pMAD is found in a broad, shallowly graded pattern in cycle 10 embryos (Fig. 3A). Over the next division cycle this gradient intensifies and becomes more dorsally restricted, and more obviously graded (Fig. 3B). By

cycle 12 it is found in an intense stripe over the dorsal midline with a very sharp lateral borders (Fig. 3C). Eventually, the stripe narrows further and begins to disappear just prior to gastrulation (Fig. 3D).

This pattern is similar to *Drosophila*, in that the gradient of BMP activity starts relatively broad and flat, and then refines and intensifies, generating a high peak at the Dorsal midline (18). However, the transformation of BMP activity all occurs in cycle 14 in *Drosophila*, while the first clear asymmetry in BMP signaling is seen in cycle 10 in *Nasonia,* and the patterns evolves over the next two division cycles.

In *Drosophila* three genes directly regulated by Toll are required for BMP signaling: the ligand *dpp*, the inhibitor *short gastrulation* (*sog*), and the metalloprotease *tolloid* (*tld*) (19). *dpp* and *tld* are expressed in broad dorsal domains and are repressed by Dorsal, while *sog* is activated by Dorsal laterally. Sog protein binds Dpp, inhibits its signaling, and facilitates its diffusion. Tld cleaves Sog, leading to its destruction, and frees Dpp to signal. The interactions among these and other BMP components are critical for the proper formation of the BMP signaling gradient, particularly the peak levels at the dorsal midline (19).

Nv-dpp is expressed maternally, and does not show spatial regulation until after gastrulation (not shown). In addition, no *sog* ortholog has been detected in any genome or transcriptome data set in *Nasonia* (7, 20). The very restricted anterior expression (Fig. 3E) and lack of patterning function of *Nv-tld* (tested by pRNAi, not shown) are also consistent with the absence of a Sog based transport system.

Other components are required for BMP signaling in *Drosophila*. One is *screw,* a highly diverged BMP 5/7 paralog related to *glass bottom boat (gbb)* (21). In *Nasonia*, *Nv-gbb* a BMP 5/7-like ligand is expressed maternally, and appears ubiquitously weak throughout early embryogenesis (not shown) and gives an identical pRNAi phenotype to *Nv-dpp* (Fig. 3F). Therefore, BMP signaling requires both *Nv-dpp* and *Nv-gbb* together to induce signaling in *Nasonia,* indicating that

Nv-Dpp+Gbb heterodimers may be required for long range BMP signaling in the *Nasonia* embryo, while such heterodimers are only required for peak levels of signaling in *Drosophila* (21).

The BMP binding protein Twisted gastrulation (Tsg), has both positive and negative effects on BMP activity in *Drosophila* (22), and is required for peak levels of BMP signaling in the embryo. pRNAi against *Nv-tsg* gives identical phenotypes to *Nv-dpp* and *Nv-gbb*, indicating that *Nv-tsg* is also required for BMP signaling in *Nasonia* (Fig. 3G). An exclusively pro-BMP, *sog*-independent role for *tsg* was also observed in *Tribolium* (23).

Finally, the receptors *thickveins* (*tkv*) and *saxophone* (*sax*) are required for BMP signaling in *Drosophila* (21). We find that both are also required in *Nasonia*, but the lack of either one alone does not completely abrogate the signal (Fig. 3H, only *Nv-tkv* RNAi result shown).

We have shown here the first example of an insect that relies almost completely on BMP signaling for DV axis patterning (Fig. 4, right side). This BMP system is independent of Toll signaling, which is in stark contrast to the *Drosophila* paradigm, where crucial BMP components are regulated by Toll signaling (Fig. 4). We have also shown that Toll signaling induces only a narrow ventral expression domain of genes whose final pattern depends on a combination dynamic expansion, and BMP mediated repression (Fig. 4), rather than on any Toll-based gradient. These results suggest that the original embryonic patterning role for Toll in insects may have been simply to induce a single ventral fate, and that the Toll pathway usurped the ancestral role of BMP some time after the divergence of the Hymenoptera from the clade containing Coleoptera and Diptera.

Furthermore, while the dynamics of BMP signaling (pMAD) are similar between wasp and fly, we have shown that the molecular mechanisms producing the dynamics must be highly diverged, due to the absence of Sog and Tld function in Nasonia, the differing roles of Tsg and BMP 5/7 genes, and the lack of any *Nasonia* BMP component with clearly localized mRNA expression during the

patterning phase. This shows that not only are the downstream regulatory networks targets of evolutionary change, but that the upstream signaling modules are also prone to significant alterations in the course of evolution.

References

1. K. V. Anderson, L. Bokla, C. Nusslein-Volhard, Establishment of dorsal-ventral polarity in the Drosophila embryo: the induction of polarity by the Toll gene product. Cell 42, 791-798 (1985); published online EpubOct (0092-8674(85)90275-2 [pii]).
2. K. V. Anderson, G. Jurgens, C. Nusslein-Volhard, Establishment of dorsal-ventral polarity in the Drosophila embryo: genetic studies on the role of the Toll gene product. Cell 42, 779-789 (1985); published online EpubOct (0092-8674(85)90274-0 [pii]).
3. B. Moussian, S. Roth, Dorsoventral axis formation in the Drosophila embryo--shaping and transducing a morphogen gradient. Curr Biol 15, R887-899 (2005); published online EpubNov 8 (S0960-9822(05)01226-1 [pii] 10.1016/j.cub.2005.10.026).
4. J. A. Lynch, S. Roth, The evolution of dorsal-ventral patterning mechanisms in insects. Genes & development 25, 107-118 (2011); published online EpubJan 15 (10.1101/gad.2010711).
5. E. M. De Robertis, Evo-devo: variations on ancestral themes. Cell 132, 185-195 (2008); published online EpubJan 25 (10.1016/j.cell.2008.01.003).
6. R. Nunes da Fonseca, C. von Levetzow, P. Kalscheuer, A. Basal, M. van der Zee, S. Roth, Self-regulatory circuits in dorsoventral axis formation of the short-germ beetle Tribolium castaneum. Developmental cell 14, 605-615 (2008); published online EpubApr (10.1016/j.devcel.2008.02.011).
7. T. Buchta, O. Ozuak, D. Stappert, S. Roth, J. A. Lynch, Patterning the dorsal-ventral axis of the wasp Nasonia vitripennis. Developmental biology 381, 189-202 (2013); published online EpubSep 1 (10.1016/j.ydbio.2013.05.026).
8. S. Roth, D. Stein, C. Nusslein-Volhard, A gradient of nuclear localization of the dorsal protein determines dorsoventral pattern in the Drosophila embryo. Cell 59, 1189-1202 (1989); published online EpubDec 22 (
9. A. Jazwinska, C. Rushlow, S. Roth, The role of brinker in mediating the graded response to Dpp in early Drosophila embryos. Development 126, 3323-3334 (1999); published online EpubAug (
10. K. A. Wharton, R. P. Ray, W. M. Gelbart, An activity gradient of decapentaplegic is necessary for the specification of dorsal pattern elements in the Drosophila embryo. Development 117, 807-822 (1993); published online EpubFeb (

11. T. von Ohlen, C. Q. Doe, Convergence of dorsal, dpp, and egfr signaling pathways subdivides the drosophila neuroectoderm into three dorsal-ventral columns. Developmental biology 224, 362-372 (2000); published online EpubAug 15 (10.1006/dbio.2000.9789).
12. V. F. Irish, W. M. Gelbart, The decapentaplegic gene is required for dorsal-ventral patterning of the Drosophila embryo. Genes & development 1, 868-879 (1987); published online EpubOct (
13. C. M. Mizutani, E. Bier, EvoD/Vo: the origins of BMP signalling in the neuroectoderm. Nature reviews. Genetics 9, 663-677 (2008); published online EpubSep (10.1038/nrg2417).
14. J. Crocker, A. Erives, A Schnurri/Mad/Medea complex attenuates the dorsal-twist gradient readout at vnd. Developmental biology 378, 64-72 (2013); published online EpubJun 1 (10.1016/j.ydbio.2013.03.002).
15. A. Hoffmann, A. Levchenko, M. L. Scott, D. Baltimore, The IkappaB-NF-kappaB signaling module: temporal control and selective gene activation. Science 298, 1241-1245 (2002); published online EpubNov 8 (10.1126/science.1071914298/5596/1241 [pii]).
16. T. Sandmann, C. Girardot, M. Brehme, W. Tongprasit, V. Stolc, E. E. Furlong, A core transcriptional network for early mesoderm development in Drosophila melanogaster. Genes & development 21, 436-449 (2007); published online EpubFeb 15 (
17. H. Tanimoto, S. Itoh, P. ten Dijke, T. Tabata, Hedgehog creates a gradient of DPP activity in Drosophila wing imaginal discs. Mol Cell 5, 59-71 (2000); published online EpubJan (S1097-2765(00)80403-7 [pii]).
18. R. Dorfman, B. Z. Shilo, Biphasic activation of the BMP pathway patterns the Drosophila embryonic dorsal region. Development 128, 965-972 (2001); published online EpubMar (
19. M. B. O'Connor, D. Umulis, H. G. Othmer, S. S. Blair, Shaping BMP morphogen gradients in the Drosophila embryo and pupal wing. Development 133, 183-193 (2006); published online EpubJan (
20. J. H. Werren, S. Richards, C. A. Desjardins, O. Niehuis, J. Gadau, J. K. Colbourne, G. Nasonia Genome Working, J. H. Werren, S. Richards, C. A. Desjardins, O. Niehuis, J. Gadau, J. K. Colbourne, L. W. Beukeboom, C. Desplan, C. G. Elsik, C. J. Grimmelikhuijzen, P. Kitts, J. A. Lynch, T. Murphy, D. C. Oliveira, C. D. Smith, L. van de Zande, K. C. Worley, E. M. Zdobnov, M. Aerts, S. Albert, V. H. Anaya, J. M. Anzola, A. R. Barchuk, S. K. Behura, A. N. Bera, M. R. Berenbaum, R. C. Bertossa, M. M. Bitondi, S. R. Bordenstein, P. Bork, E. Bornberg-Bauer, M. Brunain, G. Cazzamali, L. Chaboub, J. Chacko, D. Chavez, C. P. Childers, J. H. Choi, M. E. Clark, C. Claudianos, R. A. Clinton, A. G. Cree, A. S. Cristino, P. M. Dang, A. C. Darby, D. C. de Graaf, B. Devreese, H. H. Dinh, R. Edwards, N. Elango, E. Elhaik, O. Ermolaeva, J. D. Evans, S. Foret, G. R. Fowler, D. Gerlach, J. D. Gibson, D. G. Gilbert, D. Graur, S. Grunder, D. E. Hagen, Y. Han, F. Hauser,

D. Hultmark, H. C. t. Hunter, G. D. Hurst, S. N. Jhangian, H. Jiang, R. M. Johnson, A. K. Jones, T. Junier, T. Kadowaki, A. Kamping, Y. Kapustin, B. Kechavarzi, J. Kim, J. Kim, B. Kiryutin, T. Koevoets, C. L. Kovar, E. V. Kriventseva, R. Kucharski, H. Lee, S. L. Lee, K. Lees, L. R. Lewis, D. W. Loehlin, J. M. Logsdon, Jr., J. A. Lopez, R. J. Lozado, D. Maglott, R. Maleszka, A. Mayampurath, D. J. Mazur, M. A. McClure, A. D. Moore, M. B. Morgan, J. Muller, M. C. Munoz-Torres, D. M. Muzny, L. V. Nazareth, S. Neupert, N. B. Nguyen, F. M. Nunes, J. G. Oakeshott, G. O. Okwuonu, B. A. Pannebakker, V. R. Pejaver, Z. Peng, S. C. Pratt, R. Predel, L. L. Pu, H. Ranson, R. Raychoudhury, A. Rechtsteiner, J. T. Reese, J. G. Reid, M. Riddle, H. M. Robertson, J. Romero-Severson, M. Rosenberg, T. B. Sackton, D. B. Sattelle, H. Schluns, T. Schmitt, M. Schneider, A. Schuler, A. M. Schurko, D. M. Shuker, Z. L. Simoes, S. Sinha, Z. Smith, V. Solovyev, A. Souvorov, A. Springauf, E. Stafflinger, D. E. Stage, M. Stanke, Y. Tanaka, A. Telschow, C. Trent, S. Vattathil, E. C. Verhulst, L. Viljakainen, K. W. Wanner, R. M. Waterhouse, J. B. Whitfield, T. E. Wilkes, M. Williamson, J. H. Willis, F. Wolschin, S. Wyder, T. Yamada, S. V. Yi, C. N. Zecher, L. Zhang, R. A. Gibbs, Functional and evolutionary insights from the genomes of three parasitoid Nasonia species. Science 327, 343-348 (2010); published online EpubJan 15 (10.1126/science.1178028).

21. O. Shimmi, D. Umulis, H. Othmer, M. B. O'Connor, Facilitated transport of a Dpp/Scw heterodimer by Sog/Tsg leads to robust patterning of the Drosophila blastoderm embryo. Cell 120, 873-886 (2005); published online EpubMar 25 (10.1016/j.cell.2005.02.009).
22. Y. C. Wang, E. L. Ferguson, Spatial bistability of Dpp-receptor interactions during Drosophila dorsal-ventral patterning. Nature 434, 229-234 (2005); published online EpubMar 10 (10.1038/nature03318).
23. R. Nunes da Fonseca, M. van der Zee, S. Roth, Evolution of extracellular Dpp modulators in insects: The roles of tolloid and twisted-gastrulation in dorsoventral patterning of the Tribolium embryo. Developmental biology 345, 80-93 (2010); published online EpubSep 1 (10.1016/j.ydbio.2010.05.019).

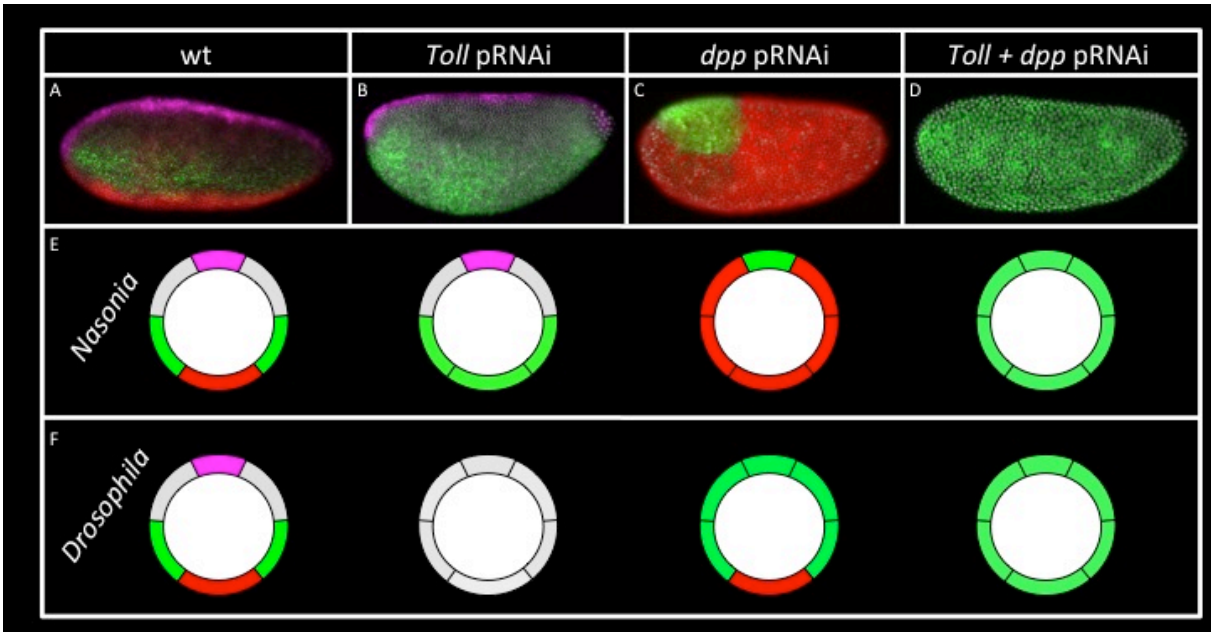

Figure 1. Effects of *Toll*, *dpp,* and *Toll/dpp* double pRNAi.
A-D, *Nv-zen* (purple), -*brk* (green) and -*twi* (red) expression in wild-type (**A**) *Nv-Toll* (**B**), *Nv-dpp* (**C**) and *Nv-Toll* /*dpp* (**D**) RNAi embryos. **E**,**F,** Schematic cross sections of *Nasonia* (**E**) and *Drosophila* (**F**) embryos corresponding to the four different conditions shown in (**A**-**D**) (Red=Mesodern, Green=Neurectoderm, Grey=Dorsal ectoderm, and Magenta=extraembryonic.

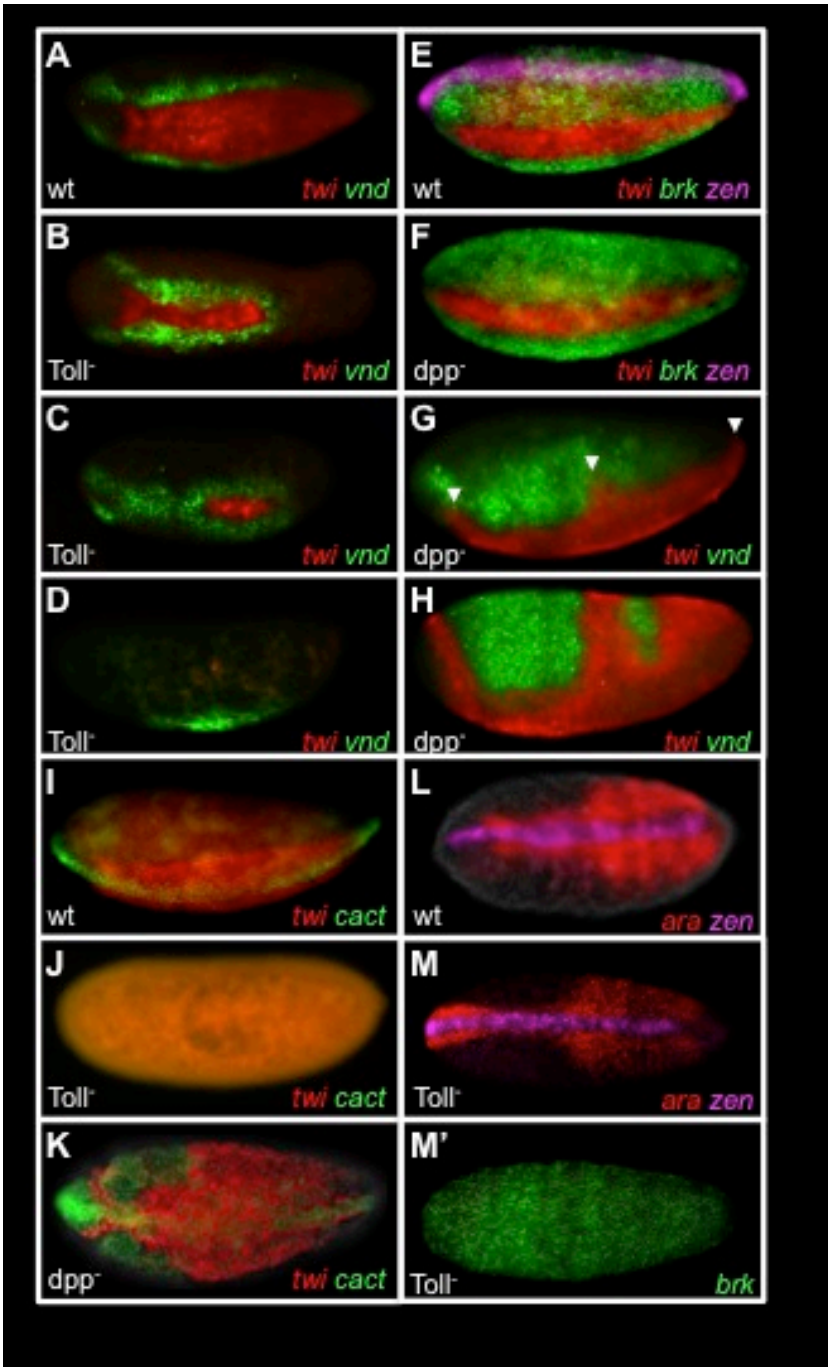

Figure 2. Detailed effects of *Nv-dpp* and *Nv-Toll* pRNAi
A-D,G-H, *Nv-vnd* (green), *Nv-twi* (red) expression in wild-type (**A**), *Nv-Toll* (**B-D**) and *Nv-dpp* **G**,**H** embryos. **E,F** *Nv-twi* (red), *Nv-brk* (green), *Nv-zen* (purple) expression in wild-type (**E**) and *Nv-dpp* (**F**) pRNAi embryos. **I-K,** *Nv-cact* (green) and *Nv-twi* (red) expression in wildtype (**I**), *Nv-Toll* (**J**) and

Nv-dpp (**K**) pRNAi embryos. **L-M,** *Nv-ara* (red), *Nv-zen* (purple) expression in wild-type (**L**) and *Nv-Toll* RNAi (**M**) embryos. **M'** is a ventral view of the same embryo in **M** showing *Nv-brk* (green).

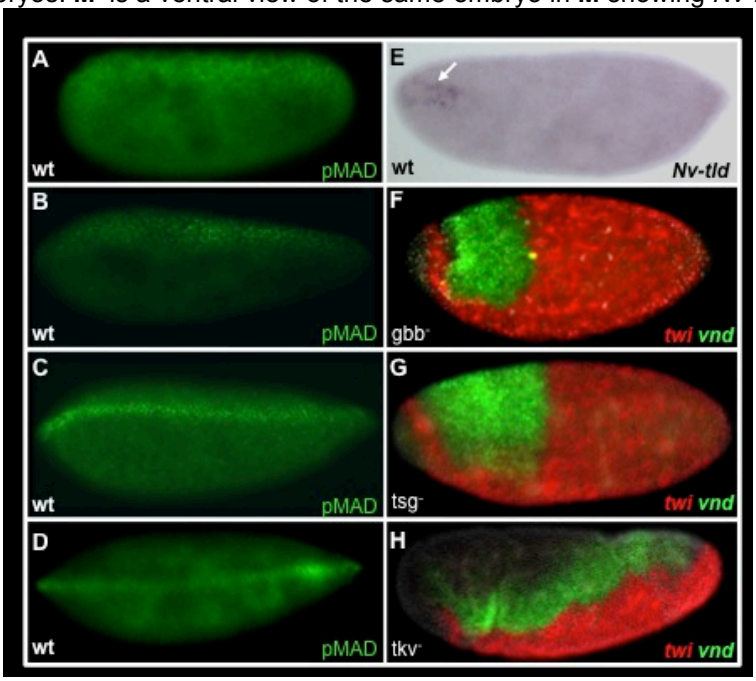

Figure 3. BMP signaling in the *Nasonia* embryo.
A,B,C,D, Distribution of pMAD (green), arranged from young (cycle 10, **A**) to old (late cycle 12, **D**). **E,** Expression of *Nv-tld* in late cycle 12. **F,H,** *Nv-twi* (red)*, Nv-brk* (green) *expression* in *Nv-gbb* (**F**), t*sg* (**G**) and *tkv* (**H**) pRNAi embryos.

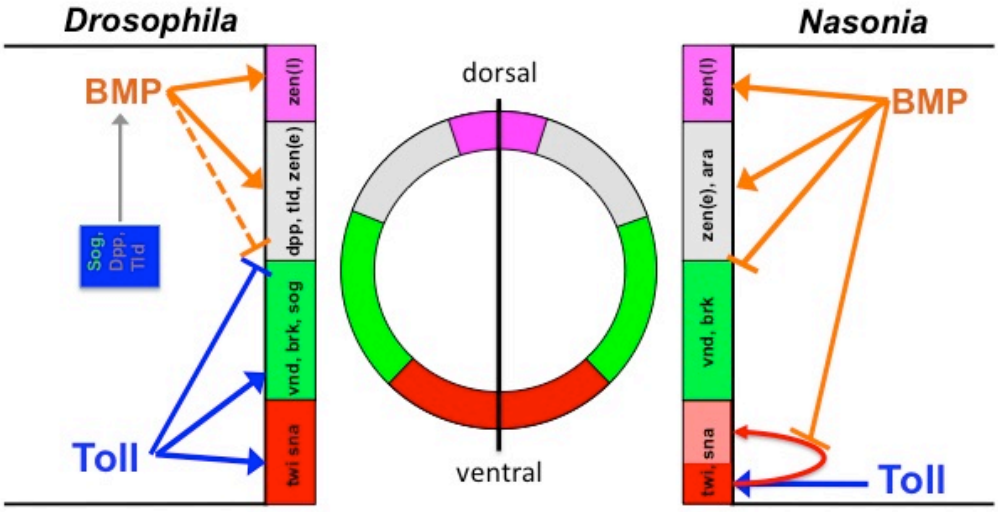

Fig. 4 Relative roles of BMP and Toll signalling in Drosophila and Nasonia embryos.

Summary of Drosophila Toll and BMP roles and regulation on left, Nasonia at right. Blue and orange arrows and lines indicate regulation by Toll and BMP, respectively. Factors in blue box on left indicate BMP signaling components whose transcription is directly regulated by Toll. Red curved arrow indicates self-activation of ventral genes. zen (e) and zen(l), indicate early and late zen expression, respectively.

Supplement:

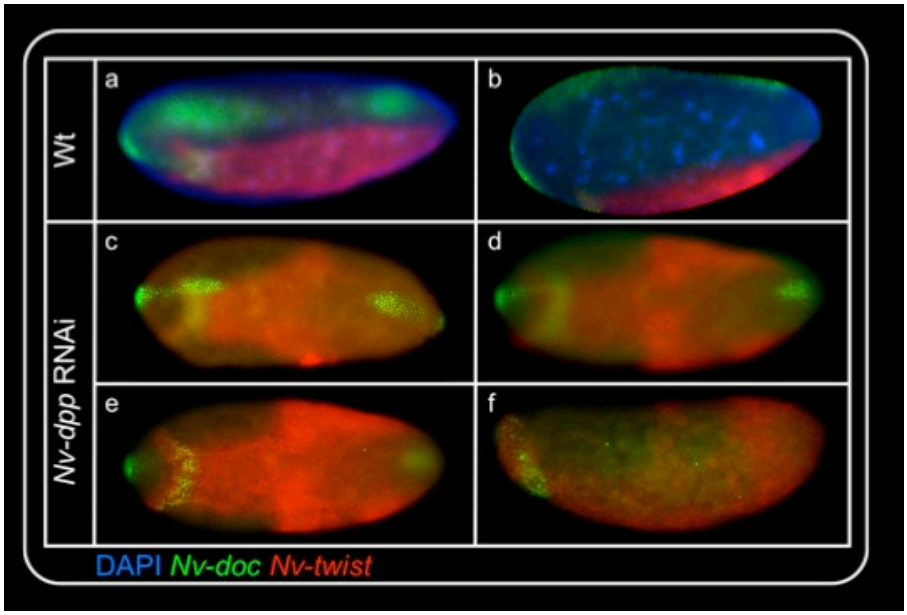

Figure S1. *Nasonia dorsocross* (*Nv-doc*) as a marker in *Nv-d*pp RNAi.

A-G, *twi* (red) and *doc* (green) expression in wild-type (**A,B**) and *dpp*$^{-}$ (**C-F**).
A, dorso-lateral view; **C-E**, dorsal view; **B,F**, lateral view.

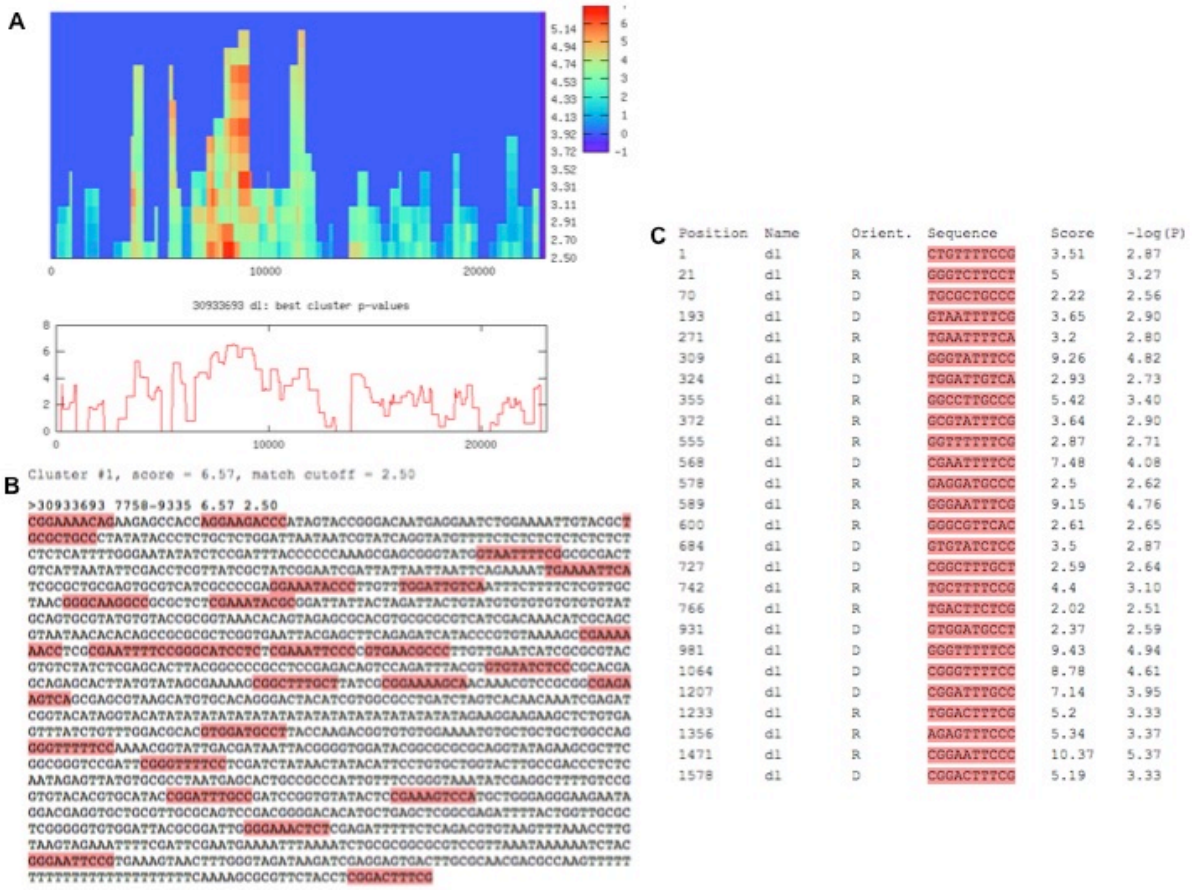

Figure S2. **Illustration of clustered Dorsal binding sites in the *Nv-cact* genomic region.** A genomic fragment including the *Nv-cact1* locus plus 10kb upstream and downstream was submitted to the Clusterdraw web server , using default parameters. Output of the highest scoring cluster is shown. **A).** Heatmap and histogram showing regions with clusters of high scoring Dorsal binding sites. Note that the strongest cluster is located just before the 10kb mark, which is the start of the *Nv-cact* coding locus. **B)** Distribution of Dorsal binding sites in best scoring cluster. **C).** Position and score (higher score~higher affinity) of Dorsal sites in best scoring cluster.

Materials and methods

Embryo collection

All *N. vitripennis* embryos were collected using the *Waspinator* and fixed as described in [4].

Double-Stranded RNA (dsRNA) primer

Toll (*Toll*)	Fw	ggccgcggGAACTCGCCAAACTGGTCTC
	Rev	cccggggcAACGGATTGTTCGTCAGCTC

decapentaplegic (*dpp*)	Fw	ggccgcgggTGGTGGGCGAGGCGGTAAA
	Rev	cccggggcCACGACCTTGTTCTCCTCGT
glass bottom boat 1 (*gbb1*)	Fw	ggccgcggATCCTGCTGCAGTTCGACTT
	Rev	cccggggcCCCTGATGATCATGTTGTGG

In Situ hybridization (ISH) primer

cactus1 (*cact1*)	Fw	ggccgcggACTTGGATATGGGCAAGTCG
	Rev	cccggggcCTACTGTCGCTGCTGCTGTC
twist (*twi*)	Fw	ggccgcgggCTTCTCGCCCAGTAACAAC
	Rev	cccggggcACGTTAGCCATGACCCTCTG
ventral nervous system defective (*vnd*)	Fw	ggccgcgggTCGGACTGCTCAACAACTG
	Rev	cccggggcAGGTTCCAGGAGCTTCGACT
brinker (*brk*)	Fw	ggccgcggATCCAAAAGTGGCTCCAGTG
	Rev	cccggggcCTGAAAGTCGTGCTCCTCGT
zerknüllt (*zen*)	Fw	ggccgcggAAGTCGGCTCCTATTCAGCA
	Rev	cccggggcTAGGAATAGTGGCCCGAAGA
araucan (*ara*)	Fw	ggccgcggCACCACCACCTTCTCATCCT
	Rev	cccggggcGCCCTTGTAGAACGGTTTGA
dorsocross1 (*doc1*)	Fw	ggccgcggATAAAATCGGCACCGAGATG
	Rev	cccggggcAAATAGGCAGCTGCAATGCT

RNAi

Young *N. vitripennis* pupae were injected as in [3].

In Situ Hybridisation (ISH) and Immunohistochemistry (IHC)

Two-color ISH was performed as described in [2]

Three-color ISH is a modified version of the two-color ISH and was perfomred in 4 days.

First day: Probe incubation using biotin-, fluorescein-, and dig labelled probes as described in [2].

Second day: Antibodies were incubated using α-fluorescein::AP antibodies (1:2500), α-digoxigen::POD antibodies (1:100) and Mouse-α-biotin antibodies (1:100) as described in [2].
Third day: Staining reaction with Fast Red and HNPP (Roche) as substrates for α-fluorescein::AP antibodies to give a red fluorescent signal with AlexaFluor 488 tyramide (Invitrogen) as a substrate α-digoxigen::POD antibodies as described in [2].
After staining reaction POD was destroyed by incubating embryos for 30 min in a 1% H_2O_2 solution diluted in PBT. Antibody incubation using α-mouse::POD (1:100) antibodies overnight.
Fourth day: Staining reaction with AlexaFluor 647 (Invitrogen) as substrate for α-mouse::POD.

Immunohistochemistry was performed as described in [1]. Rabbit monoclonal antibody 41D10, raised against phospho-Smad 1/5, was obtained from Cell Signaling Sciences, and was used at 1:100. Secondary anti-rabbit::Alexa 568 was used at a concentration of 1:500

1. Patel, N.H. (1994). Imaging neuronal subsets and other cell types in whole mount *Drosophila* embryos and larvae using antibody probes. In Methods in Cell Biology, Volume 44, L.S.B. Goldstein and E. Fyrberg, eds. (New York: Academic Press).

2. Mazzoni, E.O., Celik, A., Wernet, M.F., Vasiliauskas, D., Johnston, R.J., Cook, T.A., Pichaud, F., and Desplan, C. (2008). Iroquois complex genes induce co-expression of rhodopsins in Drosophila. PLoS Biol. 6, e97. 27.

3. Lynch, J.A., and Desplan, C. (2006). A method for parental RNA interference in the wasp *Nasonia vitripennis*. Nat. Protoc. 1, 486–494.

4. Buchta, T., Özüak, O., et al., Patterning the dorsal–ventral axis of the wasp *Nasonia vitripennis*. Dev. Biol. (2013), http://dx.doi.org/10.1016/j.ydbio.2013.05.026

2.3 Ancient and diverged TGF-β signaling components in *Nasonia vitripennis*

Ancient and diverged TGF-β signaling components in *Nasonia vitripennis*

Orhan Özüak*, Thomas Buchta*,Siegfried Roth, Jeremy A. Lynch

*These authors contributed equally

Absract

The TGF- β signaling pathway and its modulators are involved in many aspects of cellular growth and differentiation in all metazoa. Although most of the core components of the pathway are highly conserved many lineage specific adaptations have been observed including changes regarding paralog number, presence and absence of modulators and functional relevance for particular processes. In the parasitic jewel wasp *Nasonia vitripennis* the Bone Morphogenetic Proteins (BMPs), one major subgroups the of the TGF-ß superfamily, play a more fundamental role in dorsoventral (DV) patterning than in all other insects studied so far. However, *Nasonia* lacks the BMP antagonist Short gastrulation/Chordin, which is essential for polarizing the BMP gradient along the DV axis in most bilaterian animals. Here, we present a broad survey of TGF-β signaling in *Nasonia* with aim to detect other lineage specific peculiarities and to identify potential mechanisms, which explain how BMP-dependent DV pattering occurs in the early *Nasonia* embryo in the absence of Sog.

Introduction

The TGF-β signaling pathway controls various processes throughout development, which include dorsoventral axis specification, cell proliferation, appendage formation as well as central nervous system patterning (1, 2). It consists of the extracellular ligands and their modulators, which interact with each other to

control ligand availability and distribution, of the receptors and of intracellular components, which assure signaling transduction and target gene expression (1, 3).

Most of the ligands belong to either the Bone Morphogenetic Protein (BMP) subfamily or the Activin/TGF-β subfamily (4, 5). Around 30 TGF-β ligands have been described in vertebrates and 7 for *Drosophila* and *Tribolium* (6, 7). Decapentaplegic (Dpp), Glass bottom boat (Gbb) and Screw (Scw) are the BMPs in *Drosophila* (8-10). Activin (Act), Activin-like protein 23b, which is also called Dawdle (Daw), and Myoglianin (Myo) belong to the Activin/TGF-β subfamily (11-13). Maverick (Mav) is highly diverged, and is not easily placed into either of the ligand subfamilies (14).

All TGF-β ligands form dimers and bind to a heteromeric receptor complex of two type I and two type II serine-threonine kinase receptors (3). In *Drosophila* the BMPs as well as the Activins use Punt as a common type II receptor, while specificity is generated by the type I receptors. BMP ligands bind the type I receptors Thickveins (Tkv) and Saxophone (Sax), whereas Activin/TGF-β ligands signal through the type I receptor Baboon (Babo) (1).

Upon ligand binding, the type I receptors become phosphorylated, which in turn phosphorylate and thereby activate receptor-regulated SMADs (R-SMADs). Tkv and Sax activate Mothers against Dpp (Mad) and Babo activates Smad on X (Smox). Once phosphorylated, R-Smads bind to the Co-Smad Medea and form a complex that translocates into the nucleus where they regulate target gene expression (1).

Inhibitory SMADs such as Daughters against Dpp (Dad) in *Drosophila* can compete with Medea and bind to R-Smads, thereby inhibiting translocation and target gene regulation (1).

On the extracellular level, a large variety of modulators are involved in controlling ligand availability and distribution. A prominent group of modulators, which usually act as BMP antagonists are characterized by an array of conserved

cysteine-rich domains that form cysteine knot structures (15). On the basis of spacing of the cysteine residues within the cysteine ring they have been grouped into several subgroups, e.g. the Noggins, the Chordin family, the Twisted gastrulation-like proteins, the Crossveinless 2 and the Dan family (15). In *Drosophila*, the main BMP antagonist in dorsoventral patterning is the Chordin homolog Short gastrulation (Sog), which interacts with Twisted gastrulation and is cleaved by the metalloprotease Tolloid (16).

Besides diffusible, secreted proteins several membrane-bound and extracellular matrix proteins have been shown to influence the efficiency of TGF-β signaling (17). Thus, in the *Drosophila* wing two glypicans, the GPI anchored Heparan-Sulphate Proteoglycans Dally and Dally-like are required for efficient BMP signaling activity (18) while type IV collagens control the range of the BMP signaling gradient in the embryo (19).

In our previous work we showed that the parasitic jewel wasp *Nasonia vitripennis* uses the BMP pathway to pattern the DV axis despite the fact that no *sog* ortholog is present in *Nasonia* (Özüak et al, unpublished). The main goal of this work is to provide an overview of the TGF-β pathway in *Nasonia* and to identify components, which might help to explain how the BMP signaling gradient is established during DV patterning in the wasp embryo.

Similar work was already done for the short germ beetle *Tribolium castaneum*, which revealed that the beetle retained a more ancestral composition of TGF-β signaling components compared to *Drosophila* (7, 20, 21).

In this work we describe, members of all different signaling components for the wasp. Interestingly, we found a case of parallel evolution, involving the duplication and divergence of the BMP 5/6/7/8 ligands in *Nasonia* and *Drosophila.* In addition we identified the BMP ligand ADMP, which is not present in *Drosophila* and *Tribolium*, but plays an important role in vertebrates (22). As we were unable to find a *sog* homolog in *Nasonia* we were especially interested to identify

alternative BMP antagonists, which might be expressed at the ventral side of the embryo. However, we failed to identify such inhibitors corroborating our functional studies which indicated that the DV BMP gradient of *Nasonia* is not shaped by an opposing inhibitory gradient, but rather by diffusion from a dorsal source region (Özüak et al. unpublished). Interestingly, the RNA of the type I receptor Tkv is localized to the dorsal midline of the developing *Nasonia* oocyte. In addition, one of the type II receptors is dorsally expressed in the early embryo. Based on these observations we discuss a possible scenario of how the embryonic BMP gradient in *Nasonia* is established in the absence of a ventral inhibitor.

Results/Discussion:

Ligands

So far seven TGF-β ligands are described in *Drosophila* and *Tribolium*. In the wasp *Nasonia* we found eight potential TGF-β ligands in the genome. In our previous work we described the important role of *Nv-dpp* in patterning the dorsal-ventral axis of the wasp embryo (Özüak et al. unpublished). Knocking down *Nv-dpp* leads to the loss of dorsal fates and an almost complete ventralization of the embryo. In our phylogenetic analysis, *Nv-dpp* groups perfectly with other insect Dpp sequences as well as their vertebrate homologs Bmp2/4 (Fig. 1A). During oogenesis *Nv-dpp* is expressed in the nurse cells and localized at the posterior pole of the oocyte (Fig. 2A). In the early embryo, *Nv-dpp* is ubiquitously expressed and after gastrulation is completed, it is expressed in two stripes that flank the extraembryonic region on the dorsal side of the embryo (Fig. 1 B, C).

Another important ligand for embryonic DV patterning in *Drosophila* is Screw, which represents a diverged paralog of Gbb (8, 10). *Drosophila* Gbb plays no role in DV patterning, but is required in later developmental processes such as wing formation (16). We found two paralogs of Nv-Gbb, but unlike in *Tribolium*,

where both Gbb paralogs are closer related to each other than to any other Gbb (7), the *Nasonia* Gbb paralogs are not closely related. Instead, Nv-Gbb1 groups together with other insect Gbbs and the vertebrate homologs Bmp 5/6/7/8, while Nv-Gbb2 shows signs of a very fast evolving gene such as *Drosophila screw*. Both genes are ubiquitously expressed during oogenesis as well as during early embryogenesis (Fig 1 D, F; Fig. 2 B, C). After gastrulation *Nv-gbb1* is expressed like *Nv-dpp* in two stripes at the dorsal side (Fig 1 E), while *Nv-gbb2* expression is gone. The knockdown of Nv-Gbb2 leads, like the knockdown of Nv-Dpp to a ventralization of the embryo (Özüak et al. unpublished). Interestingly, the knockdown of Nv-Gbb1 has no embryonic phenotype, suggesting that it plays no role in early embryonic DV patterning. It might however play a role in later embryonic or in postembryonic stages, which we could not, targeted by parental RNAi. Thus, the situation might be similar to *Drosophila* where one Bmp 5/6/7/8 paralog (*screw*) was subject to fast evolutionary changes adapting to the special requirements of early embryonic DV patterning while the other one (*gbb*) retaining ancestral sequence features is required for later (more generic) developmental processes.

ADMP (anti-dorsalizing morphogenetic protein) has a BMP-like activity in *Xenopus* (22). Despite its important role in vertebrates during D-V patterning, ADMP is not present in *Drosophila* and *Tribolium*. However, it is present in the Honeybee and we found an ortholog of ADMP in the wasp (Fig 1 A). It will be interesting to further investigate ADMP function in *Nasonia* to see if it also plays a role in self-regulation during embryonic D-V patterning.

Orthologs of ligands belonging to the Activin subfamily such as *act, daw*, and *myo* are found in *Nasonia*. All three are ubiquitously expressed in the early embryo and later no expression is detectable (Fig 1G-I). The last of the eight detected ligands is Maverick, which is not clearly grouped into one of the two large subfamilies. In *Drosophila*, Mav is required for growth in the wing disc. A knockdown of Mav leads to wing size reduction with normal veins pattern (23). We investigated the expression pattern of *Nv-mav* and found out that there is no

expression in the early embryo, but later after completion of gastrulation *Nv-mav* is expressed in two very narrow stripes flanking the extraembryonic region on the dorsal side (Fig 1 J, K).

Receptors

The extracellular BMP signal is transmitted via tetrameric receptor complexes formed by type I and type II receptors. Altogether our analyses revealed six *Nasonia* orthologs of *Drosophila* Serine-Threonine kinase receptors: two BMP type I receptors, *tkv* and *sax*, and the Activin receptor type I ortholog *babo* as well as type II receptors *wishful thinking (wit)* and two *punt* orthologs (Fig 3A). Aside from these receptors we also found BAMBI (not shown), which in vertebrates is known to be a pseudo receptor (24) and might play a role in inhibiting BMP signaling in *Nasonia* as well .

Nv-sax is ubiquitously expressed in the nurse cells and ubiquitously distributed in the oocyte (Fig 2D). *Nv-tkv* is also expressed in all nurse cells. However, in the oocyte, it shows a striking pattern of localization. Besides an anterior accumulation the RNA is found in a narrow stripe along the dorsal midline (Fig. 2G-I). The dorsal side can be identified via the position of the oocyte nucleus. (data not shown, (25)). Thus, *Nv-tkv* RNA localization during oogenesis closely resembles that of the *Nv-tgf-a*, which is involved in establishing the DV axis in *Nasonia* (25). In early embryos *Nv-tkv* is no longer localized and shows like *Nv-sax* ubiquitous expression (Fig. 3B, C). Knock down of both receptors using pRNAi has been performed in previous studies and resulted in the case of *Nv-sax* as well as *Nv-tkv* in a strong ventralization of the embryo (Özüak et al unpublished).

Similar to the type I receptors, *Nv babo* shows a uniform expression pattern in early *Nasonia* embryos (Fig. 3D). The presence of a *babo* homolog in *Nasonia* is interesting since previous studies on *Apis mellifera* revealed a lack of this gene (7),

indicating that the loss of Activin signaling via Baboon is not a general feature of the hymenoptera.

Furthermore, two homologous genes of the type II receptor Punt are present. *punt1* is not expressed during oogenesis (Fig 2E) However, it shows a distinct expression pattern along the dorsal midline in early blastoderm embryos (Fig. 3E), which strongly resembles the early expression patterns of previously described BMP signaling target genes in *Nasonia* (26).

In contrast to this, *punt2* is expressed during oogenesis and is localized at the posterior pole of the oocyte (Fig. 2F). This localization is not present in the embryo where *punt2* mRNA is distributed ubiquitously (Fig. 3F). Because of its maternal distribution, we knocked down *punt2*. Eclosed females that were injected with *punt2* dsRNA during yellow pupae stage, laid no eggs and had degenerated ovaries (data not shown). This phenotype could be due to defects in Activin or BMP signaling as *punt2* might be essential for both pathways.

Smads

SMADs are characterized by the presence of two Mad Homology (MH1 and MH2) domains. In addition, R-Smads have a C-terminal SXS motif. Upon ligand binding, the receptors pass on the signal by phosphorylating both serines in the SXS motif thereby activating the R-Smads (27). We identified four proteins with a MH1 and MH2 domain in the *Nasonia* genome, three of which contained a SXS motif (Fig. S1). Phylogenetic analysis revealed that two of the SXS motif containing proteins group together with *Drosophila* Mad and the third one with *Drosophila* Smox (Fig. 4A). It is worth mentioning that Nv-Mad2 is, similar to Nv-Gbb2 and Nv-Punt1, significantly more diverged in comparison to Nv-Mad1 and the other insect Mad orthologs. The fourth identified protein displayed clear homology to the Co-Smad Medea (Fig 4A). We could not identify any orthologs of known inhibitory Smads like Daughters against dpp (Dad).

During oogenesis *Nv-mad1* is ubiquitously expressed in the nurse cells and oocytes while *Nv-mad2* RNA accumulates at the posterior pole of the oocyte (Fig. 2J,K). *Nv-mad1* does not seem to have a conserved role in embryogenesis since it did not show any phenotype after pRNAi mediated knockdown. However, embryos of females injected with *Nv-mad2* dsRNA were severely ventralized as seen from the expansion of the ventral *twist* domain (Fig. 4C). This phenotype closely resembles the previously described knockdown phenotype of *Nv-dpp* and *Nv-gbb2* (Özüak et al unpublished).

Nv-smox is ubiquitously expressed during oogenesis (Fig. 2L) and pRNAi mediated knockdown resulted in sterile females (not shown) indicating an important role of Activin signaling during oogenesis. The *Nv-smox* phenotype suggests that the sterility caused by *Nv-punt2* knockdown is due to interference with Activin, rather than BMP signaling.

TGF-β modulators

At the extracellular level, the TGF-β pathway is influenced in many ways to fine tune ligand and receptor activity. While antagonists bind to ligands and inhibit them, cell surface proteins modulate the flux of the ligands (17). In our previous work we provided evidence that *Nasonia* is lacking *sog*, which is the main BMP antagonist in *Drosophila* and other insects. Sog belongs to the Chordin family, one of the subgroups of BMP antagonists. We searched for orthologs of other groups such as Noggin or members of the Dan family. While in *Tribolium* two members of the Dan family, Dan and Gremlin, are present, no orthologs of members of the Dan family nor Noggin are present in the *Nasonia* genome . However, like in *Drosophila* and *Tribolium* we found an ortholog of Follistatin, which preferentially antagonizes Activin rather than BMP (28). In *Nasonia*, *follistatin* is ubiquitously expressed during early embryogenesis and later after gastrulation in two narrow stripes that flank the extraembryonic region on the dorsal side of the embryo (Fig 5. A, E)

Despite the absence of *sog* three *Nasonia* orthologs of Twisted gastrulation/Crossveinless1 (Nv-Cva-c) were discovered in an earlier study (21). In *Drosophila* Tsg is thought to be a part of the Sog–Dpp complex. In this complex Tsg can have a pro- as well as an anti-BMP function. It was suggested that Tsg acts anti-BMP by enhancing the binding of Sog to Dpp and pro-BMP by enhancing the cleavage of Sog by the metalloprotease Tolloid (16). In our previous studies with *Nasonia* using *Nv-tsg1* pRNAi a pro BMP role for Tsg during embryogenesis was observed since embryos of injected females were severely ventralized (Özüak et al, unpublished). An exclusively pro BMP role for Tsg was also observed in *Tribolium castaneum* (21). Interestingly, this pro-BMP function of Tc-Tsg was described to be Sog independent. Since *Nasonia* apparently lacks Sog, the pro-BMP function of Tsg in *Nasonia* should also be Sog-independent.

Finally, we were able to identify four Crossveinless 2 like molecules (Cv2a-Cv2d) (Fig. 5Q). Cv2 proteins consist of similar domains as Sog/chordin proteins, but are thought to tightly interact with the type I receptors and /or membrane anchored proteoglycans and therefore lack diffusibility (29). *cv2c* and *cv2d* show a uniform expression in early *Nasonia* blastoderm embryos and weak uniform expression during later embryonic development (Fig.5 C,D,G,H). *cv2a* is first expressed in small patches on the dorsal side at cellularized blastoderm stage (Fig 5B). During development these patches widen towards the anterior and elongate towards posterior. At the onset of gastrulation *cv2A* is expressed in two narrow stripes flanking the presumptive serosa (Fig. 5F). We were not able to clone *cv2b* indicating that this gene might be a pseudogene, or is expressed only during postembryonic development.

Besides the antagonists we found several orthologs of cell surface proteins that are candidates for modulating the flux of BMP ligands and facilitating long range signaling activity. Among these are orthologs of Dally, Glypican4, CollagenIV and Pentagone (17, 30). In early blastoderm embryos all are ubiquitously expressed (Fig. 5I-L). Later, after gastrulation is completed, all of

them show a distinct pattern. *Nv-dally* is expressed in a dotted pattern of two stripes flanking the ventral midline (Fig. 5M). *Nv-glypican4* is expressed in segmental stripes on the ventral half of the embryo (Fig. 5N). *Nv-collagenIV* is expressed in small patches at the anterior and posterior of the embryo (Fig. 5O). The expression pattern of *Nv-pentagone*, two ventral stripes, resembles strongly that of *Nv-ind*, a neuroectodermal marker, which we described in our previous work (Fig. 5P) (26).

Taken together this work indicates that *Nasonia* has retained some components of an ancestral TGF-β signaling network, such as ADMP and Bambi that have been lost in other insect lineages (7). However, *Nasonia* also shows high degrees of divergence in some key signaling components with essential functions for embryonic DV patterning like Gbb2, Mad2 and Punt1. The most striking observation is that *Nasonia* has lost some families of BMP antagonists including Sog, which plays a crucial in DV pattering in most bilaterian animals (31). Our earlier work indicates that *Nasonia* indeed radically deviates from the mode of DV patterning found in most other animals. Apparently, *Nasonia* establishes its DV axis in a bipolar fashion using independent signaling sources along the ventral and dorsal midline (Özüak et al., unpublished). These signaling sources are established during oogenesis. The oocytes of *Nasonia* like those of *Apis*, the other hymenopteran species studied so far, show an amazing ability to precisely localize mRNAs not only to the anterior and posterior poles (Fig. 2AG), but also along the dorsal midline (25, 32, 33). Thus, in *Nasonia* and *Apis* the RNA of TGF-a is localized in narrow dorsal stripe and the secreted TGF-a ligand initiates EGF signaling at the dorsal side of the follicular epithelium along the entire egg length (25, 34). In *Nasonia* functional studies show that EGF signaling negatively regulates the formation of eggshell cues required to localize a ventral source for embryonic DV patterning (25). However, both hymenopteran species are also able to localize the RNA for BMP signaling components along the dorsal midline of the oocyte. For *Apis* the RNA of the ligand Dpp is localized (34) while in *Nasonia* as shown in this

study the RNA of the type I receptor Tkv is localized. If proteins produced by these localized RNAs are inserted into the membrane and remain there until egg deposition and early embryogenesis they might become sources for establishing signaling gradients in the embryo. In this context our finding is interesting that one of the type II receptors punt1 is expressed along the dorsal midline in early embryos. This indicates that in *Nasonia* a positive feedback of BMP signaling is established along the dorsal midline at early stages of development. Further studies are required to investigate whether maternal receptor localization coupled to zygotic positive feedback are sufficient to account for the long range BMP gradient from which we have shown earlier that it is crucial for patterning the entire DV axis of the embryo (Özüak et al*,* unpublished).

References

1. L. Parker, D. G. Stathakis, K. Arora, Regulation of BMP and activin signaling in Drosophila., Prog. Mol. Subcell. Biol. 34, 73–101 (2004).
2. H. Chang, C. W. Brown, M. M. Matzuk, Genetic analysis of the mammalian transforming growth factor-beta superfamily., Endocr. Rev. 23, 787–823 (2002).
3. C. Sieber, J. Kopf, C. Hiepen, P. Knaus, Recent advances in BMP receptor signaling., Cytokine Growth Factor Rev. 20, 343–55 (2009).
4. Y. Yamamoto, M. Oelgeschläger, Regulation of bone morphogenetic proteins in early embryonic development., Naturwissenschaften 91, 519–34 (2004).
5. A. P. Hinck, Structural studies of the TGF-βs and their receptors - insights into evolution of the TGF-β superfamily., FEBS Lett. 586, 1860–70 (2012).
6. B. Schmierer, C. S. Hill, TGFbeta-SMAD signal transduction: molecular specificity and functional flexibility., Nat. Rev. Mol. Cell Biol. 8, 970–82 (2007).
7. M. Van der Zee, R. N. da Fonseca, S. Roth, TGFbeta signaling in Tribolium: vertebrate-like components in a beetle., Dev. Genes Evol. 218, 203–13 (2008).
8. K. Arora, M. S. Levine, M. B. O'Connor, The screw gene encodes a ubiquitously expressed member of the TGF-beta family required for specification of dorsal cell fates in the Drosophila embryo., Genes Dev. 8, 2588–601 (1994).

9. R. W. Padgett, R. D. St Johnston, W. M. Gelbart, A transcript from a Drosophila pattern gene predicts a protein homologous to the transforming growth factor-beta family., Nature 325, 81–4 (1987).
10. K. A. Wharton, G. H. Thomsen, W. M. Gelbart, Drosophila 60A gene, another transforming growth factor beta family member, is closely related to human bone morphogenetic proteins., Proc. Natl. Acad. Sci. U. S. A. 88, 9214–8 (1991).
11. G. Kutty et al., Identification of a new member of transforming growth factor-beta superfamily in Drosophila: the first invertebrate activin gene., Biochem. Biophys. Res. Commun. 246, 644–9 (1998).
12. L. Parker, J. E. Ellis, M. Q. Nguyen, K. Arora, The divergent TGF-beta ligand Dawdle utilizes an activin pathway to influence axon guidance in Drosophila., Development 133, 4981–91 (2006).
13. P. C. Lo, M. Frasch, Sequence and expression of myoglianin, a novel Drosophila gene of the TGF-beta superfamily., Mech. Dev. 86, 171–5 (1999).
14. M. Nguyen, L. Parker, K. Arora, Identification of maverick, a novel member of the TGF-beta superfamily in Drosophila., Mech. Dev. 95, 201–6 (2000).
15. D. W. Walsh, C. Godson, D. P. Brazil, F. Martin, Extracellular BMP-antagonist regulation in development and disease: tied up in knots., Trends Cell Biol. 20, 244–56 (2010).
16. M. B. O'Connor, D. Umulis, H. G. Othmer, S. S. Blair, Shaping BMP morphogen gradients in the Drosophila embryo and pupal wing., Development 133, 183–93 (2006).
17. M.-C. Ramel, C. S. Hill, Spatial regulation of BMP activity., FEBS Lett. 586, 1929–41 (2012).
18. J. L. Erickson, Formation and maintenance of morphogen gradients: an essential role for the endomembrane system in Drosophila melanogaster wing development., Fly (Austin). 5, 266–71 (2011).
19. H. L. Ashe, Type IV collagens and Dpp: positive and negative regulators of signaling., Fly (Austin). 2, 313–5 (2008).
20. M. van der Zee, O. Stockhammer, C. von Levetzow, R. Nunes da Fonseca, S. Roth, Sog/Chordin is required for ventral-to-dorsal Dpp/BMP transport and head formation in a short germ insect., Proc. Natl. Acad. Sci. U. S. A. 103, 16307–12 (2006).
21. R. Nunes da Fonseca, M. van der Zee, S. Roth, Evolution of extracellular Dpp modulators in insects: The roles of tolloid and twisted-gastrulation in dorsoventral patterning of the Tribolium embryo., Dev. Biol. 345, 80–93 (2010).

22. B. Reversade, E. M. De Robertis, Regulation of ADMP and BMP2/4/7 at opposite embryonic poles generates a self-regulating morphogenetic field., Cell 123, 1147–60 (2005).
23. C. F. Hevia, J. F. de Celis, Activation and function of TGFβ signalling during Drosophila wing development and its interactions with the BMP pathway., Dev. Biol. 377, 138–53 (2013).
24. D. Onichtchouk et al., Silencing of TGF-beta signalling by the pseudoreceptor BAMBI., Nature 401, 480–5 (1999).
25. J. A. Lynch, A. D. Peel, A. Drechsler, M. Averof, S. Roth, EGF signaling and the origin of axial polarity among the insects., Curr. Biol. 20, 1042–7 (2010).
26. T. Buchta, O. Ozüak, D. Stappert, S. Roth, J. a Lynch, Patterning the dorsal-ventral axis of the wasp Nasonia vitripennis., Dev. Biol. , 1–14 (2013).
27. X.-H. Feng, R. Derynck, Specificity and versatility in tgf-beta signaling through Smads., Annu. Rev. Cell Dev. Biol. 21, 659–93 (2005).
28. J. Pentek, L. Parker, A. Wu, K. Arora, Follistatin preferentially antagonizes activin rather than BMP signaling in Drosophila., Genesis 47, 261–73 (2009).
29. A. L. Ambrosio et al., Crossveinless-2 Is a BMP feedback inhibitor that binds Chordin/BMP to regulate Xenopus embryonic patterning., Dev. Cell 15, 248–60 (2008).
30. R. Vuilleumier et al., Control of Dpp morphogen signalling by a secreted feedback regulator., Nat. Cell Biol. 12, 611–7 (2010).
31. C. M. Mizutani, E. Bier, EvoD/Vo: the origins of BMP signalling in the neuroectoderm., Nat. Rev. Genet. 9, 663–77 (2008).
32. J. A. Lynch, A. E. Brent, D. S. Leaf, M. A. Pultz, C. Desplan, Localized maternal orthodenticle patterns anterior and posterior in the long germ wasp Nasonia., Nature 439, 728–32 (2006).
33. M. J. Wilson, P. K. Dearden, RNA localization in the honeybee (Apis mellifera) oocyte reveals insights about the evolution of RNA localization mechanisms., Dev. Biol. 375, 193–201 (2013).
34. M. J. Wilson, H. Abbott, P. K. Dearden, The evolution of oocyte patterning in insects: multiple cell-signaling pathways are active during honeybee oogenesis and are likely to play a role in axis patterning., Evol. Dev. 13, 127–37 (2011).

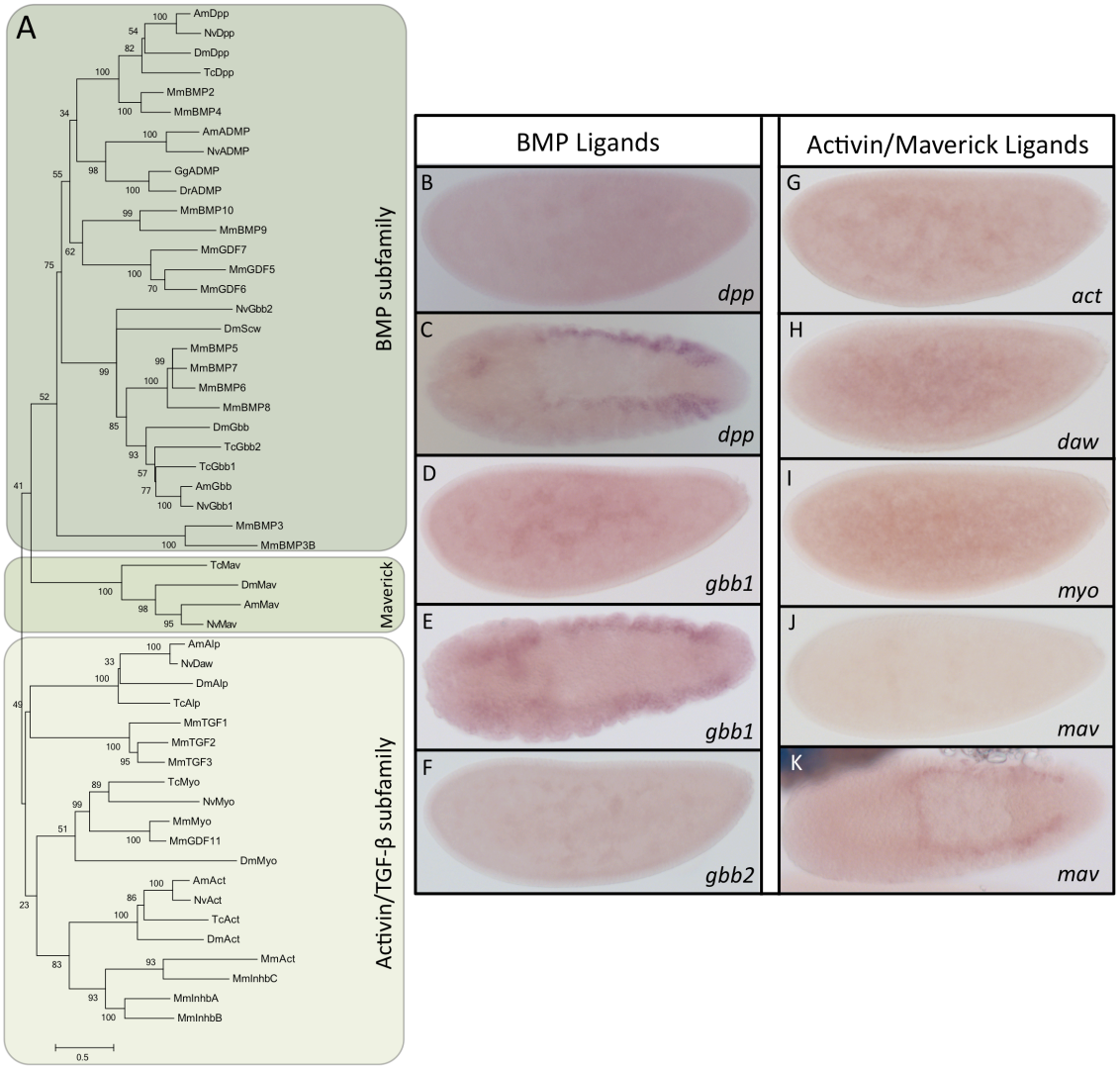

Figure 1. Ligands

(A) Maximum likelihood tree of TGF-β ligands in different insect and vertebrate species. Bootstrap values (1,000 replicates) are indicated in percentages. Amino acid substitution model: WAG+i+g. Nv *Nasonia vitripennis;* Am *Apis mellifera*; Dm *Drosophila melanogaster*; Tc *Tribolium castaneum*; Mm *Mus musculus*; Gg *Gallus gallus*; Dr *Danio rerio*.

(**B, D, F, G, H, I, J**) Early and (**C, E, K**) late ISH of BMP Ligands (**B-F**) and Activin/Maverick ligands (**G-K**) for *dpp* (**B, C**), *gbb1* (**D, E**), *gbb2* (**F**), *act* (**G**), *daw* (**H**), *myo* (**I**), *mav* (**J, K**). **B, D, F, G, H, I, J** lateral view. **C, E, K** dorsal view. Anterior is left.

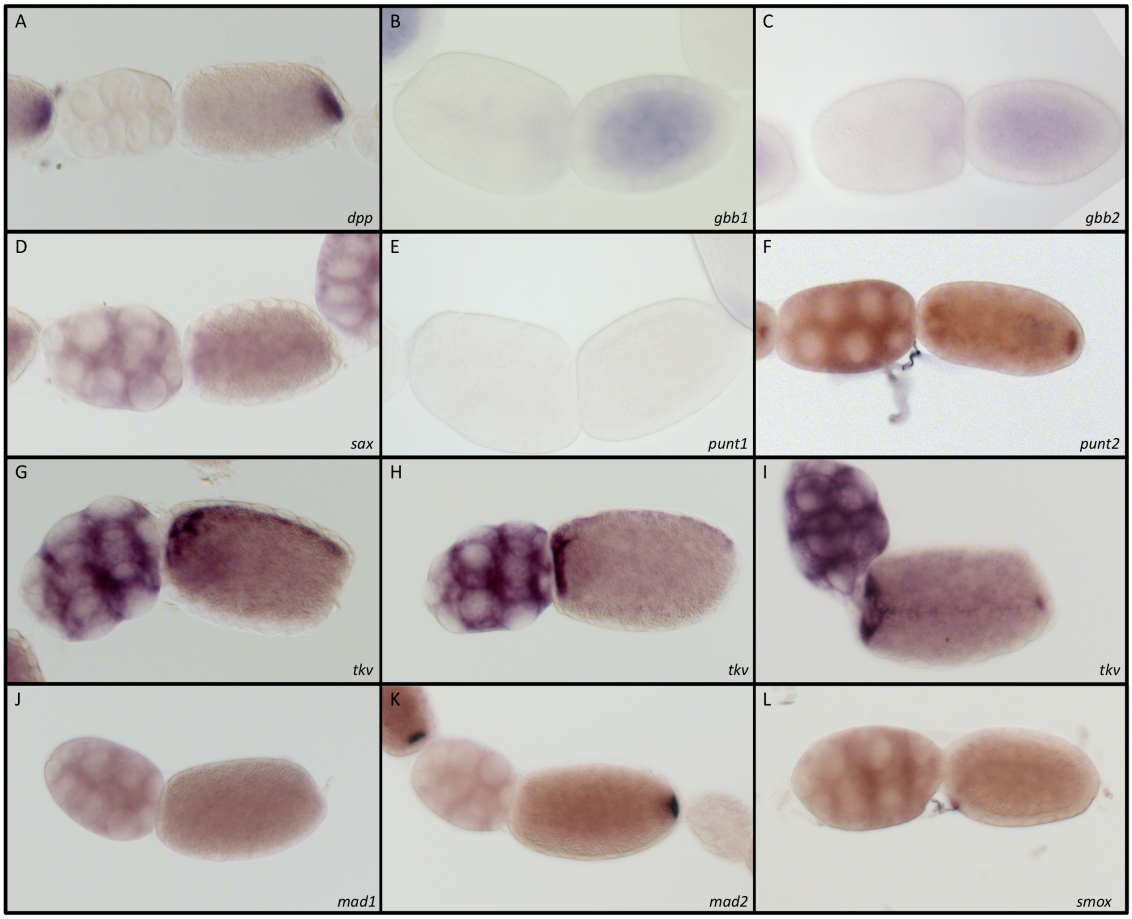

Figure 2. BMP components in Nasonia ovaries
Expression of (**A**) *dpp*, (**B**) *gbb1*, (**C**) *gbb2*, (**D**) *sax*, (**E**) *punt2*, (**F**) *punt1*, (**G-I**) *tkv* in lateral (**G-H**) and dorsal (**I**) view, *mad1* (**J**), *mad2* (**K**) and *smox* (**L**) in *Nasonia* ovaries.

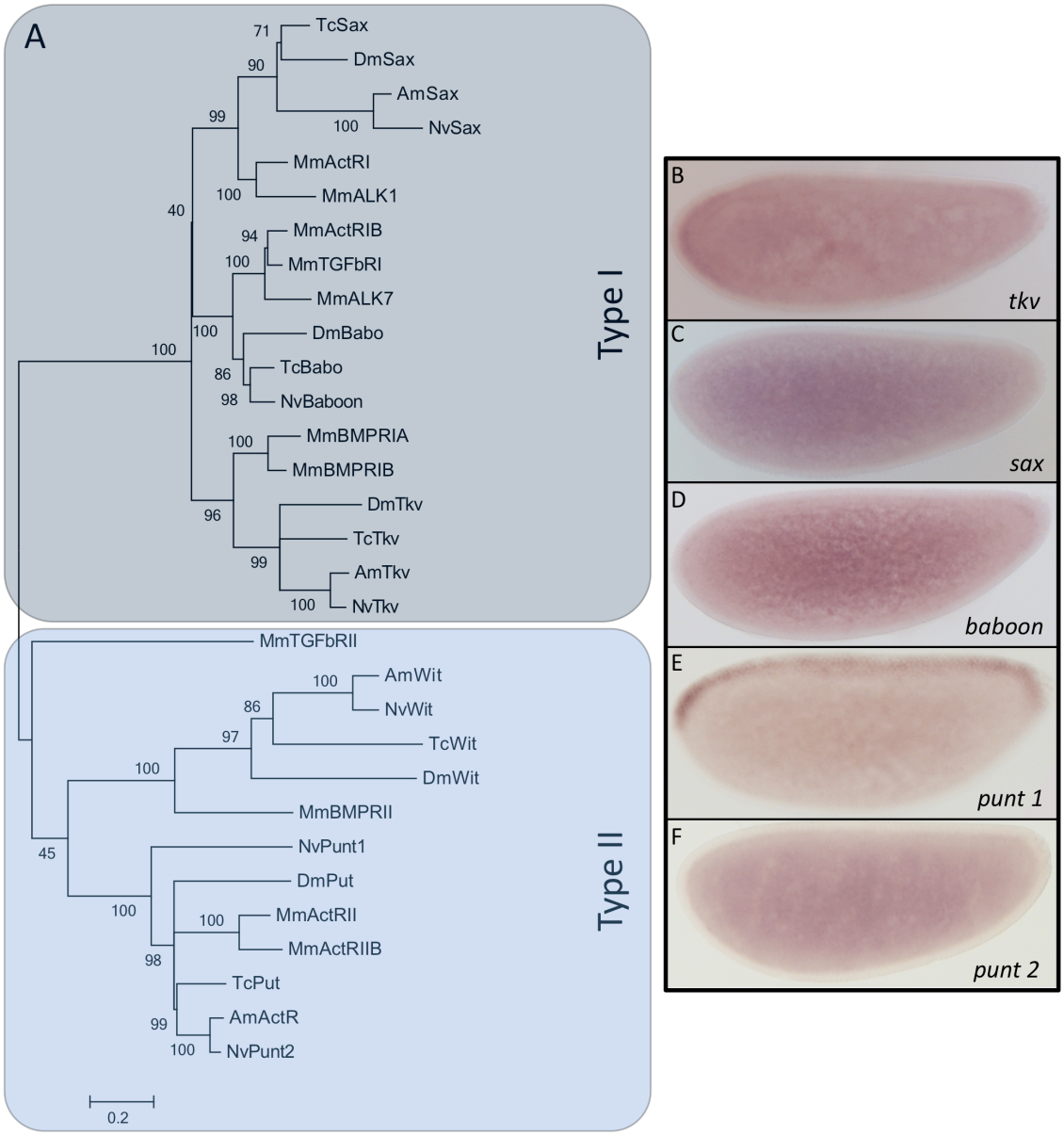

Figure 3. Receptors

(**A**) Maximum likelihood tree of type I and type II receptors in different insect and vertebrate species. Bootstrap values (1,000 replicates) in percentages. Amino acid substitution model: WAG+i+g. Nv *Nasonia vitripennis*; Am *Apis mellifera*; Dm *Drosophila melanogaster*; Tc *Tribolium castaneum*; Mm *Mus musculus*, see main text for protein abbreviations. (**B-F**) expression pattern of (**B**) *thickveins*, (**C**) *saxophone*, (**D**) *baboon*, (**E**) *punt1*, (**F**) *punt2* in *Nasonia* embryos. Anterior is left.

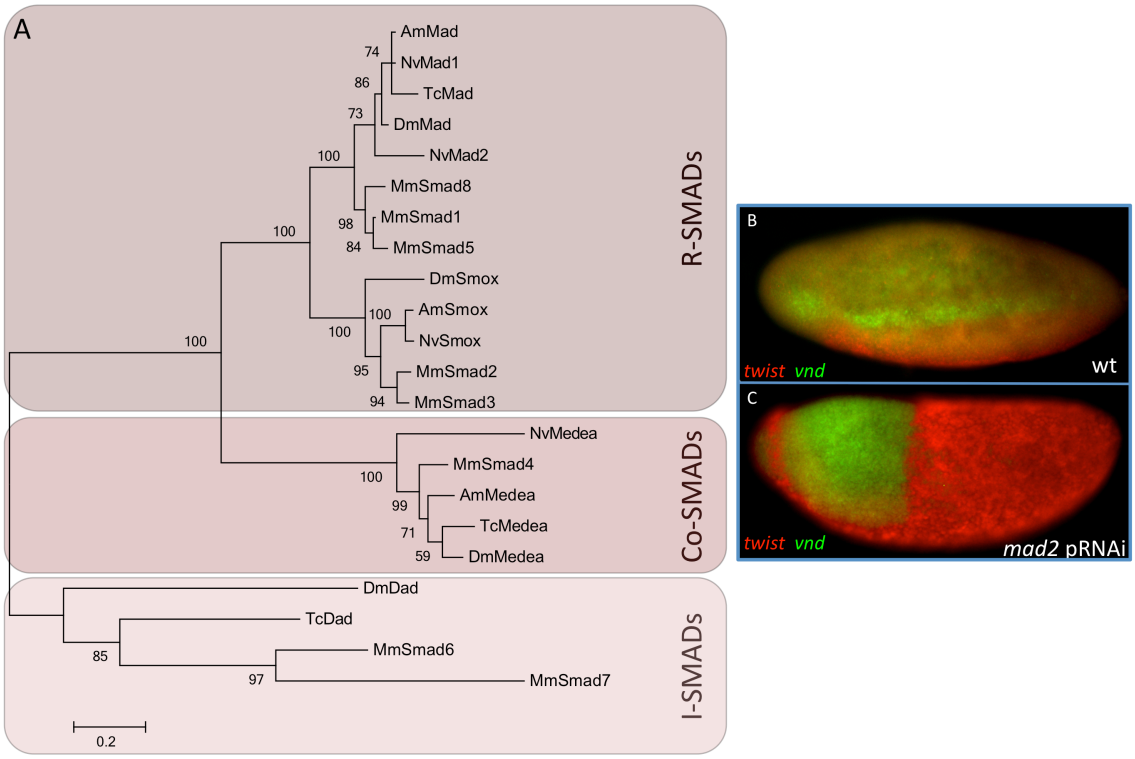

Figure 4. SMADs

(**A**) Maximum likelihood tree of SMADs in different insect and vertebrate species. Bootstrap values (1,000 replicates) in percentages. Amino acid substitution model: WAG+i+g. Nv *Nasonia vitripennis*; Am *Apis mellifera*; Dm *Drosophila melanogaster*; Tc *Tribolium castaneum*; Mm *Mus musculus*. **(B-C**) Lateral view of wildtype (**B**) and *mad2* knockdown (**C**) *Nasonia* embryos showing expression pattern of *twi* (red) and *vnd* (green). Anterior is left.

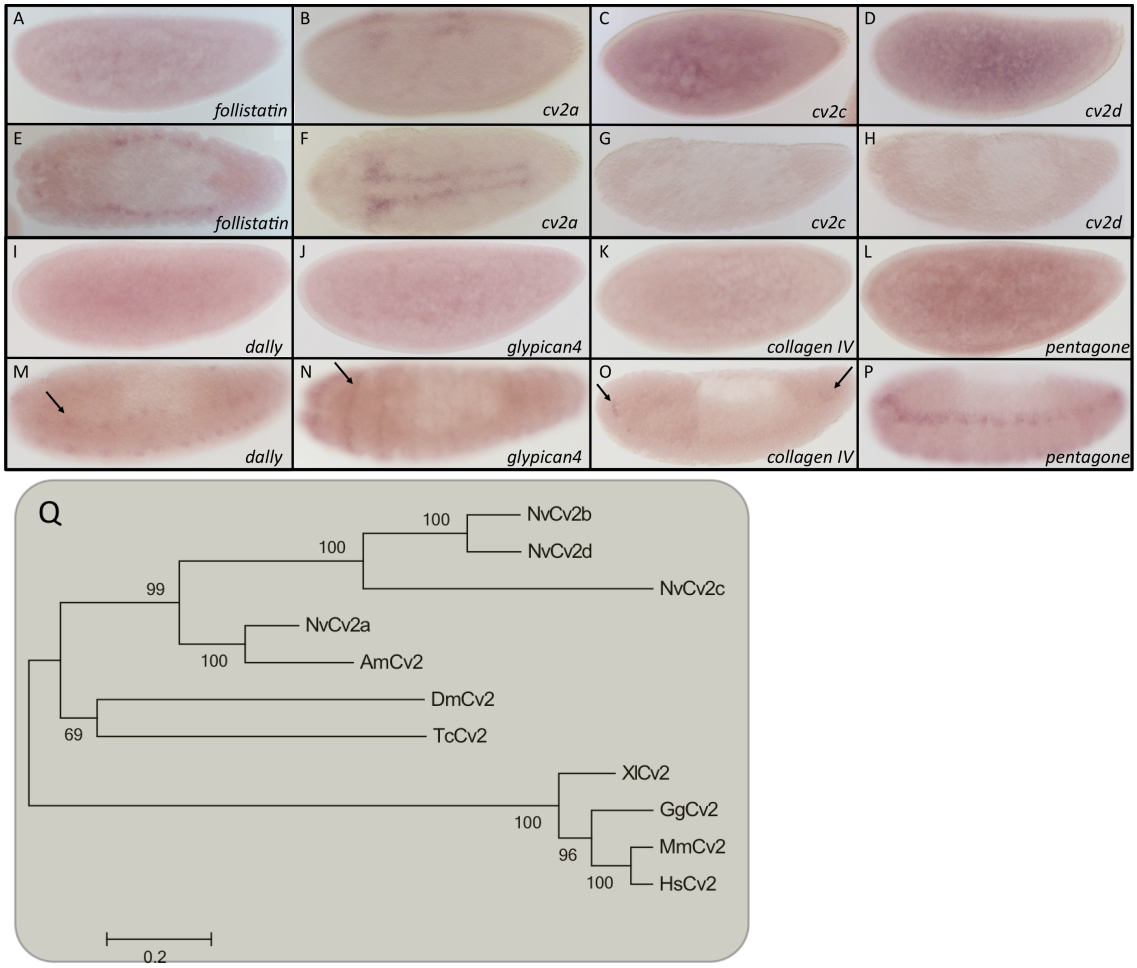

Figure 5. Extracellular modulators

Early (**A-D, I-L**) and late (**E-H, M-P**) expression of *follistatin* (**A, E**), *cv2a* (**B, F**), *cv2c* (**C, G**), *cv2d* (**D, H**), *dally* (**I, M**), *glypican4* (**J, N**), *collagen IV* (**K, O**), *pentagone* (**L, P**) in *Nasonia* embryos.

A-D, I-L, O, P lateral view. **E, F** dorsal view. **G, H, O** dorsolateral view. **N** ventral view. Anterior is the right. (**Q**) Maximum likelihood tree of *crossveinless2* in different insect and vertebrate species . Bootstrap values (1,000 replicates) in percentages. Amino acid substitution model: WAG+i+g. Nv *Nasonia vitripennis*; Am *Apis mellifera*; Dm *Drosophila melanogaster*; Tc *Tribolium castaneum*; Mm *Mus musculus;* Hs *Homo sapiens;* Gg *Gallus gallus;* Xl *Xenopus laevis*.

Supplementary Figure 1
Part of a Smad protein alignment showing the conserved MH2 and SXS domain.

Material and methods

Embryo and ovary collection

All *N. vitripennis* embryos were collected using the *Waspinator* and fixed as described in [1]. Nasonia ovaries were dissected and fixed as described in [2].

ISH

Single in Situ hybridizations for Nasonia and Drosophila were performed as previously described [3]. Two-color ISH was performed as described in [4]

RNAi

Young *N. vitripennis* pupae were injected as in [5].

1. Buchta, T., Özüak, O., et al., Patterning the dorsal–ventral axis of the wasp *Nasonia vitripennis*. Dev. Biol. (2013), http://dx.doi.org/10.1016/j.ydbio.2013.05.026

2. Lynch, J.A., Peel, A.D., Drechsler, A., Averof, M., Roth, S., 2010. EGF signaling and the origin of axial polarity among the insects. Curr. Biol.: CB 20, 1042–1047.

3. Brent, A.E., Schweitzer, R., Tabin, C.J., 2003. A somitic compartment of tendon progenitors. Cell 113, 235–248. Bull,

4. Mazzoni, E.O., Celik, A., Wernet, M.F., Vasiliauskas, D., Johnston, R.J., Cook, T.A., Pichaud, F., and Desplan, C. (2008). Iroquois complex genes induce co-expression of rhodopsins in Drosophila. PLoS Biol. 6, e97. 27.

5. Lynch, J.A., and Desplan, C. (2006). A method for parental RNA interference in the wasp *Nasonia vitripennis*. Nat. Protoc. 1, 486–494.

Gene identification, phylogenetic analysis

Conserved domains of TGFβ signaling components were identified by TBLASTN (Altschul et al. 1997) on NCBI. The protein sequences were aligned with muscle 3.7 (http://www.drive5.com/muscle/index.htm). Alignment refinement was performed using GBLOCKS 0.91b (http://molevol.cmima.csic.es/castresana/Gblocks.html). Maximum likelihood

Trees were edited in MEGA5.2.2 (Kumar et al. 2004)(http://www.megasoftware.net/index.php).

NCBI accession numbers for ligands

Am Dpp XP_001122815.2; Dm Dpp AAN10431.1; Tc Dpp EFA02913.1; Mm BMP2 NP_031579.2; Mm BMP4 AAC37698.1; Mm BMP10 NP_033886.2; Mm BMP9 AAD56961.1; Mm GDF5 NP_032135.2; Mm GDF6 NP_038554.1; Mm GDF7 NP_038555.1; Dm Scw AAN11056.2; Dm Gbb AAF47075.1; Am Gbb XP_394252.1; Tc Gbb1 EFA04645.1; Tc Gbb2 EFA04646.1; Mm BMP5 NP_031581.2; Mm BMP8 NP_001242948.1; Mm BMP6 NP_031582.1; Mm BMP7 NP_031583.2; Mm BMP3 NP_775580.1; Mm BMP3B NP_665684.2; Am ADMP XP_003251013.1; Gg ADMP AAD52011.1; Dr ADMP NP_571951.2; Tc Mav EFA11885.1; Dm Mav AAF59328.1; Am Mav XP_001122118.2; Am Alp XP_001122210.1; Dm Alp NP_523461.1; Tc Alp EFA11884.1; Am Act XP_001123044.2; Dm Act NP_651942.2; Tc Act EFA05602.1; Mm Act NP_032408.2; Mm InhbA NP_032406.1; Mm InhbB NP_032407.1; Mm InhbC NP_034695.1; Dm Myo AAF59319.1; Tc Myo EFA05753.1; Mm Myo AAO46885.1; Mm GDF11 NP_034402.1; Mm TGF1 NP_035707.1; Mm TGF2 NP_033393.2; Mm TGF3 NP_033394.2; Nv Dpp XP_001607677.1; Nv Gbb1 XP_001603876.1; Nv Gbb2 XP_001603269.2; Nv ADMP XP_001604750.2; Nv Myo XP_001602255.2; Nv Mav XP_001606148.2; Nv Act XP_001602284.1; Nv Alp XP_003425497.1

NCBI accession numbers for receptors

Tc Tkv EFA09250.1; Dm Tkv AAN10533; Am Tkv XP_391989; Mm BMPRIA P36895; Mm BMPRIB NP_031586; Tc Sax EFA07576.1; Dm Sax AAF59189; Am Sax XP_001121528; Mm ActRI NP_031420; Mm ActRIB NP_031421; Mm ALK1 Q61288;

Tc Babo EFA01312.1; Dm Babo AAF59011; Mm TGFbrI XM_006537756.1; Mm ALK7 NP_620790; Tc Wit XP_974821.1; Am Wit XP_397334; Dm Wit AAF47832; Mm BMPRII NP_031587; Tc Put EEZ97734.1; Am ActR XP_395928; Dm Put AAF55079; Mm ActRII CAM14875; Mm ActRIIB NP_031423; Nv Wit XP_003428148.1; Nv Tkv XP_001601240.2; Nv Sax XP_003426889.1; Nv Babo XP_003427942.1; Nv Put1 XP_001606053.1; Nv Put2 XP_001603863.1;

NCBI accession numbers for SMADs

Dm Mad AAF51142.1; Dm Smox NP_511079.1; Am Mad XP_392819.3; Am Smox XP_396056.4; Mm Smad1 NP_032565.2; Mm Smad5 NP_032567.1; Mm Smad8 AAF77079.2; Mm Smad2 NP_034884.2; Mm Smad3 NP_058049.3; Dm Dad NP_477260.1; Tc Dad EEZ99343.1; Mm Smad6 NP_032568.3; Mm Smad7 NP_001036125.1; Am Medea XP_392838.4; Tc Medea EFA11586.1; Dm Medea NP_524610.1; Mm Smad4 NP_032566.2; Nv Mad1 XP_001601460.2; Nv Mad2 XP_001602991.1; Nv Mad3 XP_001608214.2; Nv Medea XP_003427724.1; Tc Mad EFA05663.1

NCBI accession numbers for Crossveinless2

Nv Cv2a XP_001601040.2; Nv Cv2b XP_001599339.1; Nv Cv2c XP_001603432.2; Nv Cv2d XP_001599102.2; Dm Cv2 AAG01337.2; Tc Cv2 EFA10783.1; Am XM_006570432.1; Gg NP_001007081.1; Mm Cv2 AAN45857.1; Xl Cv2 AAX12852.1; Hs Cv2 AAP89012.1;

ISH Primers

Gene	Primer	Sequence	Accession Nr.
twist	Forward	ggCCgCgggCTTCTCgCCCAgTAACAAC	XM_001605767
	Reverse	CCCggggCACgTTAgCCATgACCCTCTg	XM_001605767
vnd	Forward	ggCCgCgggTCggACTgCTCAACAACTg	XM_001604500
	Reverse	CCCggggCAggTTCCAggAgCTTCgACT	XM_001604500
dpp	Forward	ggccgcggGTGGTGGGCGAGGCGGTAAA	XP_001607677.1
	Reverse	cccggggcCACGACCTTGTTCTCCTCGT	XP_001607677.1
gbb1	Forward	ggccgcggCCAAGTTCCTCCTGGACATC	XP_001603876.1
	Reverse	cccggggcGATGATCCAGTCCTGCCACT	XP_001603876.1
gbb2	Forward	ggccgcggATCCTGCTGCAGTTCGACTT	XP_001603269.2
	Reverse	cccggggcCCCTGATGATCATGTTGTGG	XP_001603269.2
activin	Forward	ggccgcggGACGACTTCTACGCGAGGAC	XP_001602284.1
	Reverse	cccggggcCTCGATCACGTGCGTGTAGT	XP_001602284.1
alp	Forward	ggccgcggAGCTTCTACGGCAAGACCAA	XP_003425497.1
	Reverse	cccggggcGAGCAGCAGGGCACTATTTC	XP_003425497.1
myostatin	Forward	ggccgcggCTCTCGCTTTGGATCTACGG	XP_001602255.2
	Reverse	cccggggcCGATCTGGTACTCGTTGTCG	XP_001602255.2

maverick	Forward	ggccgcggGGCGAGTCAAAGAAGTGCTG	XP_001606148.2
	Reverse	cccggggcTCAGGAGCAAGCGCACTC	XP_001606148.2
mad1	Forward	ggccgcggGCCCCACAACGTCTCATACT	XP_001601460.2
	Reverse	cccggggcACATCCTGGCGATGGTACTC	XP_001601460.2
mad2	Forward	ggccgcggTGAATCAACCATGCCTCAAA	XP_001602991.1
	Reverse	cccggggcGCATCTCGATCCAACAAGGT	XP_001602991.1
mad3	Forward	ggccgcggCAGAAGAGGGACGAGGTCTG	XP_001608214.2
	Reverse	cccggggcTGTCGTCTTGTTTGCTCGAC	XP_001608214.2
tkv	Forward	ggCCgCggTACCCCACATCCAggAgAAg	XP_001601240.2
	Reverse	CCCggggCgAAgATCTCggTgTgCAggT	XP_001601240.2
sax	Forward	ggCCgCgggCTCTTACCCTCCAgACACg	XP_003426889.1
	Reverse	CCCggggCTgCTTTTgTgTgCCAACATT	XP_003426889.1
baboon	Forward	ggccgcggTGCGAAACTGATGGCTACTG	XP_003427942.1
	Reverse	cccggggcTCCGACGATCTCCATGTGTA	XP_003427942.1
puntI	Forward	ggccgcggTCTCAAGCAGAGCAGGGAAT	XP_001606053.1
	Reverse	cccggggcGAAGCAAGTTCCCAGAGCAC	XP_001606053.1
puntII	Forward	ggccgcggGCGCCTACCTAGCGATACTG	XP_001603863.1
	Reverse	cccggggcCTTCTCAACGCCGATAAAGC	XP_001603863.1
follistatin	Forward	ggCCgCggAgCgAggAggACTACgACAA	XP_001607105.2
	Reverse	CCCggggCAgCTCggATAggTgACgTTg	XP_001607105.2
cv2a	Forward	ggccgcggGGCGTTATTACGGAATCGAA	XP_001601040.2
	Reverse	cccggggcTCGCCGAAGACAGTACACAC	XP_001601040.2
cv2c	Forward	ggccgcggGTTGTCCTCATTGCGAAGGT	XP_001603432.2
	Reverse	cccggggcTCGGTATGGCAAATCAACAA	XP_001603432.2
cv2d	Forward	ggccgcggAGCGTCACTGCACAACTGTC	XP_001599102.2
	Reverse	cccggggcCAAGTTGTCTGCTGCTCTCG	XP_001599102.2
dally	Forward	ggccgcggGCGACATTCCCAAACAGATT	XP_003425386.1
	Reverse	cccggggcGACAACCGTCTTGGCGTATT	XP_003425386.1
glypican4	Forward	ggccgcggGCACACAAGGGCCACTAAAT	XP_001607767.2
	Reverse	cccggggcCGTCGTCGATCTCTTTGTGA	XP_001607767.2
collagenIV	Forward	ggccgcggCTTCGGAACGTGGAGAGAAG	XP_003427100.1
	Reverse	cccggggcGCCAACCAGAAGCTGAACTC	XP_003427100.1
pentagone	Forward	ggccgcggCCTAGACCGGGACGAGTACA	XP_001601094.2
	Reverse	cccggggcGTACCTCGGCAGTTTCTTGC	XP_001601094.2

3 Additional Material & Methods

3.1 Stock keeping

In order to maintain a stock of *Nasonia vitripennis*, freshly eclosed wasps are first honey fed for two days, using a honey water soaked filter paper (Fig. 1). Then around 25 females are transferred together with fresh hosts (*Calliphora sp*. pupae) (Fig. 3.1) in a plastic vial and kept there for 4-5 days at room temperature. After that, the females will be removed and the parasitized hosts are stored at room temperature. In two weeks new wasps will eclose and the whole procedure can be repeated. Keeping the parasitized hosts at 18°C will extend eclosure for additional two weeks with a total developmental time of four weeks.

Figure 3.1 | Wasp stock with honey water soaked filter paper and *Calliphora sp*. pupae

3.2 Collection and fixation of embryos

The *Waspinator* is loaded with 19 fresh hosts and filled with up to 120 honey fed females. The wasps can now access all hosts at the same time and lay their eggs at the anterior tip of the hosts, as that is the only region exposed to the wasps. Egg laying time can be between an hour and a day, however it is recommended to not change the first round of hosts and leave them overnight. By doing this, females can adept to their new environment and will be less stressed.

To collect the embryos, parasitized hosts are cracked open at the anterior side and dipped into the fixing solution, which consists of 5% formaldehyde in PBS and the same amount of heptane. 3-6 hour old embryos are fixed over night. Older embryos can be fixed for an hour. After fixation, the lower formaldehyde phase is taken off and the same amount of ice cold 100% methanol is added followed by vigorous shaking of the fixation vial for at least a minute. Embryos that lost the vitelline membrane will sink to the bottom and can be collected and stored in an eppendorf tube filled with 100% methanol at -20°C.

Fixation solution: 2.5ml 10% formaldehyde
2.5ml PBS 1x
5ml heptane

3.3 *In situ* probe & dsRNA syntheses

3.3.1 Obtaining the sequence

- Go to flybase.org
- Enter the name of the gene into the quick search box
- Click on the search result corresponding to your gene
- In the text box above the "Get FASTA", chose "translations" to get the protein sequence of the gene

- Select the resulting protein sequence (highlight, then ctrl+C)
- Go back to flybase.org homepage, and click "blast" at the top of the page
    - For Database, choose GenBank protein
    - For Program, choose blastp
    - Past your sequence (ctrl+v) in the sequence box
    - Under the Species section, make sure only *Nasonia* box is checked
- Click on BLAST button, and wait for results
- Typically the *Nasonia* gene of interest will have the highest score (and lowest E-value) among multiple results. Click on the link (top-left) to the GenBank accession for the highest scoring *Nasonia* gene
- Scroll Down on this page, and click on the link for "CDS" (This will give you the DNA sequence coding for the protein that you have just found)
- On this page, change the Display box (lower right) to FASTA

Select and copy the sequence (ctrl+c) you might want to also paste into a text document for later use.

3.3.2 Designing the primers

- We will be using the online version of the program Primer3. Go to http://frodo.wi.mit.edu/
- Paste your sequence from above into large box at top of page
- Parameters:
    - Product size range should be in the range of 700-850bp. PCR products of this size work well in both making dsRNA and single stranded probes
    - The maximum primer size should be set to 22, but 20 bp is ideal
    - Leave other settings as default
- Press "pick primers" button

- By default, you will be given up to 5 primer pairs. Usually the first pair has the best characteristics (in regard to self and between primer complementarities)
- Select and copy the forward and reverse primers, and paste them into a text document (make sure you label and keep track of which is forward and which is reverse!)
- We will be using special Universal primers to make templates for RNAi and in situ probes, for this we need linker sequences on the 5′ end of each primer:
    - For the forward (sense) primer add the sequence ggccgcgg to the 5′ end

      For the reverse (antisense) add the sequence cccggggc to the 5′end

3.3.3 PCR

Primers

- Dissolve stock to 0.1 nanomole/microliter (100 microMolar) in distilled water
- Make working solution in eppi by diluting stock to 5 micromolar concentration (i.e. dilute primer stock 1:20)

First PCR:

- Do a 25 microliter reaction using the Red Taq mix from sigma
- The PCR mix is at 2x concentration
- The final concentration of each primer should be 0.2 micromolar
- Use 1 microliter of cDNA (made by the SMART RACE protocol)
- Use an annealing temperature of 57°C and do 35 cycles
- Check the reaction on a gel; you should have a single, bright band at the expected size. If this is so, purify PCR and sequence (if desired. If you will

not sequence the product, you do not have to purify and can proceed directly to second PCR). If other bands are present, either try the PCR again at a higher annealing temperature, or gel purify the correct band.

Second PCR:

- To make template for a labelled antisense probe, use the gene specific forward primer with the 3′ T7 universal primer (sequence: agggatcctaatacgactcactatagggcccggggc)
- To make a control sense probe, use the gene specific reverse primer with the T7 5′ universal (Sequence: gagaattctaatacgactcactatagggccgcgg)
- To make template for dsRNA, use both the T7 5′ and 3′ Universal primers.
- The concentrations of primers are the same as the first PCR
- Use 1 microliter of first PCR as template in each reaction
- Use same cycling parameters as first PCR

3.3.4 Making dig labelled probes

1. Make the T7 reaction master mix (Using Ambion T7 Maxiscript kit) in order below (volumes given for 1 reaction)

- 8 microliter RNAse free water
- 2 microliter transcription buffer
- 2 microliter dig labelling mix
- 2 microliter T7 RNA polymerase

- Using **Roche T7 Polymerase + Roche RNAse Inhibitor** (40U/microliter) (volumes given for 1 reaction)

- 7.5 microliter RNAse free water
- 2 microliter transcription buffer
- 2 microliter dig labelling mix

- 2 microliter T7 RNA polymerase
- 0.5 microliter RNAse inhibitor (20U/rxn)

2. Mix well, and quickly pipette into individual reaction tubes (14 microliter each)
3. Add 6 microliter PCR template to each reaction tube. Mix well.
4. Put reactions at 37 degree for 2-4 hours
5. Stop the reaction by adding 30 microliter water, and 50 microliter 2x stop solution (can remove 1-2 microliter to check on gel)
6. Add 5 microliter tRNA and 10 microliter Lithium Chloride
7. Add 300 microliter 100% ethanol, and precipitate for at least 30 minutes at -20°C
8. Centrifuge at 4 degrees 14000 rpm for 15 minutes
9. Decant supernatant
10. Add 300 microliter 70% ethanol, spin again for 5 minutes
11. Carefully remove all supernatant with pipette
12. Allow pellet to dry for about 5 minutes
13. resuspend pellet in 100 microliter resuspension solution
14. store at –20°C

resuspension solution: 50% formamide
5x SSC
in H_2O

3.3.5 Making dsRNA

1. Dilute the dsRNA template PCR reaction with an equal amount RNAse free water
2. Prepare the 20 microliter master mix, using the Ambion T7 Megascript Kit:

   a. 2 microliters each of the NTPs
   b. 2 microliters T7 transcription buffer
   c. 2 microliter of T7 polymerase mix
3. If making multiple dsRNAs, pipette 12 microliters each of master mix into individual reaction tubes
4. Add 8 microliter of dsRNA PCR template to master mix.
5. Mix well and place at 37°C for 4 hours- overnight
6. Stop reaction by adding 115 microliter RNAse free water, and 15 microliter Ammonium acetate stop solution.
7. Purify by adding 150 microliter Phenol:Chloroform
   a. Vortex or shake for about 1 minute
   b. Centrifuge at 5000 rpm for 5 minutes
   c. Take upper, aqueous layer, avoiding the interface
8. Precipitate by adding 150 microliters of isopropanol
   a. Incubate at –20°C for 30minutes-1hour
9. Spin at full speed in refrigerated centrifuge (4°C) for 15 minutes
10. Decant supernatant, add 300 microliter 70% ethanol, mix gently
11. Spin again at full speed for 5 minutes in refrigerated centrifuge
12. Carefully pipette away ethanol, and allow pellet to dry in open tube 5 minutes
13. Resuspend in 50 microliter RNAse free water.
14. Check concentration on spectrophotometer
15. Run 1 microliter of reaction on gel
16. If multiple bands, heat reaction to boiling, and allow to cool on bench at room temperature.

3.4 *In situ* Hybridization (ISH)

(Modified from Ava Brent and Jeremy A. Lynch)

The following protocol can be used for a single or double *In Situ* and will take 3 days.

1. Wash in PBT 3 x 5 min
2. Proteinase K digest 5 μg/mL (in PBT) for 5 minutes.
3. Rinse 2x in PBT
4. Fix in 5% formaldehyde/PBT 25 min
5. Wash in PBT 4x 5min
6. Wash in 50/50 PBT/Hyb 5 min
7. Prehyb 1 or more hour at 65°C
8. Remove prehyb, add diluted probe mix (1μl probe in 50μl hyb), and incubate overnight at 60°C.
9. Wash in hyb wash solution 3x 25 min each at 60°C
10. Wash in 50/50 MABT/hyb wash for 5 min at room temp
11. Wash 4x 10minutes in MABT
12. Block in 2%BBR MABT + 10% NGS 1 or more hours
13. Incubate with appropriate anti-hapten antibodies (for double in situ use a combination of anti-dig::POD (Roche) at 1:100, anti-biotin or anti-dig::AP at 1:5000 or anti-fluorescein::AP at 1:2500 overnight at 4C in 2%BBR MABT/ 10% NGS serum (for antibody+ISH experiments, add primary antibody here)
14. Wash 4x 15 minutes in MABT
15. Continue with normal HRP and/or AP detection methods (see below)
16. If you are doing antibody+ISH, block 1 or more hours, then add secondary antibody, overnight 4C
17. Wash 4x 10minutes, detect secondary antibody by preferred means

For AP NBT/BCIP detection:

1. Wash 2x 5 min each in AP buffer
2. For each mL of desired detection solution, add 20 uL of NBT/BCIP stock solution to AP buffer (Roche)
3. Add about 500uL of detection solution to each sample
4. To stop reaction, wash several times in PBT

For the red fluorescent staining use the HNPP detection kit and Fast Red tablets from Roche:

1. Wash 2x 5 minute each in AP buffer
2. Dissolve 1 fast red tablet in 2mL of AP buffer
3. Filter solution using a syringe driven filter unit, Nylon, 0.2 um
4. Add 10uL HNPP solution to each mL of filtered fast red solution you want to use.
5. Add 400uL of this to each sample, a visible red stain should appear, which will also be brightly fluorescent
6. Wash and mount, or go to green TSA staining steps

For Green tyramide (Using TSA detection kit with alex488 tyramide from Molecular Probes):

1. After last wash, rinse 2x in PBS, or PBT with only 0.05% tween
2. Dilute 30% H2O2 1:100 in amplification buffer
3. Add 1uL of above dilution to 100uL amplification buffer for a final dilution of 0.0015% H2O2
4. Add 1uL tyramide stock to above solution and immediately add to embryos
5. Stain in the dark for 1 - 2 hour at room temperature (can go longer)
6. Wash and mount in vecta shield

3.4.1 Solutions for ISH

PBT
1x PBS
0.1% Tween 20

Hybridization solution (can be stored at -20°C)

50% formamide	25ml of 100% formamide
5x SSC	12,5ml of 20x SSC
2% SDS	10ml of 10% SDS
2% BBR	1g (Roche)
250 ug/mL tRNA	0.0125g
50 μg/mL heparin	100μl
H_2O	fill up to 50ml

BBR (Boerhinger Blocking reagent for nucleic acids, available from roche)
tRNA (can also substitute ssDNA, as in other standard hyb solutions)

You will need to heat this for a while at 55-65C to dissolve the BBR. Store at –20C. Also, this must be preheated to re-dissolve the BBR before the prehyb steps

Hyb wash solution (can be stored at -20°C)

50% formamide	25ml of 100% formamide
2x SSC	5ml of 20x SSC
1% SDS	5ml of 10% SDS
0.1% Tween	250μl of 20% Tween
H_2O	fill up to 50ml

MABT (allways fresh)

1x MAB	10ml of 5x stock of MAB
0.1% Tween 20	250μl of 20% Tween
H_2O	fill up to 50ml

2%BBR MABT + 10% NGS (fresh)

1x MAB	10ml of 5x stock of MAB
0.1% Tween 20	250μl of 20% Tween
10% NGS	2,5ml of 100% NGS
2% BBR	1g (Roche)
H_2O	fill up to 50ml

5x stock of MAB:

58g Maleic Acid
approx 32g NaOH pellets
43.8g NaCl
pH to 7.5 with 10N NaOH
water to 1L

AP Buffer:	**20 mL of AP buffer** (allways fresh)
100 mM NaCl	400 uL 5M NaCl
100mM Tris pH 9.5	2mL 1M Tris pH 9.5
50mM MgCl (2)	1mL 1M MgCl
0.1% Tween 20	100 uL of 20% Tween
H_2O	fill up to 20ml

For the MABT/2%BBR solution, you will have to heat the mixture at 55-65C to dissolve the BBR. I do this during the first post-hyb wash, and check on it periodically. Once the BBR is dissolved, let it cool at room temperature.

3.4.2 Triple fluorescent *In situ*

Here is one example of a triple fish using a slightly modified protocol as described for the double in situ.

The first day is performed as described above. Three different probes are added in the end for hybridization, which are fluorescein-, dig- and biotin-labeled.

The second day is the same and the following three antibodies are used for overnight incubation:

1.) α-flu::AP 1:2500

2.) α-dig::POD 1:100

3.) mouse-α-biotin 1:100

After the third day the fast red kit is used to detect the fluorescein-labeled probe and the TSA 488 for the dig-labeled probe.

The next step, after performing the first two staining, is to destroy the POD, which is coupled to the α-dig::POD antibody. To do so incubate the embryos for 30 min. in a 1% H_2O_2 solution diluted in PBT.

- Rinse 4x in PBT
- Block in western block diluted 1:5 in PBT for 1hr or more
- Incubate the α-mouse::POD (1:100) antibody in western block/PBT overnight at 4°C

On the fourth day use the TSA 647 kit or any other appropriate wavelength to detect the third (biotin-labeled) probe.

3.4.3 High throughput *In situ*

To perform a high throughput *In situ*, we adapted the Vacuum-assisted staining method described in (Berns et al., 2012).

The protocol for the high throughput *In situ* is the same as described above for a single *In situ*, except that we use less than half amounts of solutions for washing and incubation, and we use a 1%BBR containing hybridization solution.

To perform a high throughput *In situ* you will need:

Vacuum pump

96-well filter plates (with a 0.45-µm pore size)

Multi-channel pipette

It is also recommended to synthesize the *In situ* probes in 96-well plates, so one can easily transfer them to the *In situ* well plate.

3.5 Antibody staining

The following protocol can be used for an antibody staining of ovaries or embryos and will take 2 days.

1. Wash 2x with PBT (0.1%)
2. Block in PBT 1% + BSA 1% + NGS 10%(blocking solution) for 1 hour at room temperature
3. Incubate with primary antibody in blocking solution over night at 4°C
4. Wash 2x with PBT (0.1%)
5. Block in blocking solution for 1 hour at room temperature
6. Incubate with secondary antibody (1:400) and (if needed) phalloidin (1:200) in blocking solution for 2-3 hours at room temperature. Keep in dark.
7. Wash 2x with PBT (0.1%) and mount directly in Vectashield + DAPI

3.6 dsRNA injection

1. Take a microscope slide, place a drop of water in the middle, and place a 22 x 22 mm cover slip on top of it.
2. Place a drop of non-toxic school glue on the cover slip and distribute it with a needle along the slip so that you have a nice stripe of glue on the cover slip
3. Use the same needle tip with a small amount of glue and carefully pick up a yellow staged female pupa by the head or thorax and place it laterally in the glue. Usually around 5x5 rows are convenient (Fig. 3.2).
4. Make sure that all pupae are in the same orientation and that they are not totally covered with glue.
5. Load the dsRNA into an injection needle, pulled from capillary glass (conditions described below) and attach this needle to a fine tube, which is connected to a 5ml syringe. The dsRNA should be mixed with small amounts of phenol red, which serves as a visual control during injection. Around 4μl of dsRNA per needle will be sufficient for 25-30 pupae.
6. Before you start to inject, cut the tip of the needle with a razor blade and brush it gently against the cover slip until small droplets are visible. Make sure not to cut too much, otherwise the needle will harm the pupae and eventually kill them. Often the needle will break sufficiently after the first injection attempt.
7. Inject the pupae in the abdomen and gently apply some pressure on the plunger of the syringe until the pupa visibly swells a bit. Injection is done under a dissecting microscope at room temperature.
8. After all pupae are injected, move the cover slip into a plastic vial and seal it. The wasps are able to eclose even though they are glued. There is no need to remove the injected pupae from the glue.

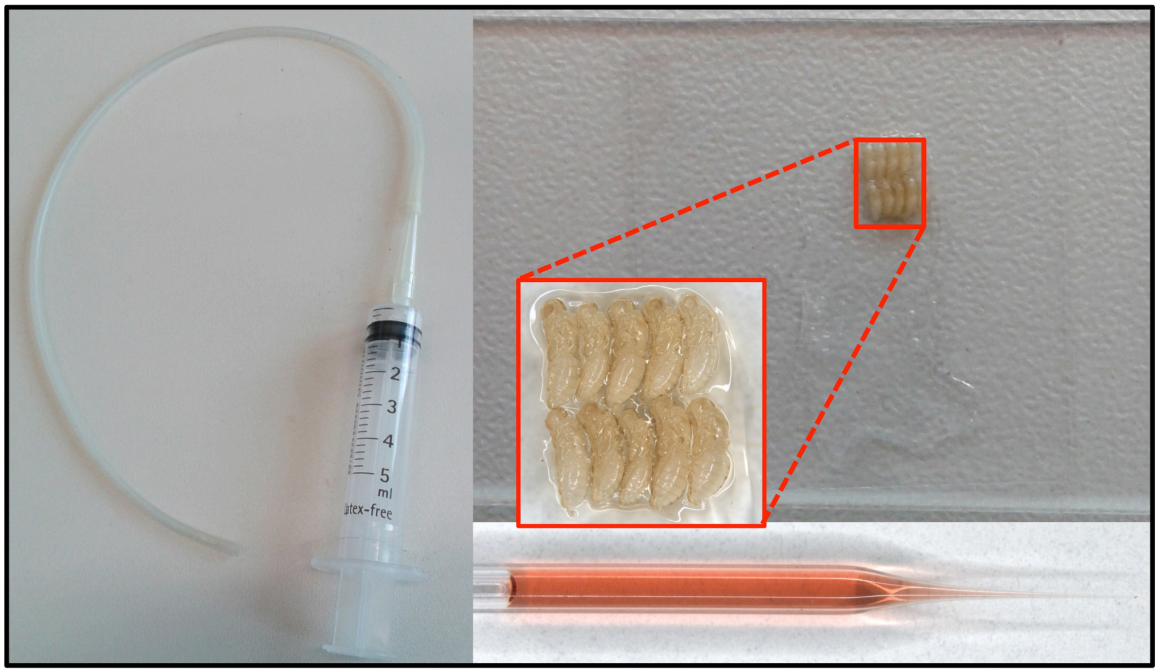

Figure 3.2 | Syringe, loaded needle and glued female pupae, ready for injection

Here is an example for injecting:

Inject on Monday and store the injected pupae in a plastic vial at 29°C.
On Friday, add honey water soaked filter paper into the vial.
The wasps will eclose over the weekend and feed on the honey water
On Monday after the weekend, freshly eclosed and honey fed wasps can be loaded on the waspinator for egg laying.

Needle puller conditions:

P= 500
H= 540
Pull= 240
Vel= 100
Time= 150

3.7 Transcriptome

3.7.1 RNA isolation

1. Homogenize *Nasonia vitripennis* embryos in 50µl TRIZOL Reagent (Invitrogen) with a pistil in a 1.5ml Eppendorf tube.
2. Incubate homogenized tissue in TRIZOL Reagent for 5 minutes at room temperature.
3. Bring volume up to 1ml TRIZOL
4. Add 200µl Chloroform
5. Shake tube vigorously by hand for 15 seconds.
6. Incubate 2 – 3 minutes at room temperature.
7. Centrifuge at 11,600 rcf for 15 minutes at 4°C.
8. Transfer upper aqueous phase to a new RNase-free 1.5ml tube.
9. Add 500µl Isopropyl alcohol.
10. Incubate overnight at -20°C.
11. Centrifuge at 11,600 rcf for 15 minutes at 4°C.
12. Remove supernatant thoroughly.
13. Add 1ml 70% ethanol.
14. Wash pellet 20-30 minutes on a shaker.
15. Centrifuge at 9,700 rcf for 15 minutes at 4°C.
16. Remove supernatant thoroughly.
17. Dry RNA pellet for 5 minutes at room temperature.
18. Re-suspend pellet in 10-20µl RNase-free water.
19. Check concentration and purity on spectrophotometer.

3.7.2 Preparing RNA samples for sequencing

In total, six different RNA samples were created for sequencing. Two Toll knockdowns, two BMP knockdowns and two water injected "wild type" samples. To knock down the Toll pathway, the Toll receptor was targeted by pRNAi, using two independent fragments of TollA for two different samples (termed TollA and TollA*). To sufficiently knock down the BMP pathway, the ligand Dpp was targeted. To create a second independent sample, the ligand Gbb2 was knocked down, since the outcome of Dpp and Gbb2 knockdowns was the same phenotype. Finally, two independently water-injected samples served as a control. Generating and injecting double stranded RNA was done as described in 3.3.5 and 3.6. Primers used for this procedure are listed in table 3.4.

Eggs laid by eclosed females, which were injected for the different fragments, were examined for the phenotype. Several steps were carried out to verify the knockdown. The first test was the hatch rate of the injected eggs. The hatch rate for TollA/TollA* as well as Dpp/Gbb2 were zero. No eggs hatched, which was a first indication for a very strong knockdown. Water-injected females on the other hand, laid eggs with a hatch rate of close to 100%. The second test was to verify the knockdown by *In Situ* hybridization. As we demonstrated in the second paper, TollA knockdown lead to a loss of the mesoderm, while Dpp/Gbb2 knockdown lead to an almost complete ventralization, which is marked by a massive expansion of *twist* expression. These two expression patterns were confirmed for the knockdowns of Toll5'/Toll3' and Dpp/Gbb2, while the control eggs showed a wild type expression of *twist*. After these two successful tests, aged embryos of 3-6 hours at 29°C were collected for each of the six different conditions. This time point was chosen, because most of the DV patterning genes are expressed during this period, which goes from early blastoderm stage (3h) to the beginning of gastrulation (6h). Subsequently, RNA was prepared of the collected embryos using the RNA extraction method described in 3.7.1. Before the RNA was

sent for sequencing a small amount was taken out for cDNA synthesis using the SuperScript® VILO cDNA Synthesis Kit from Invitrogen. With this cDNA a last test was carried out to verify the knockdown, by performing a RT qPCR for *twist*. The outcome of the RT qPCR reflected the *twist* expression pattern for both knockdown conditions. The amount of *twist* was reduced to nearly zero in Toll knockdowns and doubled in Dpp/Gbb2 knockdowns. The qPCR was done by Thomas Buchta. With this final test to verify the knockdowns, all RNA samples were ready for sequencing.

3.7.3 The tuxedo package for transcriptome analysis

The tuxedo package consists of several software components such as Bowtie, TopHat, Cufflinks package, and the CummeRbund. The TopHat software aligns millions of RNA-seq reads to the reference genome, while the Bowtie software provides the algorithmic core for TopHat. The cufflinks package assembles the TopHat's read alignments, produces a transcriptome annotation of the genome, and it quantifies this transcriptome across multiple conditions. Finally the CummeRbund software is used to find differentially expressed genes and transcripts.

Table 3.1 | List of primers used for amplification of candidate genes

#	Symbol	forward Primer	reverse Primer
1	*nfkb*	GCCTGGAGATAGCCACAAAC	ATTAGCAGCGGCTTGACTGT
2	*rel*	GGACGATTTTCGGAACTTGA	AAGCGTGCTCCTGGAGATTA
3	*kek5*	CAGTTCCGCTACCCCTTACA	CAAGAAAGGTGTGTGCTGTG
4	*crco*	TGACTGGTATCAGCCAGCAG	GCTGTTGTAGAACCACGAGGA
5	*six4*	CGACATGCTACCCCTGAACT	GTAGGGATGCTCACCGACTC
6	*chp*	TCAGCCAGAACAGCATATCG	TGCTCGACAGCCTACTGTGC
7	*zfhd*	TCATTGTACGAACCGCATGT	TCTGTATGCCGTCCTTCCTC
8	*stumps*	GACACAGAAGACCGCAGACA	GTCGACCCATCATCATGAAA
9	*fgfr*	GATTCAAGGAGGAGCTGACG	ACTTCATTTGCGGGAACATC
10	*integrin*	CTCTTGTCGACGAAGGAAGG	TGACTCCCGGGTAGTAGTCG

11	*vvl*	CAGAAGGAGAAGCGCATGAC	CCCCATTTTTCCTCCATTCT
12	*netrin*	TCCATGGACTACGGGAAGAC	CAGCCGGTGCAACTACTGT
13	*shrb*	TTTACGCGAGTGGAATCAAG	CGGGTTCTCTCACGCTAAAG
14	*ubiligase*	ACTCCGAATGGTGAATTTCG	TCGATTTCTTCGGTGGTCTC
15	*ApoLI*	GAGAGCCGAGAGCGAGTCTA	AGGCACTGTTGATGCACTTG
16	*twi*	GAGCAGAATCACCAGGAACC	CTGGCTCGGCATAGAGCTAC
17	*N.N.*	AGCAACTACAGCACGCTCAA	GGATCTTGAGGATGGCGATA
18	*transposon*	CCTCGGAGCGAATAGCTAAC	GTGCAGTCTGACGTGCTTGT
19	*tdrd7*	GTTGCACAGCAAGCTCACAT	GAGCCGAGTTCTCGGTGA
20	*novel1*	GAATTCCTGATAGCCCTGGA	CACCGGATTGTCTCGGAGAT
21	*rdh*	AGACGGTCGACGAAATCAAG	CAATTGCAAACATCGAGACG
22	*adoR*	CTGGGCCATACTCCATCCTA	GGTCGCTGTTCTCGTTCTTC
23	*novel2*	CGACCAGCCCTTAGAAGAAA	CATCTCCGCAACTTTTCCAT
24	*mirr*	ACAACAACAACGACGACGAC	ATCTGACAGCGGGCTACCTA
25	*crb*	AAAGGACATCCCAACACTCG	GGGGTCCACCGCAGAAGTTT
26	*yki*	GCAGTGCGAGTGCAAAATAA	TTGATGCTTGCAGAGAGACG
27	*Ap1*	TCGTTCTACGAGCAGGAGGT	TGAGATCCCATTAGCGAACC
28	*foxo*	TGGATGGTGAAAAATGTCCA	GTTCGGATGGTCCCTTATCA
29	*ltl*	ACCTGGAACTCGGTCACAAC	AGGGAAGTCTCGCTTGAGTG
30	*disco*	TAACAGCCTGATCGCTTACG	GCGTTGTACGGTGAAATCT
31	*sal3like*	TCAGCTTCACGCGGTCAGGA	ACGAAGCTGCCAACTTAGGG
32	*Sp67*	TCCTCCCATATCCGAAACAA	GCTGTGGAAGCAAAGGACTC
33	*zen*	CTTACGAGCATCAGCAGCAG	CTCCAGACGCTGAAGGCTAC
34	*uif*	GATGGTCTTTGTGCCAGGAT	GCGGCGATGAGAAATTACAA
35	*novel3*	CGCGGAAGTCGAGTCTAATC	GCATCCGGACTTTGAATGTT
36	*cg4782*	GAAGACGTCCTTCTCGCATC	GATCCAACCCGCTCAAATC
37	*ncRNA1*	TCGTTTATTGAATGCTCGATT	AGGTGTTGTGTCTGCACTCG
38	*rful*	GGCGTGTTGTGAAAATGAAA	GATGCGATGCAGAGCATAGA
39	*jag*	TCATTCGACTCGCTTCAGTG	ACCGGTCGAGATCTGAAGAA
40	*ncRNA2*	TCATGTTCTCCTCGTTGCTG	GCTGTAGATCACCACGACGA
41	*grn1*	TGACGATGGACAGAGTGAGC	CGGAACGTTCTCCACTTGTT
42	*pnr*	AGCTTCAGGCTCCCGTCTAT	GTTGTACGCCGCTCGTTTAT
43	*grn2*	TGCCGTGTGTGTGATGATTA	GGAGACGAGTACGGAGAACG
44	*ara*	AGCAACGTCCTACTCGTCGT	ATAGGTGAACCAGCCGAATG
45	*otd2*	TCGAGAGTCCAGGTCTGGTT	GTGGTGGGAGTTGTTGCTCT
46	*msh*	TACGAGCGTGTCTGAGCACT	CTTCCTCGCCTCAGTCTCTG
47	*at*	TCTGCTTCATCGTCAACTCG	AACGATGGATCGCTACCAAG
48	*novel4*	TAGGTTTTCAGGGCAGCATC	CCAATGGCTCCAGTTGATTT

Table 3.2 | List of candidate genes
A list of 48 genes that were used for expression pattern analysis. The arrow pointing up or down next to BMP / Toll indicates, whether the gene is up or down regulated in the respective knockdown.

#	Gene	Symbol	Pathway
1	*NF-κB*	*nfkb*	BMP ↓, Toll ↓
2	*relish*	*rel*	BMP ↓, Toll ↓
3	*kekkon5*	*kek5*	Toll ↓
4	*crocodile*	*crco*	Toll ↓
5	*six4*	*six4*	Toll ↓
6	*chaoptin*	*chp*	Toll ↓
7	*zincfingerhd*	*zfhd*	Toll ↓
8	*stumps*	*stumps*	Toll ↓
9	*fibroblastgrowthfactorreceptor*	*fgfr*	Toll ↓
10	*integrin*	*integrin*	Toll ↓
11	*ventral veinslacking*	*vvl*	BMP ↑, Toll ↓
12	*netrin*	*netrin*	BMP ↑, Toll ↓
13	*shrub*	*shrb*	BMP ↓, Toll ↓
14	*ubiligase*	*ubiligase*	BMP ↓, Toll ↓
15	*apolipophorin*	*ApoLI*	BMP ↓, Toll ↓
16	*twist*	*twi*	BMP ↑, Toll ↓
17	*LOC100118639*	*N.N.*	Toll ↓
18	*transposon*	*transposon*	Toll ↓
19	*tudordomaincontaining 7*	*tdrd7*	Toll ↓
20	*novel1*	*novel1*	Toll ↓
21	*retinoldehydrogenase*	*rdh*	Toll ↓
22	*adenosinereceptor*	*adoR*	Toll ↓
23	*novel2*	*novel2*	Toll ↓
24	*mirror*	*mirr*	Toll ↓
25	*crumbs*	*crb*	BMP ↓
26	*yorkie*	*yki*	BMP ↓
27	*Apterous1*	*Ap1*	BMP ↓
28	*forkhead box*	*foxo*	BMP ↓
29	*larval translucida*	*ltl*	BMP ↓
30	*disconnected*	*disco*	BMP ↓
31	*spalt3like*	*sal3like*	BMP ↓
32	*Seronin Protease 67*	*Sp67*	BMP ↓
33	*zerknüllt*	*zen*	BMP ↓
34	*uninflatable*	*uif*	BMP ↓
35	*novel3*	*novel3*	BMP ↓, Toll ↓

36	*cg4782*	*cg4782*	BMP ↓, Toll ↓
37	*ncRNA1*	*ncRNA1*	BMP ↓, Toll ↓
38	*ring fingerubiligase*	*rful*	BMP ↓, Toll ↓
39	*jagged*	*jag*	BMP ↓, Toll ↓
40	*ncRNA2*	*ncRNA2*	BMP ↓
41	*grain1*	*grn1*	BMP ↓
42	*pannier*	*pnr*	BMP ↓
43	*grain2*	*grn2*	BMP ↓
44	*araucan*	*ara*	BMP ↓
45	*orthodenticle2*	*otd2*	BMP ↓
46	*muscle segment homeobox*	*msh*	BMP ↓
47	*aminotransferase*	*at*	BMP ↓
48	*novel4*	*novel4*	BMP ↓

Table 3.3 | List of genes that show a dorsal expression pattern

#	Gene	Symbol
1	*aminotransferase*	*at*
2	*Apterous1*	*Ap1*
3	*disconnected*	*disco*
4	*grain1*	*grn1*
5	*grain2*	*grn2*
6	*larval translucida*	*ltl*
7	*Seronin Protease 67*	*Sp67*
8	*novel3*	*novel3*
9	*novel4*	*novel4*
10	*cg4782*	*cg4782*
11	*apolipophorin*	*ApoLI*

Table 3.4 | List of primers used for RNAi probe synthesis

Name	Sequence 5′ -> 3′
Fw Toll	GAACTCGCCAAACTGGTCTC
Rev Toll	AACGGATTGTTCGTCAGCTC
Fw Toll*	GAACTCGCCAAACTGGTCTC
Rev Toll*	AACGGATTGTTCGTCAGCTC
Fw Dpp	GTGGTGGGCGAGGCGGTAAA
Rev Dpp	CACGACCTTGTTCTCCTCGT
Fw Gbb	ATCCTGCTGCAGTTCGACTT
Rev Gbb	CCCTGATGATCATGTTGTGG

4 Additional Results

To identify new target genes of the Toll and BMP pathway, which are regulated during DV patterning in the embryo, a next generation RNA sequencing approach was carried out for three different genome conditions including knockdowns of the Toll and BMP pathways as well as water-injected control. The different RNA samples were prepared by Thomas Buchta and me and are described in more detail in 3.7. Sequencing was done by the Cologne Center for Genomics (CCG) using the Illumina HiSeq 2000. The sequencing strategy was to create a 180-200bp RNA library for 100bp paired-end reads. The raw data (around 100GB) is available in the Roth group. Assembling the transcriptome data as well as finding and calculating differentially expressed genes between the different conditions were done by Dr. Jeremy Lynch using the tuxedo package (Trapnell et al., 2012). Section 3.7.2 provides a small description of the tuxedo package. The transcriptome analysis resulted in a list with 262 significantly different expressed genes. 94 genes, comparing BMP knockdown to wild type and 168 genes when comparing wild type to the Toll knockdown. Among those 262 candidates several genes (e.g. *twist*, *zen*, and *pnr)* were included whose expression pattern upon loss of Toll or BMP signalling were known to us and matched the results of the transcriptome data. Thus, these genes served as a proof of principle.

In order to optimize time and materials for analyzing the embryonic expression pattern of 262 genes we established a 96 well *In Situ* technique, which was adapted from (Weiszmann et al., 2009; Berns et al., 2012). To test this new technique, we designed primers for cloning and *In Situ* probe synthesis of 48 genes (Table 3.1), which showed the highest variation among the 262 genes. 19 of the 48 candidates were down regulated comparing BMP knockdown to wild type, 16 were down regulated comparing Toll knockdown to wild type, 10 were in both cases down regulated, and 3 were up regulated in BMP and down regulated in Toll

(Table 3.2). The following *In Situ* probe synthesis as well as the *In Situ* were done by Selma Wolff and Jessica Pietsch in the frame of their Bachelor Thesis and were supervised by Thomas Buchta and me, respectively. All methods for this procedure are described in section 3.1-7.

18 of 48 genes showed a specific expression pattern, while the rest was either ubiquitously expressed or showed no expression. 11 of these genes (table 3.3) showed a distinct dorsal expression pattern during blastoderm stage, which is similar to the dorsal stripe pattern of *Nv-zen*. The remaining 7 genes were either expressed in a segmental pattern (*mirr*, *rdh*, *six4*, and *jag*) or on the ventral side in stripe like pattern (*intergrin*, *netrin*, and *vvl*).

5 Discussion and Outlook

5.1 Analysis of DV marker genes in *Nasonia*

Two conserved pathways pattern the embryonic DV axis of the fruit fly *Drosophila melanogaster*. The Toll pathway patterns the ventral half (mesoderm and neuroectoderm) of the embryo and controls the expression of key components of the BMP pathway, which patterns the dorsal half (non-neuroectoderm and extra embryonic tissue). Besides its ancestral role in innate immunity, the Toll pathway is not employed to pattern the DV axis outside the insects. This leads to the assumption that using the Toll pathway for DV patterning is a novelty of insects. Nevertheless, it remains still a mystery of how and when a transition occurred from using a BMP only system to a BMP + Toll system within the insects. To get a deeper understanding of the evolution of axial patterning in insects and to find out which characteristics of DV patterning are truly representatives of the ancestral mode we analyzed the DV axis of the wasp *Nasonia vitripennis*. The first step was to analyze the expression of DV target genes along the entire embryonic axis. Therefore, we cloned and analyzed the expression of *Nasonia* orthologs of *Drosophila* DV marker genes and categorized them in ventral, lateral, and dorsal genes.

5.1.1 Dynamics on the ventral side

The analysis of the ventral marker genes *twist*, *snail*, *sim*, and *cact1* in *Nasonia* revealed striking differences when compared to *Drosophila*. All four genes are initially detected in a very narrow stripe (3-4 nuclei) at the ventral midline of the

Nasonia embryo. Over the course of cycle 11 the *twist*, *snail*, and *sim* domains expand until they reach their final width and characteristic shape in cycle 12, while *Nv-cact1* remains in a narrow stripe until it is cleared again from the ventral side just prior to gastrulation. This is in stark contrast to *Drosophila*, where the initial *twist* and *snail* domains are only slightly narrower and weaker than their mature domains. The highly dynamic nature of ventral expression domains in *Nasonia* is already a first indication of a GRN that has not only dynamic but also possible self-regulatory properties, as it has been shown in *Tribolium*. However, the underlying regulatory mechanisms that produce these dynamic gene expressions must clearly be different in the wasp and beetle. While in *Tribolium* the gene expression dynamics are a consequence of the shrinking and refinement of the Dorsal nuclear gradient, the wasp expression pattern change in the opposite direction, expanding from narrow to broad.

Co-expression of *twist*, *snail*, and *sim* in *Nasonia* is yet another remarkable difference and provides new insights into the evolution of *sim* regulation among holometabolous insects. Overlapping expression of *sim* and *snail* is not observed in *Drosophila*, since *snail* represses *sim* expression. Instead, both *sim* stripes appear simultaneously very late in embryogenesis and flank the presumptive mesoderm. In *Nasonia*, the *sim* expression domain expands in concert with *twist* and *snail*, while it is always a bit broader. The expression domains for all three genes overlap for most of the development, until *Nv-sim* is finally cleared from the ventral midline by the end of cycle 12, leading to two stripes that flank the *Nv-twist* and *Nv-snail* domain. A similar pattern is also seen in *Tribolium*. Thus, comparing *sim* expression among *Drosophila*, *Nasonia*, and *Tribolium* it is very likely that the early broad *sim* expression domain represents the ancestral type within the holometabolous insects. To follow up the question of how an early broad *sim* expression pattern seen in the wasp and beetle evolved into a two stripe-only pattern in the fly, a detailed analysis of *sim* enhancer regions in *Nasonia* and *Tribolium* would be needed. Comparing these findings to *Drosophila* would clearly

point out the differences in *sim* regulation that lead to the different expression patterns.

5.1.2 Lateral markers

The neurogenic ectoderm on the ventral lateral side of the embryo is established and patterned by a set of transcription factors (*vnd*, *ind*, and *msh*) known as the columnar genes. In *Drosophila*, all three genes are expressed in symmetric lateral stripes. *vnd* expression is the first one to be initiated in a stripe that is complete along the AP axis and lies just dorsally to the stripes of *sim*. *ind* expression is initiated later and lies dorsal to *vnd*, while *msh* is the most dorsal and last of the columnar genes that is expressed. The final expression patterns of the columnar genes in *Nasonia* are quite similar to that of the fly. All are expressed in symmetric stripes with *vnd* just dorsally to the *sim* stripes and *msh* as the most dorsal one. However, these stripes in *Nasonia* are not initiated in their full length along the AP axis, as it is the case in *Drosophila*. Instead, their expression is restricted to the anterior and only present in the presumptive thoracic region. With proceeding development these initially incomplete stripes extend to the posterior end of the embryo, just at the beginning of gastrulation movements. There is basically nothing known about regulation of the columnar genes in *Nasonia* and it would be interesting to find out the underlying mechanism that cause not only the temporal gradient of gene expression along the DV axis but also along the AP axis, which is not observed in *Drosophila*.

Nv-brk is another lateral gene that marks the entire neurogenic ectoderm. In contrast to the late expression of the columnar genes, *Nv-brk* expression is initiated very early at about the same time as the ventral marker genes start in narrow stripes. This early expression of *Nv-brk* might indicate its possible role in

influencing the shape and dynamics of target genes that are observed on the ventral side.

5.1.3 Dorsal side

The dorsal part of the insect embryo is marked by the expression of a set of genes that pattern and differentiate the dorsal ectoderm and extra embryonic tissues (amnion and serosa). These extra embryonic membranes protect the embryo from the environment and are important for morphogenetic movements during gastrulation. The *Drosophila* embryo is again an exceptional case as it has only a reduced single extra embryonic membrane called amnioserosa, which is restricted to the most dorsal side of the embryo. The best marker for this tissue is the transcription factor *zen*, which is initially expressed in a broad domain and then refines to a narrow stripe along the dorsal midline. A similar pattern is observed in *Nasonia* with *Nv-zen* expression being broad in the beginning and then refining to a narrow stripe. In the fly, a ubiquitous activation of *zen*, repression by Dorsal and a subsequent refinement by the BMP pathway leads to the two phases of *zen* expression. It will be interesting to find out the underlying mechanism that produces this dynamic expression of *zen* in *Nasonia*. Although both patterns are quite similar, the *Drosophila* way of patterning can be excluded in *Nasonia* since *zen* expression and refinement takes place in Toll knockdown embryos. A different strategy for example would be a Dorsal independent system, which would require positive and negative regulation of *zen* by BMP signalling.

In *Drosophila* three different threshold outputs of gene expression on the dorsal side are generated by BMP signalling. By analyzing dorsal marker genes in *Nasonia* we also observed different threshold outputs. Genes such as *Nv-RACE* and *Nv-hnt* are expressed in a very narrow domain along the dorsal midline. *Nv-tup*

and *Nv-doc* have a moderately broader expression domain, while *Nv-ara* shows the broadest expression pattern of all examined dorsal marker genes. Thus, it is very likely that there is a gradient of positional information on the dorsal side of the *Nasonia* embryo, which leads to the different threshold outputs.

Despite these remarkable similarities between the fly and the wasp, the extra embryonic membranes behave quite different. In *Drosophila*, the amnioserosa does not migrate and maintains a border to the surrounding ectodermal cells until dorsal closure. The serosal cells in *Nasonia* eventually break their border to the surrounding cells and start to migrate over the ectoderm in order to surround the entire embryo. A similar behaviour is observed in the honeybee (Fleig and Sander, 1988) and in the scuttlefly *Megaselia* (Rafiqi et al., 2008). It might well be that this mode of serosal migration is another example of convergent evolution between hymenoptera and dipterans.

In order to find out whether *Nasonia* has, like *Drosophila*, one reduced amnioserosa or two separate membranes we analyzed the expression of genes that mark these tissues in other insects. Besides *zen* as a reliable marker of the serosa in insects we found *Nv-hnt* to have a *zen*-like expression. Both genes are expressed in a narrow stripe along the dorsal midline just prior to gastrulation. Later in development, they are expressed in the presumptive serosa and mark those cells that migrate over the ectoderm. *tup* is expressed in *Anopheles* and *Megaselia* in a region that gives rise to the amnion (Goltsev et al., 2007; Rafiqi et al., 2010), while *pnr* and *ara* are reliable amnion markers in *Tribolium* (van der Zee et al., 2006; Nunes da Fonseca et al., 2008). In *Nasonia*, all three genes are expressed on the dorsal side in a domain that flanks *Nv-zen* and *Nv-hnt* expression and therefore can be considered as amnion markers. In addition it is very likely that *Nv-ara*, with its broad expression domain, plays a role in the dorsal ectoderm. Taken together, these results clearly indicate that *Nasonia* forms two separate extra embryonic membranes. However, while we have shown that the seorsa migrates over the ectoderm in the *Nasonia* embryo, the role of the amnion remains still unclear. Live

imaging, of fluorescent protein tagged amnion markers, could reveal possible movements of the amnion and RNAi knockdowns of amniotic marker genes could provide new insights about the role of the amnion.

5.2 Functional analysis of Toll- and BMP signalling

The detailed analysis of the expression pattern of DV target genes in *Nasonia* revealed similarities but also striking differences when compared to *Drosophila*. These results clearly indicated that the upstream mechanisms, which produce these patterns, are highly diverged. In order to analyze the roles of the Toll and BMP pathways in patterning the DV axis of the *Nasonia* embryo, we knocked down the gene expression of key components of both pathways, using the pRNAi technique. To fully interpret these data we developed a fluorescent triple *in situ* protocol. Simultaneous staining of *Nv-twist* (mesoderm), *Nv-brk* (ventral and lateral ectoderm), and *Nv-zen* (extra embryonic) allowed a global view of the DV axis and helped to interpret losses or shifts of different embryonic fates.

5.2.1 The role of Toll signalling

To sufficiently knock down the Toll signalling pathway, we targeted the Toll receptor by pRNAi. A triple *in situ* of *Nv-twi*, *Nv-brk*, and *Nv-zen* on Toll pRNAi embryos revealed the loss of *Nv-twi* expression, which indicates a conserved role of Toll signalling in inducing the mesoderm. *twi* expression is also gone in *Drosophila* embryos that lack Toll signalling. In addition, *Drosophila* embryos are completely dorsalized and show no polarity at all (Anderson, Bokla, et al., 1985; Anderson, Jürgens, et al., 1985). Although *Nasonia* Toll pRNAi embryos

loose the ability to induce mesoderm, they are not completely dorsalized. Instead, the dorsal half of the *Nasonia* embryo remains highly polarized indicated by *zen* expression. The fact that even genes like *Nv-ara* together with *Nv-zen* are expressed in Toll knockdown embryos, indicates that the dorsal half of the embryo remains completely in tact and produces several threshold outputs of gene expression that are identical to wt embryos. Taken together these results clearly indicate that the dorsal side of the wasp embryo is patterned by a Toll independent system. Another interesting observation is the expansion of the ventral border of *Nv-brk* towards the ventral midline upon loss of Toll signalling. That is again not observed in *Drosophila* and thus indicates another Toll independent mode of ventro-lateral ectoderm specification in *Nasonia*. In contrast to the broad ventral lateral *Nv-brk* domain we also examined the expression of *Nv-vnd*, which is a narrow ventral ectoderm marker. In strong knockdowns *Nv-vnd* expression is gone as is *Nv-twi*. In mild knockdowns however, *Nv-vnd* shifts in concert with the shrinking *Nv-twi* domain towards the ventral midline. These results show that at least small amounts of Toll signalling are required to induce *Nv-vnd* expression, which is the case in weak phenotypes. A second interpretation of these results is that *Nv-vnd* could directly respond to lower levels of Toll signalling, since its expression domain always flanks the *Nv-twi* domain and is thus further dorsal than *Nv-twi.* To test this idea, analysis of *Nv-vnd* enhancer regions would provide useful insights. The ability to respond to low amounts of Dorsal protein is reflected in high affinity Dorsal binding sites. The presence of these binding sites in the *Nv-vnd* enhancers would strongly support the idea that *Nv-vnd* responds to lower levels of Toll signalling. Nevertheless, it could also be that *Nv-vnd* is not responding to lower amounts of Toll signalling but rather to the presumptive mesoderm. In wild type embryos, *Nv-vnd* expression starts well after the final domain of *Nv-twi* is established, which would indicate that *Nv-vnd* expression is rather influenced by the presumptive mesoderm and not directly by lower amounts of Toll signalling.

5.2.2 The role of BMP signalling

Knockdown of the BMP ligand *Nv-dpp* allowed us to investigate the role of the BMP signalling pathway. A triple *in situ* (*twi, brk,* and *zen*) of *Nv-dpp* knockdown embryos revealed the loss of dorsal fates and a massive expansion of the mesoderm marked by *Nv-twi* expression. This result is in strong contrast to the *dpp* phenotype in *Drosophila*, where dorsal fates are also lost but the mesoderm is unaffected. Further analysis of the *Nv-dpp* knockdown pointed out that the *Nv-twi* domain is always initiated in a narrow stripe (as in wild type), before it starts to cover the entire embryo. These results provided useful insights about the patterning of the ventral side of the wasp embryo, which involves at least two steps. At first, expression of the ventral most genes is initiated as a narrow stripe in a Toll dependent and at the same time BMP independent manner. These narrow stripes expand over time, probably due to self-enhancing interactions, until they reach their final width, which is clearly defined by repressive BMP signalling from the dorsal side. Besides the negative influence of the BMP pathway on the mesoderm, it became clear from intermediate phenotypes that BMP signalling has also a strong influence of the dorsal border of *Nv-vnd* expression, which is quite similar to what has been described for vertebrates (Mizutani and Bier, 2008).

Regarding the massive *Nv-twi* expansion and almost complete ventralization of the embryo we wanted to know if this expansion is due to an expansion of Toll activity. As a useful indicator of Toll signalling we chose the gene *Nv-cact1*, which is not only the inhibitor of Dorsal but also a direct target gene of Toll signalling (*Nv-cact1* expression is lost in *Nv-Toll* RNAi). In *Nv-dpp* knockdowns, *Nv-cact1* expression was unaffected. This clearly indicates that Toll signalling is not increased in BMP knockdowns and that it is not directly regulated

by BMP signalling. Furthermore, it shows that expansion of ventral genes is Toll independent and rather due to possible self-enhancing interactions.

Finally we wanted to find out what happens if both pathways are knocked down. A double knockdown of *Nv-Toll* and *Nv-dpp* resulted in completely lateralized embryos that expressed *Nv-brk* only when stained for *Nv-twi*, *-brk*, and *-zen*. This ectodermal ground state of the wasp embryo is also observed in *Drosophila*. In addition, this result demonstrates that ventralization of *Nv-dpp* RNAi embryos requires the induction of the mesoderm by Toll signalling.

Taken together, the functional analyses of the Toll and BMP pathway and their role in patterning the DV axis of *Nasonia* revealed many striking features that are in stark contrast to *Drosophila*. First, BMP signalling is completely independent of Toll signalling. Second, BMP signalling is required for almost all DV patterning and polarity of the *Nasonia* embryo, and finally, Toll signalling plays only a role in inducing the mesoderm. These results show that Toll signalling was ancestrally a limited component of the DV patterning system in insects, while BMP signalling provided global polarity of the embryo.

5.3 Establishment of the BMP signalling gradient

The fact that the BMP pathway polarizes the entire *Nasonia* embryo and that several threshold outputs of gene expressions are generated on the dorsal side, indicates a BMP signalling gradient with peak levels at the dorsal midline. To find out more about the gradient and the establishment of it we first performed a pMAD antibody staining of *Nasonia* embryos, which is a useful marker to visualize BMP signalling activity. In early cycle 10 embryos, pMAD is found in a broad graded domain, which narrows and intensifies over the next division cycles until an intense stripe with sharp borders is left along the dorsal midline at cycle 12.

This pattern is similar to *Drosophila* except that all changes of BMP activity occur in cycle 14 and not over several cycles. The generation of a BMP signalling gradient in *Drosophila* is a result of the interactions of several components like *sog*, *dpp,* and *tld*, which are all regulated by Toll signalling. Laterally activated Sog protein binds Dpp, inhibits its signalling, and facilitates its diffusion towards the dorsal side. The metalloprotease Tld cleaves Sog on the dorsal side thereby releasing Dpp, which is then free to signal. In *Nasonia* however, no *sog* ortholog has been detected in any sequenced genome or transcriptome data set, including our own transcriptome project, which raises the idea that a Sog based transport system is not present in *Nasonia*. To further investigate this idea, we searched and found an ortholog of *tld* in the *Nasonia* genome, which had no patterning function, since *Nv-tld* RNAi embryos developed normal. These results clearly indicate that the molecular mechanism to create a BMP signalling gradient is quite diverged between *Drosophila* and *Nasonia*, despite the similar pMAD pattern.

In order to gain more insights of how the BMP gradient is established in *Nasonia*, we performed a thorough analysis of the BMP signalling pathway, which included extracellular modulators, ligands, receptors, and downstream components of the pathway. Many factors besides *sog* and *tld* that are required for the establishment of a BMP gradient in *Drosophila* such as *tsg* and *screw* (a highly diverged *gbb* paralog) are also present in *Nasonia*. Knockdowns of *Nv-tsg* and *Nv-gbb* resulted both in very strong ventralized embryos that were identical to *Nv-dpp* knockdowns. This clearly underlined their importance for BMP signalling and indicated that there is a long range BMP signalling activity in *Nasonia*. In addition, it became clear that *Nasonia* retained some components of an ancestral TGF-ß signalling network, such as ADMP and Bambi, which have been lost in *Drosophila*. Another interesting result was the presence of several duplication and divergence cases in *Nasonia*. For example two *Nv-gbb* orthologs were identified, while only one was important for DV patterning in the embryo. A similar result was observed for *Nv-mad1/2*, indicating that the patterning system is highly specialized in *Nasonia*.

Nevertheless, we were not able to identify a BMP antagonist, which might have taken the role of Sog in establishing a transport-based gradient. Instead, we found very interesting expression patterns of the type I receptor *Nv-tkv* in ovaries and the type II receptor *Nv-punt1* in the embryo, which indicates an alternative way of forming a graded signalling activity. This possibility involves a two-step process of direct localization of BMP signalling components and possible positive feedback loops. The first step involves localization of Tkv protein at the dorsal side in the ovary. *Nv-tkv* mRNA is localized in a narrow stripe at the dorsal side of the ovary which is easily distinguishable by the position of the oocyte nucleus. Once the egg is laid, *Nv-tkv* mRNA becomes ubiquitously distributed in the embryo. It could be that localized Tkv protein in the ovary is still present in the embryo although the mRNA is not localized. Activation of this receptor would be the initial pulse to create a signalling activity bias on the dorsal side. The second step in creating a signalling gradient would involve a positive feedback loop, in which BMP pathway components are activated in distinct domains by BMP signalling itself. One such example is the type two receptor *Nv-punt1*. It is not expressed in the ovary but later turned on in early blastoderm embryos in a very narrow stripe along the dorsal midline. This localized receptor could then amplify the establishment of the gradient and help to create peak levels of signalling activity along the dorsal midline during early blastoderm stage. In contrast to *Nv-punt1*, *Nv-punt2* is expressed in the ovaries, ubiquitously in the embryo, and the knockdown leads to sterility. This result indicates that *Nv-punt2* is employed for general BMP signalling, while *Nv-punt1* is mainly used for generating a signalling gradient. This case of duplication and divergence of the *punt* gene shows how specialized *Nasonia* is, which might well be a consequence of the loss of *sog* and the need to establish a different way of creating a signalling gradient.

To test these hypotheses several experiments should be carried out. A starting point would be the generation of an Nv-Tkv antibody, which could be used to visualize possible dorsal localization of the protein. Next would be the

analysis of *Nv-punt1* knockdowns. Embryos lacking *Nv-punt1* could for example fail to establish peak levels of BMP signalling. We already tried to generate *Nv-punt1* knockdowns but were not successful. While maternally expressed genes are easily knocked down, we observed that the pRNAi technique is not only failing for *Nv-punt1* but also for all zygotically expressed genes we analyzed so far. This general problem can be overcome by establishing new techniques in *Nasonia*. For example, the CRSIPR/CAS system (Cong et al., 2013) could be introduced to generate reliable knockouts.

5.4 Transcriptome analysis

Despite the descriptive and functional analyses of the Toll and BMP pathways we still have not fully understood how the BMP gradient is formed or what genes are regulated by Toll signalling. The strategy was always to search for components and targets of the pathway that were already known in other insects or vertebrates. To gain new insights and find possibly new target genes of both pathways we chose and performed an unbiased approach, by creating and comparing transcriptome data sets of wild type, Toll knockdown, and Dpp knockdown conditions. The outcome of this was a set of more than 260 genes that were either significantly down or up regulated, when compared among the different data sets. To efficiently analyze the expression pattern of these genes we established a high throughput *in situ* technique where 96 samples can be analyzed in one single experiment. Positive aspects of this method were the massively reduced amounts of materials that are used for 96 samples and the time that is saved during the *in situ* procedure. On the other hand, mounting 96 different samples on microscope slides were quite challenging and required a lot of time, which can definitely be improved. A first analysis of half of the 260 candidates

revealed several genes, which had a localized expression pattern. Among those that had a dorsally localized expression pattern we found several genes that have no homolog outside the Hymenoptera. These so called novel genes could be new components of the signalling pathway and could play a role in generating a BMP gradient. Further functional analyses are needed to test their possible roles. Another very interesting gene that we found was *omb*, which is a target of BMP signalling and plays a role in patterning the wing in *Drosophila* (del Alamo Rodríguez et al., 2004). In *Nasonia*, however this gene is dorsally expressed in the early blastoderm embryo, which indicates a possible role of *Nv-omb* in patterning the embryo instead of the wing. Without the transcriptome data, we would have not tested *omb* in *Nasonia*, because of its well known role in patterning the *Drosophila* wing. Therefore, the novel genes as well as *Nv-omb* are very good examples, of how valuable and fruitful the transcriptome analysis is.

Taken together, the generated transcriptome sets provide a huge amount of data that needs to be further analyzed. At first, all differentially expressed genes should be analyzed for their expression patterns. Interesting candidates, for example those with localized expression pattern, should be further functionally tested to reveal a possible role in DV patterning. Future projects, in addition to the transcriptome analysis, would be the establishment of new molecular techniques that help to analyze the *Nasonia* embryo. Examples would be the establishment of the previously mentioned knockout techniques that would circumvent the pRNAi problems. Generating transgenic wasps that express an altered version or a fluorescently tagged version of the gene of interest could as well provide useful insights about patterning mechanisms and morphogenetic movements during gastrulation.

A. References

Anderson, K., 1995. One signal, two body axes. Science 269, 489–90.

Anderson, K. V, Bokla, L., Nüsslein-Volhard, C., 1985. Establishment of dorsal-ventral polarity in the Drosophila embryo: the induction of polarity by the Toll gene product. Cell 42, 791–8.

Anderson, K. V, Jürgens, G., Nüsslein-Volhard, C., 1985. Establishment of dorsal-ventral polarity in the Drosophila embryo: genetic studies on the role of the Toll gene product. Cell 42, 779–89.

Andreu, M.J., González-Pérez, E., Ajuria, L., Samper, N., González-Crespo, S., Campuzano, S., Jiménez, G., 2012. Mirror represses pipe expression in follicle cells to initiate dorsoventral axis formation in Drosophila. Development 139, 1110–4.

Assa-Kunik, E., Torres, I.L., Schejter, E.D., Johnston, D.S., Shilo, B.-Z., 2007. Drosophila follicle cells are patterned by multiple levels of Notch signaling and antagonism between the Notch and JAK/STAT pathways. Development 134, 1161–9.

Bergmann, A., Stein, D., Geisler, R., Hagenmaier, S., Schmid, B., Fernandez, N., Schnell, B., Nüsslein-Volhard, C., 1996. A gradient of cytoplasmic Cactus degradation establishes the nuclear localization gradient of the dorsal morphogen in Drosophila. Mech. Dev. 60, 109–23.

Berns, N., Woichansky, I., Kraft, N., Hüsken, U., Carl, M., Riechmann, V., 2012. "Vacuum-assisted staining": a simple and efficient method for screening in Drosophila. Dev. Genes Evol. 222, 113–8.

Brendza, R.P., Serbus, L.R., Duffy, J.B., Saxton, W.M., 2000. A function for kinesin I in the posterior transport of oskar mRNA and Staufen protein. Science 289, 2120–2.

Brummel, T.J., Twombly, V., Marqués, G., Wrana, J.L., Newfeld, S.J., Attisano, L., Massagué, J., O'Connor, M.B., Gelbart, W.M., 1994. Characterization and relationship of Dpp receptors encoded by the saxophone and thick veins genes in Drosophila. Cell 78, 251–61.

Chang, W.-L., Liou, W., Pen, H.-C., Chou, H.-Y., Chang, Y.-W., Li, W.-H., Chiang, W., Pai, L.-M., 2008. The gradient of Gurken, a long-range morphogen, is directly regulated by Cbl-mediated endocytosis. Development 135, 1923–33.

Chasan, R., Anderson, K. V, 1989. The role of easter, an apparent serine protease, in organizing the dorsal-ventral pattern of the Drosophila embryo. Cell 56, 391–400.

Chasan, R., Jin, Y., Anderson, K. V, 1992. Activation of the easter zymogen is regulated by five other genes to define dorsal-ventral polarity in the Drosophila embryo. Development 115, 607–16.

Chen, G., Handel, K., Roth, S., 2000. The maternal NF-kappaB/dorsal gradient of Tribolium castaneum: dynamics of early dorsoventral patterning in a short-germ beetle. Development 127, 5145–56.

Cho, Y.S., Stevens, L.M., Stein, D., 2010. Pipe-dependent ventral processing of Easter by Snake is the defining step in Drosophila embryo DV axis formation. Curr. Biol. 20, 1133–7.

Cong, L., Ran, F.A., Cox, D., Lin, S., Barretto, R., Habib, N., Hsu, P.D., Wu, X., Jiang, W., Marraffini, L.A., Zhang, F., 2013. Multiplex genome engineering using CRISPR/Cas systems. Science 339, 819–23.

Crocker, J., Tamori, Y., Erives, A., 2008. Evolution acts on enhancer organization to fine-tune gradient threshold readouts. PLoS Biol. 6, e263.

Das, P., Maduzia, L.L., Wang, H., Finelli, A.L., Cho, S.H., Smith, M.M., Padgett, R.W., 1998. The Drosophila gene Medea demonstrates the requirement for different classes of Smads in dpp signaling. Development 125, 1519–28.

Davis, G.K., Patel, N.H., 2002. Short, long, and beyond: molecular and embryological approaches to insect segmentation. Annu. Rev. Entomol. 47, 669–99.

Del Alamo Rodríguez, D., Terriente Felix, J., Díaz-Benjumea, F.J., 2004. The role of the T-box gene optomotor-blind in patterning the Drosophila wing. Dev. Biol. 268, 481–92.

DeLotto, R., Spierer, P., 1986. A gene required for the specification of dorsal-ventral pattern in Drosophila appears to encode a serine protease. Nature 323, 688–92.

Deng, W., Lin, H., 1997. Spectrosomes and fusomes anchor mitotic spindles during asymmetric germ cell divisions and facilitate the formation of a polarized microtubule array for oocyte specification in Drosophila. Dev. Biol. 189, 79–94.

Edwards, D.N., Towb, P., Wasserman, S.A., 1997. An activity-dependent network of interactions links the Rel protein Dorsal with its cytoplasmic regulators. Development 124, 3855–64.

Eldar, A., Dorfman, R., Weiss, D., Ashe, H., Shilo, B.-Z., Barkai, N., 2002. Robustness of the BMP morphogen gradient in Drosophila embryonic patterning. Nature 419, 304–8.

Ephrussi, A., Dickinson, L.K., Lehmann, R., 1991. Oskar organizes the germ plasm and directs localization of the posterior determinant nanos. Cell 66, 37–50.

Fleig, R., Sander, K., 1988. Honeybee morphogenesis: embryonic cell movements that shape the larval body. Development 103, 525–534.

François, V., Bier, E., 1995. Xenopus chordin and Drosophila short gastrulation genes encode homologous proteins functioning in dorsal-ventral axis formation. Cell 80, 19–20.

Fuller, M.T., Spradling, A.C., 2007. Male and female Drosophila germline stem cells: two versions of immortality. Science 316, 402–4.

Ghiglione, C., Carraway, K.L., Amundadottir, L.T., Boswell, R.E., Perrimon, N., Duffy, J.B., 1999. The transmembrane molecule kekkon 1 acts in a feedback loop to negatively regulate the activity of the Drosophila EGF receptor during oogenesis. Cell 96, 847–56.

Goltsev, Y., Fuse, N., Frasch, M., Zinzen, R.P., Lanzaro, G., Levine, M., 2007. Evolution of the dorsal-ventral patterning network in the mosquito, Anopheles gambiae. Development 134, 2415–24.

González-Reyes, A., Elliott, H., St Johnston, D., 1995. Polarization of both major body axes in Drosophila by gurken-torpedo signalling. Nature 375, 654–8.

González-Reyes, A., St Johnston, D., 1994. Role of oocyte position in establishment of anterior-posterior polarity in Drosophila. Science 266, 639–42.

Grieder, N.C., de Cuevas, M., Spradling, A.C., 2000. The fusome organizes the microtubule network during oocyte differentiation in Drosophila. Development 127, 4253–64.

Hong, J.-W., Hendrix, D.A., Papatsenko, D., Levine, M.S., 2008. How the Dorsal gradient works: insights from postgenome technologies. Proc. Natl. Acad. Sci. U. S. A. 105, 20072–6.

Horng, T., Medzhitov, R., 2001. Drosophila MyD88 is an adapter in the Toll signaling pathway. Proc. Natl. Acad. Sci. U. S. A. 98, 12654–8.

Hu, X., Yagi, Y., Tanji, T., Zhou, S., Ip, Y.T., 2004. Multimerization and interaction of Toll and Spätzle in Drosophila. Proc. Natl. Acad. Sci. U. S. A. 101, 9369–74.

Hudson, J.B., Podos, S.D., Keith, K., Simpson, S.L., Ferguson, E.L., 1998. The Drosophila Medea gene is required downstream of dpp and encodes a functional homolog of human Smad4. Development 125, 1407–20.

Januschke, J., Gervais, L., Dass, S., Kaltschmidt, J.A., Lopez-Schier, H., St Johnston, D., Brand, A.H., Roth, S., Guichet, A., 2002. Polar transport in the Drosophila oocyte requires Dynein and Kinesin I cooperation. Curr. Biol. 12, 1971–81.

Jaźwińska, a, Rushlow, C., Roth, S., 1999. The role of brinker in mediating the graded response to Dpp in early Drosophila embryos. Development 126, 3323–34.

Kambris, Z., Bilak, H., D'Alessandro, R., Belvin, M., Imler, J.-L., Capovilla, M., 2003. DmMyD88 controls dorsoventral patterning of the Drosophila embryo. EMBO Rep. 4, 64–9.

Kanodia, J.S., Rikhy, R., Kim, Y., Lund, V.K., DeLotto, R., Lippincott-Schwartz, J., Shvartsman, S.Y., 2009. Dynamics of the Dorsal morphogen gradient. Proc. Natl. Acad. Sci. U. S. A. 106, 21707–12.

Kim-Ha, J., Smith, J.L., Macdonald, P.M., 1991. oskar mRNA is localized to the posterior pole of the Drosophila oocyte. Cell 66, 23–35.

Kirkpatrick, H., Johnson, K., Laughon, A., 2001. Repression of dpp targets by binding of brinker to mad sites. J. Biol. Chem. 276, 18216–22.

Konrad, K.D., Goralski, T.J., Mahowald, A.P., Marsh, J.L., 1998. The gastrulation defective gene of Drosophila melanogaster is a member of the serine protease superfamily. Proc. Natl. Acad. Sci. U. S. A. 95, 6819–24.

Letsou, A., Arora, K., Wrana, J.L., Simin, K., Twombly, V., Jamal, J., Staehling-Hampton, K., Hoffmann, F.M., Gelbart, W.M., Massagué, J., 1995. Drosophila Dpp signaling is mediated by the punt gene product: a dual ligand-binding type II receptor of the TGF beta receptor family. Cell 80, 899–908.

Liberman, L.M., Reeves, G.T., Stathopoulos, A., 2009. Quantitative imaging of the Dorsal nuclear gradient reveals limitations to threshold-dependent patterning in Drosophila. Proc. Natl. Acad. Sci. U. S. A. 106, 22317–22.

Liberman, L.M., Stathopoulos, A., 2009. Design flexibility in cis-regulatory control of gene expression: synthetic and comparative evidence. Dev. Biol. 327, 578–89.

Lin, H., Spradling, A.C., 1995. Fusome asymmetry and oocyte determination in Drosophila. Dev. Genet. 16, 6–12.

Lynch, J.A., Desplan, C., 2006. A method for parental RNA interference in the wasp Nasonia vitripennis. Nat. Protoc. 1, 486–94.

Lynch, J.A., Roth, S., 2011. The evolution of dorsal-ventral patterning mechanisms in insects. Genes Dev. 25, 107–18.

Marqués, G., Musacchio, M., Shimell, M.J., Wünnenberg-Stapleton, K., Cho, K.W., O'Connor, M.B., 1997. Production of a DPP activity gradient in the early Drosophila embryo through the opposing actions of the SOG and TLD proteins. Cell 91, 417–26.

Mason, E.D., Konrad, K.D., Webb, C.D., Marsh, J.L., 1994. Dorsal midline fate in Drosophila embryos requires twisted gastrulation, a gene encoding a secreted protein related to human connective tissue growth factor. Genes Dev. 8, 1489–501.

McGrail, M., Hays, T.S., 1997. The microtubule motor cytoplasmic dynein is required for spindle orientation during germline cell divisions and oocyte differentiation in Drosophila. Development 124, 2409–19.

Medzhitov, R., Preston-Hurlburt, P., Kopp, E., Stadlen, A., Chen, C., Ghosh, S., Janeway, C.A., 1998. MyD88 is an adaptor protein in the hToll/IL-1 receptor family signaling pathways. Mol. Cell 2, 253–8.

Minakhina, S., Yang, J., Steward, R., 2003. Tamo selectively modulates nuclear import in Drosophila. Genes Cells 8, 299–310.

Mizutani, C.M., Bier, E., 2008. EvoD/Vo: the origins of BMP signalling in the neuroectoderm. Nat. Rev. Genet. 9, 663–77.

Mizutani, C.M., Nie, Q., Wan, F.Y.M., Zhang, Y.-T., Vilmos, P., Sousa-Neves, R., Bier, E., Marsh, J.L., Lander, A.D., 2005. Formation of the BMP activity gradient in the Drosophila embryo. Dev. Cell 8, 915–24.

Morimoto, A.M., Jordan, K.C., Tietze, K., Britton, J.S., O'Neill, E.M., Ruohola-Baker, H., 1996. Pointed, an ETS domain transcription factor, negatively regulates the EGF receptor pathway in Drosophila oogenesis. Development 122, 3745–54.

Morisato, D., 2001. Spätzle regulates the shape of the Dorsal gradient in the Drosophila embryo. Development 128, 2309–19.

Moussian, B., Roth, S., 2005. Dorsoventral axis formation in the Drosophila embryo--shaping and transducing a morphogen gradient. Curr. Biol. 15, R887–99.

Neuman-Silberberg, F.S., Schüpbach, T., 1993. The Drosophila dorsoventral patterning gene gurken produces a dorsally localized RNA and encodes a TGF alpha-like protein. Cell 75, 165–74.

Nunes da Fonseca, R., von Levetzow, C., Kalscheuer, P., Basal, A., van der Zee, M., Roth, S., 2008. Self-regulatory circuits in dorsoventral axis formation of the short-germ beetle Tribolium castaneum. Dev. Cell 14, 605–15.

O'Connor, M.B., Umulis, D., Othmer, H.G., Blair, S.S., 2006. Shaping BMP morphogen gradients in the Drosophila embryo and pupal wing. Development 133, 183–93.

Oelgeschläger, M., Larraín, J., Geissert, D., De Robertis, E.M., 2000. The evolutionarily conserved BMP-binding protein Twisted gastrulation promotes BMP signalling. Nature 405, 757–63.

Oelgeschläger, M., Reversade, B., Larraín, J., Little, S., Mullins, M.C., De Robertis, E.M., 2003. The pro-BMP activity of Twisted gastrulation is independent of BMP binding. Development 130, 4047–56.

Penton, A., Chen, Y., Staehling-Hampton, K., Wrana, J.L., Attisano, L., Szidonya, J., Cassill, J.A., Massagué, J., Hoffmann, F.M., 1994. Identification of two bone morphogenetic protein type I receptors in Drosophila and evidence that Brk25D is a decapentaplegic receptor. Cell 78, 239–50.

Peri, F., Bökel, C., Roth, S., 1999. Local Gurken signaling and dynamic MAPK activation during Drosophila oogenesis. Mech. Dev. 81, 75–88.

Queenan, A.M., Barcelo, G., Van Buskirk, C., Schüpbach, T., 1999. The transmembrane region of Gurken is not required for biological activity, but is necessary for transport to the oocyte membrane in Drosophila. Mech. Dev. 89, 35–42.

Rafiqi, A.M., Lemke, S., Ferguson, S., Stauber, M., Schmidt-Ott, U., 2008. Evolutionary origin of the amnioserosa in cyclorrhaphan flies correlates with spatial and temporal expression changes of zen. Proc. Natl. Acad. Sci. U. S. A. 105, 234–9.

Rafiqi, A.M., Lemke, S., Schmidt-Ott, U., 2010. Postgastrular zen expression is required to develop distinct amniotic and serosal epithelia in the scuttle fly Megaselia. Dev. Biol. 341, 282–90.

Raftery, L.A., Twombly, V., Wharton, K., Gelbart, W.M., 1995. Genetic screens to identify elements of the decapentaplegic signaling pathway in Drosophila. Genetics 139, 241–54.

Raftery, L.A., Wisotzkey, R.G., 1996. Characterization of Medea, a gene required for maximal function of the Drosophila BMP homolog Decapentaplegic. Ann. N. Y. Acad. Sci. 785, 318–20.

Reach, M., Galindo, R.L., Towb, P., Allen, J.L., Karin, M., Wasserman, S.A., 1996. A gradient of cactus protein degradation establishes dorsoventral polarity in the Drosophila embryo. Dev. Biol. 180, 353–64.

Reeves, G.T., Stathopoulos, A., 2009. Graded dorsal and differential gene regulation in the Drosophila embryo. Cold Spring Harb. Perspect. Biol. 1, a000836.

Reich, A., Sapir, A., Shilo, B., 1999. Sprouty is a general inhibitor of receptor tyrosine kinase signaling. Development 126, 4139–47.

Ross, J.J., Shimmi, O., Vilmos, P., Petryk, A., Kim, H., Gaudenz, K., Hermanson, S., Ekker, S.C., O'Connor, M.B., Marsh, J.L., 2001. Twisted gastrulation is a conserved extracellular BMP antagonist. Nature 410, 479–83.

Roth, S., 2003. The origin of dorsoventral polarity in Drosophila. Philos. Trans. R. Soc. Lond. B. Biol. Sci. 358, 1317–29; discussion 1329.

Roth, S., Lynch, J.A., 2009. Symmetry breaking during Drosophila oogenesis. Cold Spring Harb. Perspect. Biol. 1, a001891.

Roth, S., Neuman-Silberberg, F.S., Barcelo, G., Schüpbach, T., 1995. cornichon and the EGF receptor signaling process are necessary for both anterior-posterior and dorsal-ventral pattern formation in Drosophila. Cell 81, 967–78.

Rusch, J., Levine, M., 1996. Threshold responses to the dorsal regulatory gradient and the subdivision of primary tissue territories in the Drosophila embryo. Curr. Opin. Genet. Dev. 6, 416–23.

Schmierer, B., Hill, C.S., 2007. TGFbeta-SMAD signal transduction: molecular specificity and functional flexibility. Nat. Rev. Mol. Cell Biol. 8, 970–82.

Scott, I.C., Blitz, I.L., Pappano, W.N., Maas, S.A., Cho, K.W., Greenspan, D.S., 2001. Homologues of Twisted gastrulation are extracellular cofactors in antagonism of BMP signalling. Nature 410, 475–8.

Sekelsky, J.J., Newfeld, S.J., Raftery, L.A., Chartoff, E.H., Gelbart, W.M., 1995. Genetic characterization and cloning of mothers against dpp, a gene required for decapentaplegic function in Drosophila melanogaster. Genetics 139, 1347–58.

Sen, J., Goltz, J.S., Stevens, L., Stein, D., 1998. Spatially restricted expression of pipe in the Drosophila egg chamber defines embryonic dorsal-ventral polarity. Cell 95, 471–81.

Shimell, M.J., Ferguson, E.L., Childs, S.R., O'Connor, M.B., 1991. The Drosophila dorsal-ventral patterning gene tolloid is related to human bone morphogenetic protein 1. Cell 67, 469–81.

Shimmi, O., O'Connor, M.B., 2003. Physical properties of Tld, Sog, Tsg and Dpp protein interactions are predicted to help create a sharp boundary in Bmp signals during dorsoventral patterning of the Drosophila embryo. Development 130, 4673–82.

Shimmi, O., Umulis, D., Othmer, H., O'Connor, M.B., 2005. Facilitated transport of a Dpp/Scw heterodimer by Sog/Tsg leads to robust patterning of the Drosophila blastoderm embryo. Cell 120, 873–86.

Spradling, A., 1993. Developmental genetics of oogenesis. In The development of Drosophila melanogaster. Cold Spring Harb. Lab. Press. NY.

Stathopoulos, A., Levine, M., 2004. Whole-genome analysis of Drosophila gastrulation. Curr. Opin. Genet. Dev. 14, 477–84.

Stathopoulos, A., Van Drenth, M., Erives, A., Markstein, M., Levine, M., 2002. Whole-genome analysis of dorsal-ventral patterning in the Drosophila embryo. Cell 111, 687–701.

Sun, H., Towb, P., Chiem, D.N., Foster, B.A., Wasserman, S.A., 2004. Regulated assembly of the Toll signaling complex drives Drosophila dorsoventral patterning. EMBO J. 23, 100–10.

Torres, I.L., López-Schier, H., St Johnston, D., 2003. A Notch/Delta-dependent relay mechanism establishes anterior-posterior polarity in Drosophila. Dev. Cell 5, 547–58.

Towb, P., Galindo, R.L., Wasserman, S.A., 1998. Recruitment of Tube and Pelle to signaling sites at the surface of the Drosophila embryo. Development 125, 2443–50.

Trapnell, C., Roberts, A., Goff, L., Pertea, G., Kim, D., Kelley, D.R., Pimentel, H., Salzberg, S.L., Rinn, J.L., Pachter, L., 2012. Differential gene and transcript expression analysis of RNA-seq experiments with TopHat and Cufflinks. Nat. Protoc. 7, 562–78.

Uv, A.E., Roth, P., Xylourgidis, N., Wickberg, A., Cantera, R., Samakovlis, C., 2000. members only encodes a Drosophila nucleoporin required for rel protein import and immune response activation. Genes Dev. 14, 1945–57.

Van der Zee, M., Stockhammer, O., von Levetzow, C., Nunes da Fonseca, R., Roth, S., 2006. Sog/Chordin is required for ventral-to-dorsal Dpp/BMP transport

and head formation in a short germ insect. Proc. Natl. Acad. Sci. U. S. A. 103, 16307–12.

Wang, Y.-C., Ferguson, E.L., 2005. Spatial bistability of Dpp-receptor interactions during Drosophila dorsal-ventral patterning. Nature 434, 229–34.

Weiszmann, R., Hammonds, A.S., Celniker, S.E., 2009. Determination of gene expression patterns using high-throughput RNA in situ hybridization to whole-mount Drosophila embryos. Nat. Protoc. 4, 605–18.

Werren, J.H., Richards, S., Desjardins, C.A., Niehuis, O., Gadau, J., Colbourne, J.K., Beukeboom, L.W., Desplan, C., Elsik, C.G., Grimmelikhuijzen, C.J.P., Kitts, P., Lynch, J.A., Murphy, T., Oliveira, D.C.S.G., Smith, C.D., van de Zande, L., Worley, K.C., Zdobnov, E.M., Aerts, M., Albert, S., Anaya, V.H., Anzola, J.M., Barchuk, A.R., Behura, S.K., Bera, A.N., Berenbaum, M.R., Bertossa, R.C., Bitondi, M.M.G., Bordenstein, S.R., Bork, P., Bornberg-Bauer, E., Brunain, M., Cazzamali, G., Chaboub, L., Chacko, J., Chavez, D., Childers, C.P., Choi, J.-H., Clark, M.E., Claudianos, C., Clinton, R.A., Cree, A.G., Cristino, A.S., Dang, P.M., Darby, A.C., de Graaf, D.C., Devreese, B., Dinh, H.H., Edwards, R., Elango, N., Elhaik, E., Ermolaeva, O., Evans, J.D., Foret, S., Fowler, G.R., Gerlach, D., Gibson, J.D., Gilbert, D.G., Graur, D., Gründer, S., Hagen, D.E., Han, Y., Hauser, F., Hultmark, D., Hunter, H.C., Hurst, G.D.D., Jhangian, S.N., Jiang, H., Johnson, R.M., Jones, A.K., Junier, T., Kadowaki, T., Kamping, A., Kapustin, Y., Kechavarzi, B., Kim, J., Kim, J., Kiryutin, B., Koevoets, T., Kovar, C.L., Kriventseva, E. V, Kucharski, R., Lee, H., Lee, S.L., Lees, K., Lewis, L.R., Loehlin, D.W., Logsdon, J.M., Lopez, J.A., Lozado, R.J., Maglott, D., Maleszka, R., Mayampurath, A., Mazur, D.J., McClure, M.A., Moore, A.D., Morgan, M.B., Muller, J., Munoz-Torres, M.C., Muzny, D.M., Nazareth, L. V, Neupert, S., Nguyen, N.B., Nunes, F.M.F., Oakeshott, J.G., Okwuonu, G.O., Pannebakker, B.A., Pejaver, V.R., Peng, Z., Pratt, S.C., Predel, R., Pu, L.-L., Ranson, H., Raychoudhury, R., Rechtsteiner, A., Reese, J.T., Reid, J.G., Riddle, M., Robertson, H.M., Romero-Severson, J., Rosenberg, M., Sackton, T.B., Sattelle, D.B., Schlüns, H., Schmitt, T., Schneider, M., Schüler, A., Schurko, A.M., Shuker, D.M., Simões, Z.L.P., Sinha, S., Smith, Z., Solovyev, V., Souvorov, A., Springauf, A., Stafflinger, E., Stage, D.E., Stanke, M., Tanaka, Y., Telschow, A., Trent, C., Vattathil, S., Verhulst, E.C., Viljakainen, L., Wanner, K.W., Waterhouse, R.M., Whitfield, J.B., Wilkes, T.E., Williamson, M., Willis, J.H., Wolschin, F., Wyder, S., Yamada, T., Yi, S. V, Zecher, C.N., Zhang, L., Gibbs, R.A., 2010. Functional and evolutionary insights from the genomes of three parasitoid Nasonia species. Science 327, 343–8.

Winter, S.E., Campbell, G., 2004. Repression of Dpp targets in the Drosophila wing by Brinker. Development 131, 6071–81.

Wisotzkey, R.G., Mehra, A., Sutherland, D.J., Dobens, L.L., Liu, X., Dohrmann, C., Attisano, L., Raftery, L.A., 1998. Medea is a Drosophila Smad4 homolog that is differentially required to potentiate DPP responses. Development 125, 1433–45.

Zhang, Z., Zhu, X., Stevens, L.M., Stein, D., 2009. Distinct functional specificities are associated with protein isoforms encoded by the Drosophila dorsal-ventral patterning gene pipe. Development 136, 2779–89.

Zhao, T., Graham, O.S., Raposo, A., St Johnston, D., 2012. Growing microtubules push the oocyte nucleus to polarize the Drosophila dorsal-ventral axis. Science 336, 999–1003.

B. Summary

Two conserved pathways (Toll and BMP) pattern the embryonic DV axis of *Drosophila melanogaster*. The Toll pathway dominates this process and is the source of all polarity and most of the patterning along the DV axis of the embryo. This is in contrast to other animals, where Toll signalling is not employed for DV patterning, and BMP signalling plays the major role. The early patterning role of Toll can therefore be considered as an evolutionary novelty, which appeared within the insect lineage. To further investigate the evolution of axial patterning in insects we analyzed the DV axis of the wasp *Nasonia vitripennis*, which is a member of the Hymenoptera, the most basally branching order of the Holometabola.

A detailed analysis of the expression of DV marker genes that cover the entire embryonic axis revealed that the expression pattern just prior to the onset of gastrulation is almost identical in *Nasonia* and *Drosophila*. However, in *Nasonia* these patterns are initially very dynamic and evolve over time, which indicates that the upstream network for generating this pattern is highly diverged.

In order to examine the functional basis of DV patterning in *Nasonia* we knocked down Toll and BMP signalling and showed that BMP is required for almost all DV patterning and that Toll has only a limited role. These results indicate that the ancestral role of Toll in insect embryos was only to induce mesoderm, while BMP played the dominant role.

To further analyze and identify new target genes or possible new components of both pathways, we performed a transcriptome analysis of wild type, Toll knockdown, and BMP knockdown embryos. The outcome was a set of 262 genes that were significantly up or down regulated when compared among the different data sets. To analyze the expression pattern of those genes, we established a high throughput *in situ* technique. A first round of analysis revealed many interesting candidates that might play a role in DV patterning. However, further descriptive and functional analyses of all 262 identified genes are needed.

C. Zusammenfassung

In *Drosophila melanogaster* sind zwei konservierte Signalwege (Toll und BMP) für die Musterbildung der embryonalen DV-Achse verantwortlich. Der Toll Signalweg dominiert diesen Prozess und ist für die gesamte Polarität sowie den Großteil der Musterbildung entlang der DV-Achse des Embryos zuständig. Im Gegensatz dazu wird der Toll Signalweg außerhalb der Insekten nicht für die DV Musterbildung benutzt, sondern nur der BMP Signalweg. Daher kann die Rolle des Toll Signalwegs, die er während der frühen embryonalen Musterbildung einnimmt, als evolutionäre Neuheit bezeichnet werden, welche innerhalb der Abstammungslinie der Insekten entstanden ist. Zur weiteren Untersuchung der Evolution der axialen Musterbildung, haben wir die DV-Achse der Wespe *Nasonia vitripennis* untersucht. Diese gehört zu den Hymenopteren, welche die basalste Gruppe der Holometabolen Insekten darstellt.

Eine detaillierte Analyse der Expression von DV Markergenen hat gezeigt, dass die Expressionsmuster kurz vor Beginn der Gastrulation sowohl in *Nasonia* als auch in *Drosophila* fast identisch sind. Jedoch ist die Entwicklung der Muster in *Nasonia* sehr dynamisch was darauf hindeutet, dass das musterbildende Netzwerk in *Nasonia* im Gegensatz zu *Drosophila* stark abgeleitet ist.

Um die funktionelle Basis der DV Musterbildung in *Nasonia* zu untersuchen haben wir den Toll und BMP Signalweg mittels RNAi inhibiert. Das Ergebnis hat ergeben, dass BMP für die fast gesamte DV-Achse benötigt wird und Toll nur eine kleine limitierte Rolle besitzt. Somit deuten die Resultate darauf hin, dass Toll ursprünglich in Insektenembryos benutzt wurde, um Mesoderm zu induzieren und, dass BMP die Hauptrolle in der DV Musterbildung spielte.

Um weitere Zielgene und mögliche neue Komponenten beider Signalwege zu identifizieren haben wir eine Transkriptomanalyse von Wildtyp-, Toll RNAi- und BMP RNAi-Embryonen durchgeführt. Das Ergebnis war eine Liste von 262 Genen, welche im Vergleich zwischen den verschiedenen Transkriptomdaten

signifikant hoch oder runterreguliert waren. Um die Expressionsmuster dieser Gene zu analysieren, haben wir eine Hochdurchsatzvariante der *In situ* Technik entwickelt. Erste vorläufige Analysen haben viele interessante Kandidaten ergeben, welche eine mögliche Rolle in der DV Musterbildung erfüllen könnten. Jedoch sind weitere deskriptive und funktionelle Analysen aller 262 identifizierten Gene notwendig.

D. Anhang über die eigene Beteiligung an den aufgeführten Veröffentlichungen

D.1 Patterning the dorsal–ventral axis of the wasp *Nasonia vitripennis*

Thomas Buchta, Orhan Özüak, Dominik Stappert, Siegfried Roth, JeremyA. Lynch

D.1.1 Gene identification

Conserved domains of the following genes have been identified using TBLASTN (homepage) in the *Nasonia vitripennis* genome:

muscle segment homeobox 1	*(Nv-msh1)*
zerknüllt	*(Nv-zen)*
RACE	*(Nv-RACE)*
hindsight	*(Nv-hnt)*
tail-up	*(Nv-tup)*
dorsocross	*(Nv-doc)*
pannier	*(Nv-pnr)*
araucan	*(Nv-ara)*

Conserved domains of the following genes have been identified using TBLASTN in the *Drosophila melanogaster* genome:

muscle segment homeobox	*(Dm-msh)*
hindsight	*(Dm-hnt)*
zerknüllt	*(Dm-zen)*
pannier	*(Dm-pnr)*
dorsocross	*(Dm-doc)*

D.1.2 Primer design

For all in D.1.1 identified genes specific primers were designed using Primer3 (http://bioinfo.ut.ee/primer3-0.4.0/)

D.1.3 cDNA generation

cDNA used for specific gene amplification was created using superscript 3 (invitrogen).

D.1.4 *In situ* hybridization (ISH) probe synthesis

Amplicons created using gene specific primers described in D.1.2 were used for ISH probe synthesis.

D.1.5 Single/two color fluorescent ISH with DAPI

ISH with DAPI was performed for the following genes:

Dm-msh / *Dm-ind*	(Figure 5 G-I)
Nv-msh1 / *Nv-ind*	(Figure 5 J-L)
Nv-zen	(Figure 6)
Nv-zen / *Nv-RACE*	(Figure 7 A)
Nv-hnt / *Nv-zen*	(Figure 7 B-D)
Nv-tup / *Nv-zen*	(Figure 8 A-C)
Nv-doc / *Nv-zen*	(Figure 8 D-F)
Nv-zen / *Nv-pnr*	(Figure 9 A-C)

Nv-zen / *Nv-ara*	(Figure 9 D-F)
Dm-hnt / *Dm-zen*	(Supplementary Figure 4)
Dm-hnt / *Dm-pnr*	(Supplementary Figure 5)
Dm-doc / *Dm-zen*	(Supplementary Figure 6)
Nv-RACE	(Supplementary Figure 7)

D.1.6 Microscopy, picture processing and figure design

Pictures for the following figures were taken, processed and assembled

Figure 5. Comparsion of columnar gene dynamics in *Drosophila* and *Nasonia*. (G-L)

Figure 6. Dynamics of *Nv-zen* expression in *Nasonia* embryos.

Figure 7. Dynamics of *Nv-RACE* and *Nv-hnt* in relation to those of *Nv-zen*.

Figure 8. Dynamics of *Nv-tup* and *Nv-doc* in relation to those of *Nv-zen*.

Figure 9. Dynamics of *Nv-pnr* and *Nv-ara* expression in relation to those of *Nv-zen*.

Supplementary Figure 4	Double fluorescent ISH of *hnt* (green) and *zen* (red) in *Drosophila*
Supplementary Figure 5	Double fluorescent ISH of *hnt* (green) and *pnr* (red) in *Drosophila*
Supplementary Figure 6	Double fluorescent ISH of *doc* (green) and *zen* (red) in *Drosophila*
Supplementary Figure 7	Fluorescent ISH of *RACE* (red) in late (gastrulating and post- gastrulation) *Nasonia* embryos.

D.1.7 Embryo collection and fixation

Embryos used in D.1.3 and D.1.5 were collected by using the Waspinator and fixed as described in the paper

D.1.8 Waspinator

Idea and design for the *Waspinator* by T. Buchta & O. Özüak.

D.1.9 Text

Orhan Özüak wrote the manuscript of "Patterning the dorsal–ventral axis of the wasp *Nasonia vitripennis"*.

The manuscript was proofread and finalized in co-operation with Thomas Buchta.

D.2 Novel deployment of Toll and BMP signaling pathways leads to a convergent patterning output in a wasp.

Orhan Özüak*, Thomas Buchta*, Siegfried Roth, Jeremy A. Lynch

D.2.1 Gene identification

Conserved domains of the following genes have been identified using TBLASTN in the *Nasonia vitripennis* genome:

zerknüllt	(*Nv-zen*)
araucan	(*Nv-ara*)
dorsocross	(*Nv-doc*)
tolloid	(*Nv-tld*)
glass bottom boat	(*Nv-gbb*)
twisted gastrulation	(*Nv-tsg*)
thick veins	(*Nv-tkv*)
saxophone	(*Nv-sax*)

D.2.2 Primer design

For all in D.21 identified genes specific primers were designed using Primer3 (http://bioinfo.ut.ee/primer3-0.4.0/)

D.2.3 cDNA generation

cDNA used for specific gene amplification was created.

D.2.4 *In situ* hybridization (ISH) probe synthesis

Amplicons created using gene specific primers for

zerknüllt	(*Nv-zen*)
araucan	(*Nv-ara*)

dorsocross	(*Nv-doc*)
tolloid	(*Nv-tld*)

were used for ISH probe synthesis.

D.2.5 Two-color and three-color fluorescent ISH with DAPI

ISH with DAPI for the following genes:

Nv-zen / *Nv-brk* / *Nv-twi*	(Figure 1 C)
Nv-zen / *Nv-brk* / *Nv-twi*	(Figure 2 E, F)
Nv-twi / *Nv-vnd*	(Figure 2 G, H)
Nv-tld	(Figure 3 E)
Nv-twi / *Nv-vnd*	(Figure 3 F,G,H)
Nv-twi / *Nv-doc*	(Supplementary Figure 1 C-F)

D.2.6 Immunohistochemistry

pMad antibody staining	(Figure 3 A-D)

D.2.7 Double standed RNA synthesis

Amplicons created using gene specific primers for

glass bottom boat	(*Nv-gbb*)
twisted gastrulation	(*Nv-tsg*)
thick veins	(*Nv-tkv*)
saxophone	(*Nv-sax*)

were used for dsRNA synthesis.

D.2.8 dsRNA single injections

Following dsRNA were injected:

Nv-dpp
Nv-gbb
Nv-tkv
Nv-sax

D.2.9 Microscopy, picture processing and figure design

Pictures for the following figures were taken, process and assembled*:

Figure 1. Effects of *Toll*, *dpp,* and *Toll*/*dpp* double pRNAi.

Figure 2. Detailed effects of *Nv-dpp* and *Nv-Toll* pRNAi.

Figure 3. BMP signaling in the *Nasonia* embryo.

Supplementary Figure 1. *Nasonia dorsocross* (*Nv-doc*) as a marker in *Nv-dpp* RNAi

*except Figure 1 A,B,D
Figure 2 A-D, I-M'
Suppl. Fig. 1 A,B
by T. Buchta

D.2.10 Embryo collection and fixation

Embryos used in D.2.3 and D.2.5 were collected by using the *Waspinator* and fixed as described in the paper

D.2.11 Text

Thomas Buchta wrote the manuscript of "Novel deployment of Toll and BMP signaling pathways leads to a convergent patterning output in a wasp."
The manuscript was proofread and finalized in co-operation with Orhan Özüak.

D.3 Ancient and diverged TGF-ß signaling components in *Nasonia vitripennis*

Orhan Özüak*, Thomas Buchta*, Siegfried Roth, Jeremy A. Lynch

D.3.1 Gene identification

Conserved domains of the following genes have been identified using TBLASTN in the Nasonia vitripennis genome:

decapentaplegic	(*Nv-dpp*)
glass bottom boat 1	(*Nv-gbb1*)
glass bottom boat 2	(*Nv-gbb2*)
anti-dorsalizing morphogenetic protein	(*Nv-ADMP)*
maverick	(*Nv-mav*)
activin	(*Nv-act*)
activin like protein 23b	(*Nv-alp/dawdle*)
myostatin	(*Nv-myo*)
saxophone	(*Nv-sax*)
thick veins	(*Nv-tkv*)
baboon	(*Nv-babo)*

wishful thinking	(*Nv-wit*)
punt 1	(*Nv-punt1*)
punt 2	(*Nv-punt2*)

The putative Nasonia protein sequences were aligned with muscle 3.7
(http://www.drive5.com/muscle/index.htm)
Alignment refinement was performed using GBLOCKS 0.91b
(http://molevol.cmima.csic.es/castresana/Gblocks.html)
Maximum likelihood phylogenies were generated with PhyML 3.0 aLRT
(http://atgc.lirmm.fr/phyml/binaries.html)
Trees were edited in MEGA5.2.2
(http://www.megasoftware.net/index.php)

D.3.2 Primer design

For all in D.3.1 identified genes specific primers were designed using Primer3 (http://bioinfo.ut.ee/primer3-0.4.0/)

D.3.3 cDNA generation

cDNA used for specific gene amplification was created using *Superscript 3* (Invitrogen)

D.3.4 *In situ* hybridization (ISH) probe synthesis

Amplicons created using gene specific primers described in D.3.2 were used for ISH probe synthesis.

D.3.5 Single/ two color fluorescent ISH with DAPI

ISH with DAPI was performed for the following genes:

decapentaplegic	(Figure 1B, C)
glass bottom boat 1	(Figure 1D, E)
glass bottom boat 2	(Figure 1F)
activin	(Figure 1G)
activin like protein 23b / dawdle	(Figure 1H)
myostatin	(Figure 1I)
maverick	(Figure 1J, K)
thick veins	(Figure 2B)
saxophone	(Figure 2C)
baboon	(Figure 2D)
punt 1	(Figure 2E)
punt 2	(Figure 2F)

D.3.6 Double standed RNA synthesis

Amplicons created using gene specific primers described in D.3.2 were used for dsRNA synthesis.

D.3.7 dsRNA injection

Following dsRNA were injected:

glass bottom boat 1	(*Nv-gbb1*)
punt 2	(*Nv-punt2*)

D.3.8 Microscopy, picture processing, tree generation and figure design

Figure 1. Ligands.

Figure 2. Receptors

D.3.9 Embryo collection and fixation

Embryos used in 8.3.3 and 8.3.5 were collected by using the *Waspinator* and fixed as described in the paper

D.3.10 Text

Thomas Buchta wrote the manuscript of "Ancient and highly diverged TGF- ß Pathway signaling components in *Nasonia vitripennis*".

The manuscript will be proofread and finalized in co-operation with Orhan Özüak.

E. Danksagung

Ich möchte mich ganz herzlich bei Prof. Dr. Siegfried Roth für die Aufnahme in seine Arbeitsgruppe, die Möglichkeit der Mitforschung an diesem spannenden Thema, sowie für seine professionelle Unterstützung und permanente Diskussionsbereitschaft bedanken.
Vielen Dank Siegfried!

Frau Prof. Dr. Henrike Scholz danke ich für die Übernahme des Zweitgutachtens.

Herrn Prof. Dr. Jeremy A. Lynch danke ich für seine intensive Betreuung.
Vielen Dank Jeremy!

Ich danke dem SFB 680 „Molecular Basis of Evolutionary Innovations“ für die Finanzierung dieser Arbeit.

Ich danke all meinen aktuellen und ehemaligen Arbeitskollegen für ihre tägliche Hilfsbereitschaft, für die vielen wissenschaftlichen und nicht wissenschaftlichen Diskussionen sowie für die sehr angenehme Arbeitsatmosphäre.

Letztlich gilt mein größtes Dankeschön meinen Eltern Yildiz und Mehmet, meinem Bruder Ozan, meinem Onkel Ayhan, meinem Freund Tommy sowie meiner herzallerliebsten Cindy für die unendliche Unterstützung und die stets aufmunternden Worte. Ohne euch wäre ich nichts. Vielen Dank!

F. Erklärung

Ich versichere, dass ich die von mir vorgelegte Dissertation selbstständig angefertigt, die benutzten Quellen und Hilfsmittel vollständig angegeben und die Stellen der Arbeit – einschließlich Tabellen, Karten und Abbildungen -, die anderen Werken im Wortlaut oder dem Sinn nach entnommen sind, in jedem Einzelfall als Entlehnung kenntlich gemacht habe; dass diese Dissertation noch keiner anderen Fakultät oder Universität zur Prüfung vorgelegen hat; dass sie – abgesehen von unten angegebenen Teilpublikationen – noch nicht veröffentlicht worden ist sowie, dass ich eine solche Veröffentlichung vor Abschluss des Promotionsverfahrens nicht vornehmen werde.
Die Bestimmungen der Promotionsordnung sind mir bekannt. Die von mir vorgelegte Dissertation ist von Prof. Dr. Siegfried Roth betreut worden.

Teilpublikationen:

Buchta T, Ozüak O, Stappert D, Roth S, Lynch JA. (2013) Patterning the dorsal-ventral axis of the wasp Nasonia vitripennis. Dev Biol. 2013 Sep 1;381(1):189-202. doi: 10.1016/j.ydbio.2013.05.026. Epub 2013 Jun 2.

In review process:

Orhan Özüak, Thomas Buchta, Siegfried Roth, Jeremy A. Lynch
Novel deployment of Toll and BMP signaling pathways leads to a convergent patterning output in a wasp.

Orhan Özüak, Thomas Buchta, Siegfried Roth, Jeremy A. Lynch
Ancient and highly diverged TGF- ß Pathway signaling components in Nasonia vitripennis

Ich versichere, dass ich alle Angaben wahrheitsgemäß nach bestem Wissen und Gewissen gemacht habe und verpflichte mich, jedmögliche, die obigen Angaben betreffenden Veränderungen, dem Dekanat unverzüglich mitzuteilen.

Köln, 17.02.2014 Orhan Özüak

G. Lebenslauf

Persönliche Daten	
Name	Orhan Özüak
Anschrift	Rurstr. 3
	50937 Köln
Geburtsdatum / -ort	21.03.1983 Köln
Schulische Ausbildung	
1989 – 1993	Grundschule Riphahnstraße Köln
1993 – 2002	Heinrich-Mann Gymnasium Köln
Zivildienst	
2002 – 2003	Marie-Juchacz Altersheim Köln
Studium	
2003 – 2009	Biologie an der Universität zu Köln
	Diplom-Prüfungsfächer: Genetik, Entwicklungsbiologie, Biochemie
	Diplomarbeit bei Prof. Dr. Siegfried Roth am Institut für Entwicklungsbiologie der Universität zu Köln
	Titel „Functional comparison of the oskar genes from *D. melanogaster* and *N. vitripennis*."
Seit 2010	Doktorarbeit bei Prof. Dr. Siegfried Roth am Institut für Entwicklungsbiologie der Universität zu Köln
	Titel: „The role of the BMP and Toll pathways in patterning the dorsal-ventral axis of the jewel wasp *Nasonia vitripennis*."

Publikationen:

Lynch, J. A., Ozüak, O., Khila, A., Abouheif, E., Desplan, C., & Roth, S. (2011). The phylogenetic origin of oskar coincided with the origin of maternally provisioned germ plasm and pole cells at the base of the Holometabola. PLoS Genetics, 7(4), e1002029. doi:10.1371/journal.pgen.1002029

Buchta T, Ozüak O, Stappert D, Roth S, Lynch JA. (2013) Patterning the dorsal-ventral axis of the wasp Nasonia vitripennis. Dev Biol. 2013 Sep 1;381(1):189-202. doi: 10.1016/j.ydbio.2013.05.026. Epub 2013 Jun 2.

In review process:

Orhan Özüak, Thomas Buchta, Siegfried Roth, Jeremy A. Lynch
Novel deployment of Toll and BMP signaling pathways leads to a convergent patterning output in a wasp.

Orhan Özüak, Thomas Buchta, Siegfried Roth, Jeremy A. Lynch
Ancient and highly diverged TGF- ß Pathway signaling components in Nasonia vitripennis